Rodrigo Atique Ferraz de Toledo

Identificação e análise funcional de mutação associadas às craniossinostoses.

Identification and functional analysis of mutations associated with craniosynostosis.

São Paulo

2016

Rodrigo Atique Ferraz de Toledo

Identificação e análise funcional de mutação associadas às craniossinostoses.

Identification and functional analysis of mutations associated with craniosynostosis.

Tese apresentada ao Instituto de Biociências da Universidade de São Paulo, para a obtenção de Título de Doutor em Ciências, na Área de Genética e Biologia Evolutiva.

Orientador(a): Maria Rita dos Santos e Passos-Bueno

São Paulo

2016

Ficha Catalográfica

Atique Ferraz de Toledo, Rodrigo
Identificação e análise funcional de mutação associadas às craniossinostoses.
102 páginas

Tese (Doutorado) - Instituto de Biociências da Universidade de São Paulo. Departamento de Genética e Biologia Evolutiva

1. Craniossinostoses 2. NGS I.Universidade de São Paulo. Instituto de Biociências. Departamento de Genética e Biologia Evolutiva.

Comissão Julgadora:

_____ _____

Prof(a). Dr(a). Prof(a). Dr(a).

_____ _____

Prof(a). Dr(a). Prof(a). Dr(a).

_____

Prof(a). Dr(a). Orientador(a)

The world is a thing of utter inordinate complexity and richness and strangeness that is absolutely awesome. I mean the idea that such complexity can arise not only out of such simplicity, but probably absolutely out of nothing, is the most fabulous extraordinary idea. And once you get some kind of inkling of how that might have happened, it's just wonderful. And … the opportunity to spend 70 or 80 years of your life in such a universe is time well spent as far as I am concerned.

Douglas Adams

AGRADECIMENTOS

Primeiramente gostaria de agradecer os pacientes e suas famílias que confiaram em nós o suficiente para partilhar suas histórias e seus genomas. A perspectiva de podermos reduzir o sofrimento dos outros é o que faz com que os obstáculos da ciência se tornem transponíveis.

Gostaria de agradecer também à minha orientadora Maria Rita Passos-Bueno que com sua paciência e seu conhecimento foi capaz de orientar não só esse trabalho quanto tantos outros, ao mesmo tempo em que criou um ambiente de trabalho notavelmente leve e produtivo.

Também agradeço aos meus colegas de laboratório que no passar de 7 anos se tornaram mais que amigos. Se o laboratório se tornou uma segunda casa para muitos de nós, esses também se tornaram uma segunda família. Os momentos divididos, as lamentações das falhas e a celebração das vitórias são hoje parte de mim, por isso, muito obrigado a todos.

Agradeço à minha esposa e à minha família pelo suporte e encorajamento que sempre me deram. O apoio incontestável que me deram durante todos esses anos foi sempre fundamental para o meu sucesso. Sem o apoio de vocês essa tese não seria possível.

Agradeço aos meus amigos que por mais que não tenham contribuído diretamente para os trabalhos aqui apresentados sempre foram o alívio ao stress do dia a dia.

Por fim agradeço à FAPESP, CNPq e CAPES que financiaram os trabalhos aqui apresentados

ÍNDICE

O Crânio

O crânio é a estrutura esquelética mais complexa presente nos vertebrados. Anatomicamente, o crânio dos vertebrados é subdivido em neurocrânio e viscerocrânio (KURATANI; MATSUO; AIZAWA, 1997)(Figura 1A). O Neurocrânio, comumente chamado de caixa craniana, compreende os ossos atmóide, frontal, occipital, parietal, esfenoide e temporais. Esses ossos ocupam a parte superior e posterior do crânio. O viscerocrânio, ou esqueleto facial, e inclui os ossos mandibular, maxilares, lacrimais, a concha inferior nasal, os ossos nasais, palatinos, vômer e zigomáticos formando a mandíbula e maxila, além das estruturas faciais.

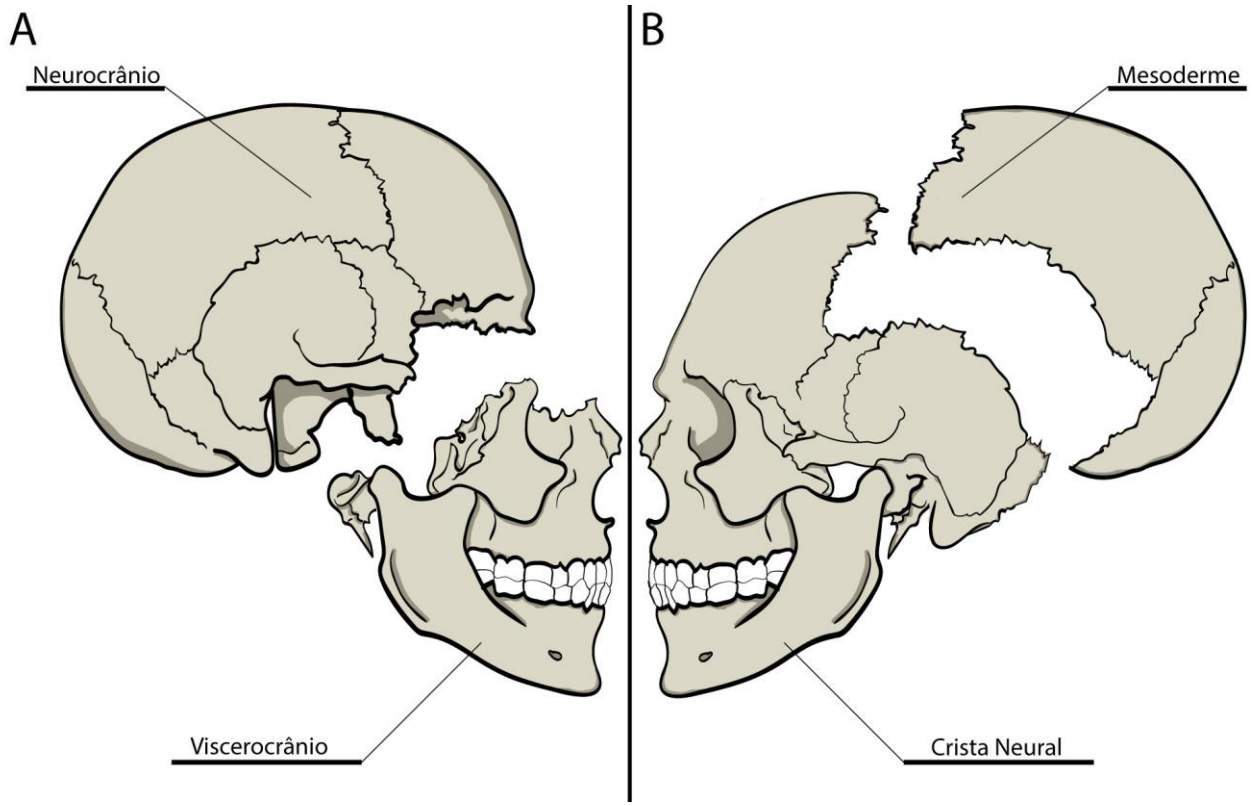

Figura 1: Esquemas representando a separação dos ossos cranianos entre pertencentes ao neurocrânio ou ao viscerocrânio (A); ou com origem embriológica da mesoderme ou crista neural (B).

As Suturas e as craniossinostoses

Suturas cranianas são os tecidos fibrosos que unem os ossos do crânio. As suturas são o principal sítio de crescimento ósseo de ossos cranianos durante o desenvolvimento craniofacial, especialmente durante a rápida expansão do neurocrânio (PRITCHARD; SCOTT; GIRGIS, 1956). Para que o crescimento ósseo aconteça, é fundamental que as suturas se mantenham fibrosas permitindo a rápida formação de tecido ósseo em suas margens.

Nos humanos, as suturas ocorrem entre os ossos frontais (sutura metópica), entre os ossos parietais (sutura sagital), entre os ossos frontais e parietais (sutura coronal) e entre os ossos parietais e occipitais (suturas lambdoides) (figura 2). Durante o desenvolvimento, as suturas sofrem um processo de ossificação, passando de tecidos fibrosos e lineares entre os ossos para complexas estruturas ósseas interdigitadas (MIURA et al., 2009). Cada sutura se ossifica em períodos distintos: nos humanos esse período varia de 2 anos de idade (sutura metópica) até os 26 (sutura lambdoide) (COHEN JR.; MACLEAN, 2000)

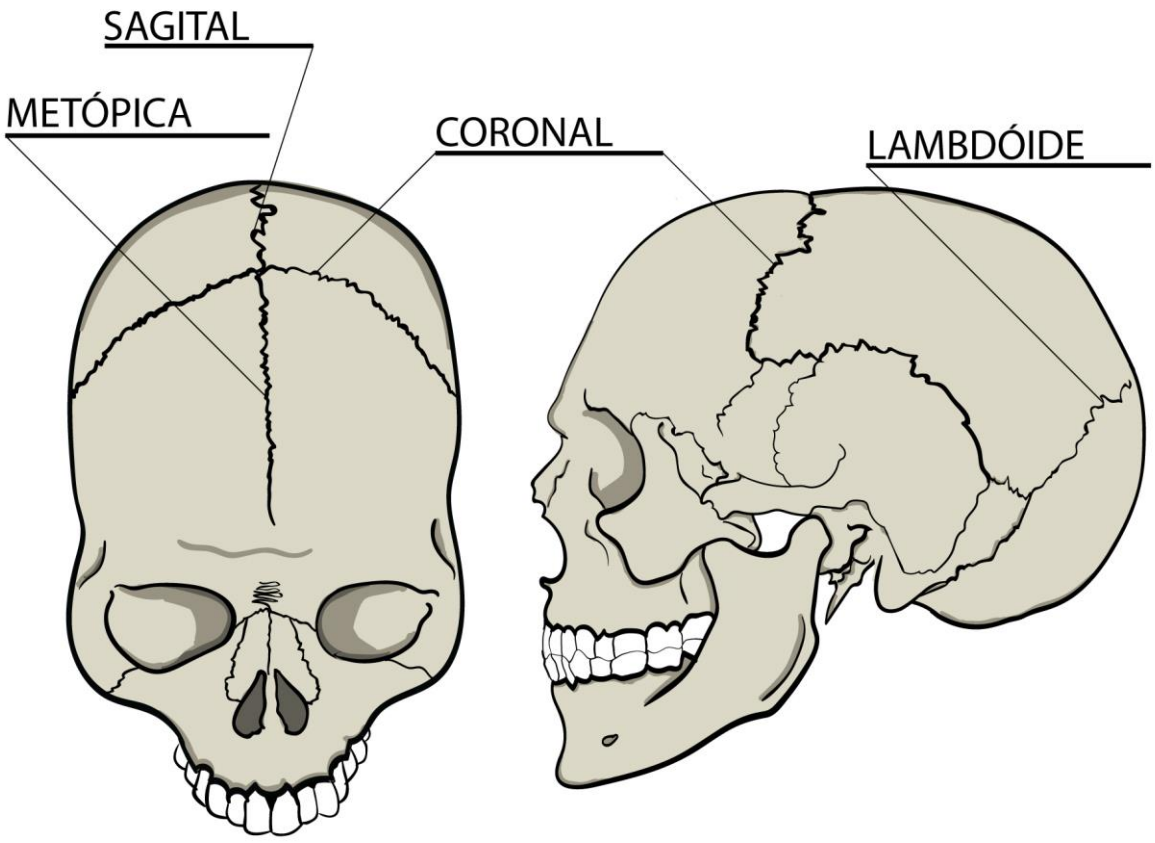

Figura 2: Localização das suturas cranianas.

Além de serem fundamentais para o crescimento dos ossos craniano, as suturas têm outras funções como permitir o movimento dos ossos durante o nascimento transvaginal, de modo que o crânio possa se ajustar à pressão que ocorre sobre ele durante a passagem pelo canal vaginal. Além disso, durante a infância, enquanto o desenvolvimento do encéfalo ocorre, todas as outras suturas cranianas continuam abertas de maneira a permitir o correto desenvolvimento e crescimento do encéfalo, com exceção da sutura metópica. Também especula-se que as suturas ajudem a absorver pequenos estresses mecânicos durante a infância (COHEN JR.; MACLEAN, 2000).

O fechamento precoce de qualquer uma das suturas cranianas é chamado de craniossinostose. As craniossinostoses são malformações congênitas que acometem cerca de 1 em cada 2.500 crianças nascidas. A ossificação prematura das suturas pode ocorrer antes ou depois do nascimento, sendo que, quanto mais cedo a sinostose ocorrer, maiores serão os efeitos no formato do crânio. As craniossinostoses podem ser classificadas de acordo com o número de suturas acometidas, simples se somente uma sutura estiver ossificada ou complexa se múltiplas suturas estiverem fusionadas.

As craniossinostoses também podem ser classificadas como sindrômicas ou não-sindrômicas.

As craniossinostoses não sindrômicas ou isoladas, onde a fusão da sutura craniana é o único defeito primário do indivíduo, são as formas de craniossinostoses mais comuns, representando cerca de 80% dos casos totais. Sintomas secundários, como manifestações neurológicas ou oftalmológicas, podem estar presentes como consequência de compressão de nervos por parte do fechamento precoce das suturas (COHEN JR.; MACLEAN, 2000), em contraste com as formas sindrômicas, onde a craniossinostose ocorre associada a outros defeitos primários de morfogênese. Na prática, esta distinção é menos clara, particularmente no período neonatal ou mesmo durante os primeiros anos da infância. Isso ocorre porque alguns dos sinais clínicos são difíceis de serem diagnosticados logo ao nascimento, enquanto outros podem surgir mais tardiamente. Estima-se ainda, que uma proporção dos casos não sindrômicos na verdade represente formas subclínicas de casos sindrômicos, o que tem sido demonstrado por estudos moleculares (PASSOS-BUENO et al., 2008).

A grande maioria dos casos de craniossinostose não sindrômica são únicos na família. Possivelmente se trata de um grupo de várias doenças, envolvendo algumas com padrão de herança monogênico - dominante ou recessivo, e ainda outras com padrão de herança multifatorial, onde os fatores genéticos e ambientais contribuem para a ocorrência da malformação. O risco de recorrência em famílias que tiveram uma primeira criança com

sinostose da sutura metópica ou sagital é relativamente baixo (menor que 10%), por outro lado, observa-se uma maior recorrência familial (estimada em 14%) quando a criança afetada apresenta sinostose das suturas coronais.

As craniossinostoses sindrômicas são formas geralmente graves onde outros defeitos no desenvolvimento acompanham a fusão prematura das suturas. Há pelo menos 150 síndromes onde uma das principais características clínicas é a sinostose de pelo menos uma sutura craniana(PASSOS-BUENO et al., 2008). As formas mais frequentes e conhecidas são as síndromes de Apert, Crouzon, Pfeiffer, Saethre-Chotzen, Muenke, displasia craniofrontonasal além de formas sindrômicas com mutações em *TCF12*. Há algumas formas raras clinicamente e geneticamente bem delineadas, como as síndromes de Carpenter, Beare-Stevenson, Crouzon com Acanthosis Nigricans; porém, a grande maioria se refere a relatos de poucos casos clínicos e cuja variabilidade clínica e mecanismo genético ainda não estão bem caracterizados.

A embriologia do crânio e das suturas

A origem embriológica do crânio é mista, com tecidos provenientes da crista neural e da mesoderme (Figura 1B)(JIANG et al., 2002). A origem dos ossos cranianos foi investigada utilizando camundongos Wnt1-Cre/R26R, de maneira a distinguir quais tecidos eram de origem de crista neural. O viscerocrânio é derivado de crista neural, com origem nos três primeiros arcos branquiais, enquanto o neurocrânio tem, em sua maior parte origem mesenquimal, exceto os ossos frontais, esfenoide e temporais, que tem origem na crista neural.

As suturas crânianas também tem origem na crista neural e mesoderme, no entanto as suturas tem origens opostas aos ossos adjacentes, tendo a coronal origem mesodérmica e a sagital origem na crista neural. A exceção a essa regra é a sutura metópica que tem origem de crista neural tal qual os ossos frontais, o que pode explicar seu fechamento precoce no crânio humano. As células que formam as suturas coronais primeiramente se organizam na região supra orbital, entre E9,5 e E11,5 (DECKELBAUM et al., 2012). Nesse sítio, localizado acima do olho em formação, se juntam células provenientes da crista neural e do mesoderme, que futuramente darão origem aos ossos frontais e parietais, e uma população de origem da

mesoderme paraxial que cria uma barreira entre essas populações. Mantendo essa organização, essas células migram apicalmente pela barreira telencefálica-diencefálica de maneira coordenada com o crescimento do encéfalo. Na sutura coronal definitiva ainda é possível se observar células filhas dessa população.

As principais vias que controlam o desenvolvimento das suturas

O desenvolvimento das suturas é influenciado tanto por fatores extrínsecos quanto fatores intrínsecos. As forças mecânicas agindo sobre o crânio são os principais fatores extrínsecos do desenvolvimento sutural, forças essas que podem ser geradas tanto por fatores externos quanto pelo crescimento do encéfalo. A relação entre o crescimento do encéfalo e craniossinostose é complexa e ainda pouco estudada, sabe-se que microcefalia é um fator de risco para craniossinostoses, no entanto a maior parte dos indivíduos com microcefalia não têm fechamento precoce de suturas(WILKIE et al., 2010). Forças mecânicas externas também podem causar craniossinostose, dados epidemiológicos mostram um maior risco de craniossinostose não sindrômica e de sutura única em gravidez múltipla, nascimento prematuro e peso alto ao nascimento.

Os fatores intrínsecos que levam ao fechamento precoce da sutura se referem a alterações no controle interno de crescimento e diferenciação celular da própria sutura. Os fatores intrínsecos podem ser subdivididos em cinco principais etapas da formação do complexo sutural: Migração das células tronco, comprometimento de linhagem, formação de barreira, controle do balanço entre diferenciação osteogênica e proliferação; e, por fim reabsorção e homeostase óssea. (TWIGG; WILKIE, 2015a).

Primariamente, as células que irão migrar da mesoderme paraxial para a região supra orbital expressam Gli1, um marcador de sinalização hedgehog (HH), de maneira transiente. Uma vez que migraram para a região supra orbital, dois processos simultâneos têm o início: o comprometimento das células mesenquimais com a linhagem osteogênica e a formação das barreiras entre os diferentes componentes da sutura. O processo de diferenciação é controlado pelos fatores de transcrição EN1, MSX2 e TWIST1, expressos nas células da região supra orbital, que por sua vez regulam direta e indiretamente a expressão de membros das famílias WNT, BMP e FGF que atuam no início da diferenciação osteogênica comprometendo as células

mesenquimais com esse destino, culminando na expressão de RUNX2 e SP7, os principais reguladores do processo de ossificação.

Simultaneamente, as células na região supra orbital de diferentes origens expressam membros das famílias EPH/EPHRIN e JAGGED/NOTCH. A família EPH/EPHRIN, a maior família de receptores tirosina cinase, regula a formação de barreiras entre tecidos por contatos célula a célula. Em geral, células que expressam o receptor EPHRIN são repelidas por células que expressam o ligante EPH com afinidade pelo respectivo receptor. Funcionalmente, esse processo ocorre pela capacidade de EPH/EPHRIN reorganizarem o citoesqueleto e, portanto, alterarem a morfologia e migração celular (KLEIN et al., 2012). Já a via NOTCH/JAGGED atua alterando a expressão gênica, uma vez que NOTCH é um receptor transmembrana que, quando ativado, cliva sua porção intracelular que migra da membrana para o núcleo e então atua como regulador de expressão de WNT e BMPs (HORI et al., 2013). A expressão desses genes leva a manutenção das células de diferentes origens que irão compor o complexo sutural da sutura coronal enquanto se organizam na região supra orbital e enquanto migram para o local da sutura.

Uma vez estabelecidas as células que participarão da formação inicial dos ossos e da sutura, é necessário que as mesmas continuem proliferando para haver crescimento ósseo no crânio. Inicialmente, como dito anteriormente, as células do mesênquima paraxial expressam Gli1(ZHAO et al., 2015), um marcador da expressão de IHH e SHH, SHH é necessário para a migração das células do mesênquima paraxial no início da embriogênese da sutura, e rapidamente perde o efeito sobre essas células. IHH atua no complexo sutural já estabelecido, e é responsável pelo recrutamento de progenitores mesenquimais do centro da sutura para a porção calcificada, aumentando assim o tamanho do osso craniano. Para a expansão da caixa craniana ocorrer de maneira sustentável, é necessário que esse recrutamento seja finamente coordenado com a proliferação das células indiferenciadas do mesênquima sutural. Dessa maneira, genes que atuam na proliferação agem de maneira antagônica à genes que atuam na diferenciação dessas células. É o caso de *TWIST1*, expresso no mesênquima sutural e *RUNX2*, *TWIST1*(JOHNSON et al., 2000a) tem efeito inibitório sobre RUNX2(KRONENBERG et al., 2004), impedindo que a expressão deste ossifique prematuramente o mesênquima sutural. *TCF12*, cuja proteína interage com TWIST1 também regula a ossificação do mesênquima sutural(SHARMA et al., 2013).

As moléculas da família FGF participam da regulação do equilíbrio entre proliferação e diferenciação (LEMMON; SCHLESSINGER, 2010; ORNITZ, 2000; YEH et al., 2011). Os ligantes dessas moléculas, os FGFRs, têm afinidade específica por diferentes ligantes, dessa maneira, FGFs específicos só têm ação sobre células que expressem os receptores que a ele se

ligam(GREEN; WALSH; DOHERTY, 1996; MOHAMMADI; OLSEN; IBRAHIMI, 2005). O osteóide, a matriz de colágeno não mineralizada feita por osteoblastos, participa do processo de diferenciação secretando moléculas como FGF2, FGF9, FGF10 e FGF18(HARADA et al., 2009; LAZARUS et al., 2007; YANG et al., 2008a), que atuam promovendo a diferenciação osteogênica das células mesenquimais. A secreção desses ligantes atua promovendo a troca do perfil de expressão dos osteoblastos. Osteoblastos menos diferenciados e com um perfil de rápida proliferação expressam FGFR2, os FGFs liberados pelo osteóide promovem a diminuição da expressão do *FGFR2* e o aumento da expressão de *FGFR1*, o que faz com que os osteoblastos se comprometam mais com a linhagem osteogênica. Além do osteóide, a dura mater também promove a proliferação com a liberação de fatores de crescimento como FGF2, BMP4 e TGFB1 (LEVI et al., 2012). Além da ação de fatores de crescimento na diferenciação osteogênica, também há evidências da participação da estereidogenese. Mutações em POR e em CYP26B1 (FLÜCK et al., 2004), ambos ligados a atividade de enzimas de P450, levam à craniossinostose, embora ainda não se saiba ao certo como ocorre esse processo.

A sutura estabelecida apresenta um estado de equilíbrio dinâmico entre proliferação e diferenciação, dessa maneira, genes que interfiram no processo de reabsorção e homeostase óssea podem interferir na manutenção de quantidades adequadas de tecido mineralizado na sutura. Um dos genes participantes nesse processo é IL11RA (NIEMINEN et al., 2011), gene que participa do processo de diferenciação dos osteoclastos, células responsáveis pela reabsorção óssea. Mutações do tipo perda de função em IL11RA causam craniossinostose ao diminuir a quantidade de osteoclastos funcionais, o que leva a diminuição da reabsorção óssea e alterando o equilíbrio do complexo sutural. Outro gene participante no processo de homeostase do complexo sutural é FAM20C, uma proteína cinase com afinidade por membros da família SIBLING como OPN, DPP1 e DMP1(SIMPSON et al., 2007a; WANG et al., 2012), moléculas que regulam a mineralização do tecido ósseo. A fosforilação das proteínas SIBLINGS é essencial para a sua atividade como reguladoras da mineralização óssea, prova disso é que mutações de perda de função em FAM20C levam a síndrome de Raine, uma osteoesclerose com uma série de defeitos esqueléticos incluindo, em alguns casos, craniossinostose. No entanto, apesar do avanço considerável no entendimento da patofisiologia das craniossinostoses, existem muitas questões em aberto, tal qual como os diferentes FGFs atuam no equilíbrio do complexo sutural.

A genética das craniossinostoses

Devido ao grande número de processos e genes envolvidos na embriologia e na manutenção do equilíbrio dinâmico do complexo sutural, como esperado, um grande número de mutações em genes que participem direta ou indiretamente desse processo leva ao fechamento prematuro das suturas cranianas (Tabela I). Ao todo, no momento foram identificados 57 genes com mutações que causem craniossinostose como *FGFR1*, *FGFR2* e *FGFR3* (Síndromes de Apert, Crouzon, Pfeiffer, Muenke e Baller-Gerold), *TWIST1* (Síndrome de Saethre-Chotzen), *ERF*, *TCF12*, *IL11RA* e *TGFBR1*(TWIGG; WILKIE, 2015a). De todas as síndromes com genes associados, trinta e sete têm herança autossômica dominante, dezoito são autossômicas recessivas, uma tem herança ligado ao X dominante e uma ligada ao X recessiva(HEUZÉ et al., 2014b). Embora um grande número de loci já tenha sido associado às craniossinostoses, 76% de todos os casos ainda não tem um diagnóstico molecular definitivo, especialmente entre as formas não sindrômicas. Mutações muito raras nos genes *FGFR2, TWIST1, FREM1, LRT3, EFNA4* e duplicações de *RUNX2* foram descritas em alguns poucos pacientes com craniossinostose não sindrômica, a grande maioria associada a sinostose de suturas coronais (JOHNSON et al., 2000b; JUSTICE et al., 2012; MEFFORD et al., 2010; MERRILL et al., 2006; SETO et al., 2007; VISSERS et al., 2011; WILKIE et al., 2007) Estudos de associação sugeriram que marcadores próximos aos genes BMP2 e BBS9 conferem risco de susceptibilidade para sinostose de sutura sagital não sindrômica, neste caso considerou-se o modelo de herança multifatorial (JUSTICE et al., 2012).

Tabela I: Principais genes associados às craniossinostoses e suas síndromes. Adaptado de HEUZÉ et al., 2014; TWIGG; WILKIE, 2015

Gene	Sindrome/ Fenótipo
ABCC9	Síndrome de Cantu
ALPL	Hipofosfatasia tipo infantil
ALX4	Craniossinostose não sindrômica
CD96	Trigonocefalia de Optiz
CHST3	Síndrome de Larsen autossômica recessiva
CYP26B1	Craniossinostose com fusão radiohumeral
EFNA4	Craniossinostose coronal não sindrômica
EFNB1	Síndrome Craniofrontonasal
ERF	Craniossinostose complexa, sinostose sagital ou lambdoide não sindromica
FAM20C	Síndrome de Raine
FBN1	Síndrome de Shprintzen–Goldberg
FGF3,	Craniossinostoses múltiplas sindrômicas
FGF4	
FGFR1	Displasia osteoglofnônica ; Síndrome de Pfeifer, Trigonocefalia, Craniossinostose metópica
FGFR2	Síndrome de Antley-Bixler sem anomalias genitais; Síndrome de Apert, Síndrome de Baere-Stevenson,

	Displasia “Bent-Bones”, Síndrome de Crouzon, Síndrome de Jackson-Weiss, Síndrome de Pfeifer
FGFR3	Síndrome Crouzon dermoesqueletal, Síndrome de Muenke, Craniossinostose coronal não sindrômica, Displasia tanatofórica tipo II
FREM1	Trigonocefalia não sindrômica
GLI3	Síndrome de Greig com cefalopolisindactilia
GPC3	Síndrome de Simpson–Golabi–Behmel
IFT122	Displasia cranioectodermal 1
IFT43	Displasia cranioectodermal 3
IGF1R	Craniossinostoses de sutura única
IHH	Craniossinostose e sindactilia
IL11RA	Síndrome da craniossinostose e anomalias dentais
JAGGED1	Síndrome de Alagille
LMX1B	Síndrome da Unha–patela
LRIT3	Sinostose sagital não sindrômica
MEGF8	Síndrome de Carpenter
MSX2	Craniossinostose Boston-type
OSTM1	Osteopetrose infantil, craniosinostose, malformação de Chiari
POR	Síndrome de POR com anomalias genitais
RAB23	Síndrome de Carpenter
RECQL4	Síndrome de Bailer–Gerold
RUNX2	Craniossinostose não sindrômica
SH3PXD2B	Síndrome de Frank–ter Haar
SKI	Síndrome de Shprintzen–Goldberg
SOX6	Disostose craniofacial
TCF12	Craniossinostose Bicoronal
TGFBR1	Loeys–Dietz tipo 1
TGFBR2	Loeys–Dietz tipo 2
TWIST1	Síndrome de Saethre–Chotzen, Craniossinostose coronal ou sagital não sindrômica
WDR19	Displasia cranioectodermal 4
WDR35	Displasia cranioectodermal 2
ZEB2	Síndrome de Mowat–Wilson com craniosinostose
ZIC1	Craniossinostose associada a ZIC1
HUWE1	-

Etiologia molecular das craniossinostoses sindrômicas mais comuns.

Síndrome de Apert

Cerca de 98% dos casos de síndrome de Apert é causada pelas mutações p.S252W (66%) ou p.P253R (32%), em *FGFR2*(WILKIE et al., 1995), que é uma proteína localizada na membrana celular capaz de regular vários processos celulares, como proliferação, migração e diferenciação celular. O FGFR2 se caracteriza por uma região extracelular que interage com os seus ligantes (domínios semelhantes a imunoglobulinas, IgI, IgII e IgIII), uma região que atravessa a membrana plasmática (transmembrana) e dois domínios tirosina cinase na porção citoplasmática da célula (TK1 e TK2). As mutações, localizadas entre as alças IgII e IgIII do receptor, consideradas como do tipo ganho de função, causam o aumento da afinidade de FGFR2 por seus ligantes (FGFs), de forma que tornam possível a ativação do receptor por outros FGFs que naturalmente não tem afinidade pela forma selvagem de FGFR2 (IBRAHIMI et al., 2004) . Duas outras mutações de ganho de função em FGFR2 (c.755_756CG->TT/ p.Ser252Phe e c.940-2A->G) foram também associadas à síndrome de Apert, porém são muito raras (LAJEUNIE et al., 1999; OLDRIDGE et al., 1999; PASSOS-BUENO et al., 1997). Há pouca variabilidade do quadro clínico entre os pacientes com síndrome de Apert, sendo que a mutação p.S252W está mais associada a ocorrência de fissura palatina, porém a uma menor gravidade da sindactilia dos membros (SLANEY et al., 1996). A penetrância da doença é completa e não há heterogeneidade genética de loco, ou seja, todos os casos de síndrome de Apert são causados por mutações em FGFR2, as quais são geralmente *de novo* e todas de origem paterna. Somente os afetados pela síndrome tem risco alto (50%) de virem a ter descendentes com síndrome de Apert.

Síndrome de Crouzon

Várias dezenas de mutações em *FGFR2*, a grande maioria localizada na alça IgIII da proteína codificado por este gene, já foram descritas como causativas da síndrome de Crouzon . As mutações que causam Crouzon, são também do tipo ganho de função, e ativam constitutivamente o receptor, fazendo com que a transdução do sinal ocorra independentemente da ligação com FGF (FRIESEL, 1995; GALVIN et al., 1996). Embora haja uma grande variedade de mutações descritas, as mais prevalentes são p.C342Y (16% das mutações encontradas) e p.C278F (14,5%). O quadro clinico da síndrome de Crouzon causada por mutações em FGFR2 é bastante variável, havendo pacientes que nunca precisaram ser submetidos a procedimentos cirúrgicos. A penetrancia da síndrome de Crouzon é completa,

contudo, a expressividade clínica da doença é variável. Ainda, há heterogeneidade genética de loco, ou seja, uma proporção de casos é causada por mutações em outros genes

Síndrome de Pfeiffer

A síndrome de Pfeiffer, que inclui pacientes anteriormente classificados como Jackson-Weiss, pode ocorrer por mutações nos genes FGFR1 (<10% dos casos) e FGFR2. Em FGFR1, um outro parálogo de FGFR2, apenas a mutação na posição p.P252R localizada entre as alças IgII e IgIII da proteína foi descrita. Em FGFR2, existem várias diferentes mutações causativas da síndrome de Pfeiffer, a grande maioria localizada na alça IgIII (PASSOS-BUENO et al., 2008). As mutações p.Trp290Cys, p.Ser351Cys e p.Tyr340Cys são preditivas da gravidade do quadro clinico, estando associados apenas a formas mais graves de Pffeifer, ou Pffeifer tipos 2 e 3 (LAJEUNIE et al., 2006; NAZZARO et al., 2004; OLIVEIRA et al., 2006; TARTAGLIA et al., 1997) . Porém a grande maioria das mutações não apresenta uma correlação com a variabilidade clínica da síndrome de Pfeiffer e uma grande proporção destas mutações também estão associadas a síndrome de Crouzon. Apesar da penetrância da doença ser completa, há um grande espectro de variabilidade do quadro clinico, onde as formas mais graves apresentam sinostoses de múltiplas suturas dentre outras alterações craniofaciais e de membros.

Síndrome de Muenke

O mecanismo genético responsável por esta síndrome é a mutação p.P250R, no gene FGFR3, um outro parálogo de FGFR2, com uma estrutura de domínios funcionais muito semelhante. A síndrome de Muenke, recentemente caracterizada, é a forma mais comum das craniossinostoses sindrômicas, correspondendo a cerca de 6-8% de todos os casos de craniossinostose. Caracteriza-se por uma ampla variabilidade clínica, com envolvimento da sinostose coronal uni ou bilateral; contudo, uma proporção alta de portadores da mutação (cerca de 20%) não apresentam sinostose das suturas. As características faciais variam de normais a dismórficas, e nestes casos apresentam sobreposição clínica com o da síndrome de Saethre-Chotzen ou Crouzon. Uma complicação frequente é a perda da audição de baixa frequência, que uma vez identificada pode auxiliar no diagnostico diferencial entre os vários possíveis diagnósticos clínicos (MORRISS-KAY; WILKIE, 2005; WILKIE et al., 2010)

Saethre-Chotzen

A grande maioria dos casos de síndrome de Saethre-Chotzen é causada por mutações no gene TWIST1, que é um fator de transcrição da classe basic helix-loop-helix (bHLH) (PAN et al., 2009). As mutações causativas da síndrome de Saethre-Chotzen podem ser de diversos tipos, tais como pequenas variantes da sequência do DNA, pequenas deleções ou até mesmo deleções maiores

envolvendo o gene TWIST1. Todas estas alterações levam a perda de função do TWIST1, de forma que haploinsuficiência (insuficiência) da proteína TWIST1 é o mecanismo causativo desta síndrome (JOHNSON; WILKIE, 2011). O quadro clínico é extremamente variável, e não raro observa-se penetrância incompleta da craniossinostose. Não existe correlações entre os tipos de mutação e o fenótipo.

Displasia Craniofrontonasal

Cerca de 95% dos casos é determinada por mutações no gene EFNB1, que codifica a proteína efrina-B1. Esta proteína está envolvida em reconhecimento celular, de forma que células que expressam esta proteína tendem a se agregar. Há diversos tipos de mutações, e todas levam a perda de função da proteína. A displasia craniofrontonasal é uma forma ligada ao X, onde, diferentemente do que normalmente ocorre em doenças ligadas ao X, os casos mais graves são as mulheres heterozigotas, e não os homens, neste caso chamados de hemizigotos, portadores da mutação em EFNB1. Uma das explicações propostas para esse fenômeno é que devido ao processo de compensação de dose, no qual um dos cromossomos X de cada célula das mulheres é inativado, se cria um mosaico de células expressando ou não EFNB1, o que se supõe que interfere no processo de delimitação dos tecidos durante a embriogênese. Por outro lado, nos homens hemizigotos para a mutação, nenhuma das células expressa a forma selvagem de EFNB1, o que é compensado por outros receptores e ligantes da família das efrinas (TWIGG et al., 2006; WIELAND et al., 2004). Mais recentemente, foram identificados meninos com quadro típico da síndrome, incluindo craniossinostose de sutura coronal. Demonstrou-se que o quadro mais grave presente nestes meninos é decorrente de mosaicismo somático, ou seja, eles são portadores de duas linhagens celulares, uma normal e outra com mutação no gene EFNB1, de forma a simular o que acontece nas meninas (TWIGG et al., 2006).

Questões não respondidas

A genética e a etiologia molecular das craniossinostoses, embora profundamente estudadas, explicam apenas uma pequena parcela dos casos de craniossinostose. Acredita-se que boa parte dos casos não explicados sejam devidos a mutações *de novo* em famílias com casos únicos ou a mutações raras em loci não previamente associados às craniossinostoses. O estudo desses casos, até então inviável, hoje se torna possível pelo advento de tecnologias de sequenciamento em larga escala, conhecidas coletivamente como *Next Generation Sequencing* (NGS). Usando esse

tipo de abordagem, outros grupos foram bem-sucedidos em detectar novos loci associados às craniossinostoses como *TCF12* e *ERF*.

A importância de se conhecer melhor a etiologia molecular das craniossinostoses fica clara na ausência de possíveis tratamentos que atuem de forma paralela ou mesmo substituam a intervenção cirúrgica, hoje o único tratamento disponível. Além da aplicação direta do conhecimento sobre as causas genéticas nas diferentes síndromes no aconselhamento genético das famílias, o melhor entendimento dos processos que levam ao fechamento precoce das suturas é essencial para a perspectiva de alternativas não cirúrgicas de tratamento. Para tal, deve-se conhecer desde os loci envolvidos como os mecanismos moleculares que levam à patologia, fazendo essencial o estudo funcional das craniossinostoses sindrômicas mais comuns como a síndrome de Apert. Hoje ainda temos aberta a questão do efeito da ação dos ligantes não específicos sobre as células tronco mesenquimais que compõem a sutura portadora da mutação p.S252W em FGFR2.

Por fim, síndromes raras de expressividade variável da craniossinostose são frequentemente desconsideradas ao se estudar o processo de fechamento da sutura O estudo dessas pode levar à um melhor entendimento de fatores genéticos e ambientais que possam predispor ao fechamento da sutura.

Objetivos

Nesse trabalho trabalhamos com duas hipóteses distintas: Que as mutações causativas de casos raros de craniossinostose e casos únicos podem ser elucidados pelo sequenciamento do exoma; e, que as células da sutura de pacientes com Síndrome de Apert reagem de maneira diferente aos ligantes não específicos às quais ganharam afinidade.

Para isso traçamos os seguintes objetivos:

I) Para melhor entender a etiologia das craniossinostoses pretendemos nesse trabalho utilizar sequenciamento de larga escala para estudar casos familiais raros sem diagnóstico molecular definido.

II) Estudar os efeitos de ligantes não específicos sobre células tronco mesenquimais e fibroblastos provenientes da sutura de pacientes com síndrome de Apert.

I. Craniosynostosis in Raine syndrome: Is there a genotype and phenotype correlation?

Atique, R; Bertola, B; Rocha, K; Ezquina, S; Yamamoto, G; Faria, MEJ; Valente, M; Passos-Bueno, MR.

Abstract

Raine syndrome is a rare autosomal recessive disease caused by Loss of Function mutations in *FAM20C* that causes increased ossification, intracranial calcifications, craniofacial dysmorphisms and amelogenesis defects and in some cases perinatal death occurs. Craniosynostosis has been reported in less than 20% of the cases and the suture involved varies. Here we describe two novel apparently unrelated cases with the p.P496L mutation and present a review of the literature pertaining to the described mutations and the presence of craniosynostosis. Our analysis suggests that some missense mutations in *FAM20C* are more likely to result in premature fusion of the cranial sutures.

Resumo

A síndrome de Raine é uma doença autossômica recessiva rara causada por mutações do tipo perda de função no gene *FAM20C* que casa aumento da ossificação, calcificações intracranianas, dismorfismos craniofaciais e defeitos na amelogênese, e, em alguns casos, pode levar à morte no período perinatal. Craniossinostose foi reportada em menos de 20% dos casos e afeta diferentes suturas. Nesse trabalho nós descrevemos dois novos casos sem relação familiar com a

mutação p.P496L e apresentamos uma revisão da literatura com enfoque nas mutações já descritas e a presença de craniossinostose. Nossa análise sugere que certas mutações em *FAM20C* têm maior chance de resultar na fusão prematura das suturas cranianas.

Introduction

Raine syndrome (RS) is a rare autosomal recessive disease, with an estimated prevalence of < 1/1,000,000, with 41 cases so far characterized (Seidhahmed et al., 2015). A variety of alleles, mostly missense changes, in *FAM20C*have been shown to explain the RS phenotype in most of these cases (SIMPSON et al., 2007a). Affected individuals present craniofacial dysplasia, midfacial hypoplasia, short stature, abnormal teeth, enamel defects, intracranial calcifications, overall increased bone density, narrow forehead, proptosis and periosteal bone formation(FAUNDES; CASTILLO-TAUCHER, 2014)(KAN; KOZLOWSKI, 1992b).Up until 2009 all reported cases were stillborn or died perinatally due to respiratory deficiency. However, after the first report of non-lethal cases of Raine syndrome by Simpson et al, 2009,several other cases have since been reported. It is still unclear if there is any correlation between genotype and clinical severity and variability.

Craniosynostosis, early closure of the cranial sutures, was only reported in 4 cases so far(ACEVEDO; POULTER, 2015; CHITAYAT et al., 2007; SIMPSON et al., 2007a), however, there is evidence of early closure of cranial sutures, such as altered skull morphology, in approximately 40% of the cases, of the affected individuals in both lethal and non-lethal cases (table I). Suture agenesis has also been reported, in some cases, with wide fontanelles. Presence of craniosynostosis in Raine syndrome patients has not yet been linked to specific genotypes or environmental factors, mostly due to the small number of cases reported and the allelic heterogeneity of the syndrome. Therefore, description of novel cases is essential to delineate

the phenotypic variability in addition to better characterize the molecular pathogenicity of Raine syndrome.

In this paper we present two novel unrelated cases of Raine syndrome bearing the p.P496L in *FAM20C* mutation. Based on our patients and the review of the literature we discuss the possibility of phenotype/genotype correlation between the FAM20Cmutations and craniosynostosis.

Methods

DNA Preparation

DNA was purified from peripheral blood (according to standard protocols) or saliva (collected with Oragene® saliva collection kits OG-500 and OG-575; DNA GenotekInc, Ottawa, Canada), following manufacturer's instructions.

Library Construction and Exome Sequencing

Library preparation and exome capture were performed with Nextera Rapid Capture Exome. Library quantification was performed with KAPA Library Quantification kit (KAPA Biosystems), through real-time quantitative PCR. Paired-end sequencing was performed on a HiScanSQ (Illumina)

Exome Data Processing

Sequences were aligned to the hg19 reference genome with Burrows-Wheller Aligner (BWA; http://bio-bwa.sourceforge.net). Genome indexing, realignment of reads and duplicate removal were performed with Picard (http://broadinstitute.github.io/picard/). Variants were then called using Genome Analysis Toolkit package (GATK; https://www.broadinstitute.org/gatk/), and subsequently annotated with ANNOVAR (http://www.openbioinformatics.org/annovar/).

Variant Filtering

We applied a "frequency filter", to exclude variants with minor allele frequency (MAF) > 0.1% in public databases (1000 Genomes Project (1kGP; Abecasis et al., 2012), NHLBI Exome Sequencing Project (ESP6500; http://evs.gs.washington.edu/EVS/), Exome Aggregation Consortium (ExAC; http://exac.broadinstitute.org/)). To account for local polymorphisms, we also used our in-house

database (CEGH60+, a collection of exome sequencing data of 609 elderly Brazilians from the biobank of the Centro de Pesquisa sobre o Genoma Humano e Células Tronco, coordinated by M. Zatz), and additional exomes of patients affected by unrelated conditions sequenced in our core facility.

To avoid false positive calls, we applied a "quality filter", that removed variants with low quality (minimum GATK quality score threshold fixed as 30), low coverage (<10x), and displaying allelic imbalance greater than 75:25. Synonymous variants or variants located in hypervariable genes (Fuentes Fajardo et al., 2012) were also removed from further analysis. Due to consanguinity of the parents of Family 1 we further refined the search for homozygous mutations.

Variant Validation

Variants classified as best candidates were visually inspected using Integrative Genomics Viewer (IGV) software (Broad Institute of MIT and Harvard). Sanger sequencing was used for variant validation and, whenever appropriate, for mutation screening in additional relatives. PCR primers were designed with Primer Designing Tool web interface (NCBI). The primers used were: Forward sequence: TTCTGGAAGGTTTGGGAAGTAT, reverse sequence: AATTCAGGGCTGTGGTTGAAT. PCR products were sequenced with ABI 3730 DNA Analyzer (Applied Biosystems), and sequences were visualized using Sequencher® 5.2 analysis software (Gene Codes).

Statistical Analysis

The groups were compared for enrichment using Fisher's Exact Test using the QuickCalcs tool available at http://graphpad.com/quickcalcs/contingency2.

Results

Case reports and genomic data

Family 1

The index, female, was first evaluated at 7 years old. Parents are healthy first cousins. The patient was delivered via caesarian at 38weeksofgestation and hipotonia was noted at the time of birth.

Early closure of the metopic and sagittal sutures was disclosed at 5 years of age. The propositus was diagnosed with syndromic craniosynostosis and referred for genetic evaluation.

On physical examination at 7 years old the child showed facial dysmorphism (Fig. 1) with frontal bossing, proptosis, midface hypoplasia, depressed nasal bridge, low-set ears, teeth with enamel defects, and, clinodactyly. Brain CT scans showed multiple bilateral intracranial calcifications in the basal ganglia, and in the periventricular and subependymal regions

Assuming an autosomal recessive pattern of inheritance as the most likely, we have filtered the variants from whole exome sequencing (WES) for homozygous variants, and it was revealed the c.C1487T; p.P496L mutation in both alleles of FAM20C. This result was later confirmed by Sanger sequencing. The p.P496L mutation is localized within CR3 and close to two highly conserved cysteines (according to Tagliabracci et al, 2012) within the FAM family.

Family 2

The index is a 6 years old female, second child of healthy, unrelated parents. The patient was born at 38 weeks, with a birth weight of 4150g. The child was evaluated at 6 years old and showed craniofacial anomalies including frontal bossing, midfacial hypoplasia, bitemporal narrowing, ocular proptosis, and enamel defects, the mother reported tooth loss since the first year of life and yellowish coloration. She presented with recurrent abscesses and pulpal necrosis. Dental evaluation disclosed hypoplastic enamel. She evolved with recurrent seizures since the age of 2 years, requiring antiepileptic drugs until the age of 6. Her milestones were normal, but she presents learning disability. She was evaluated periodically for abnormalities in bone metabolism and serum levels of calcium and phosphorus were normal until the age of 6 years of age, but at the age of 9 years of age, serum levels of phosphorus have shown low levels, ranging from 2.5mg/dL to 2.9mg/dL (NV: 4.50-5.50mg/dL). Skeletal survey showed short clavicles, scoliosis and ivory epiphysis in hands and feet, CT scans revealed bilateral and multiple intracranial calcifications similar to the ones observed in patient 1, but no premature suture closure, only radiographic signs of metopic ridge and ortophantogram revealed early loss of deciduous teeth and vertical maxillary deficiency. Raine Syndrome diagnosis was proposed.

Sanger sequencing of *FAM20C* revealed the c.1487C>T; p.P496L mutation in both alleles.

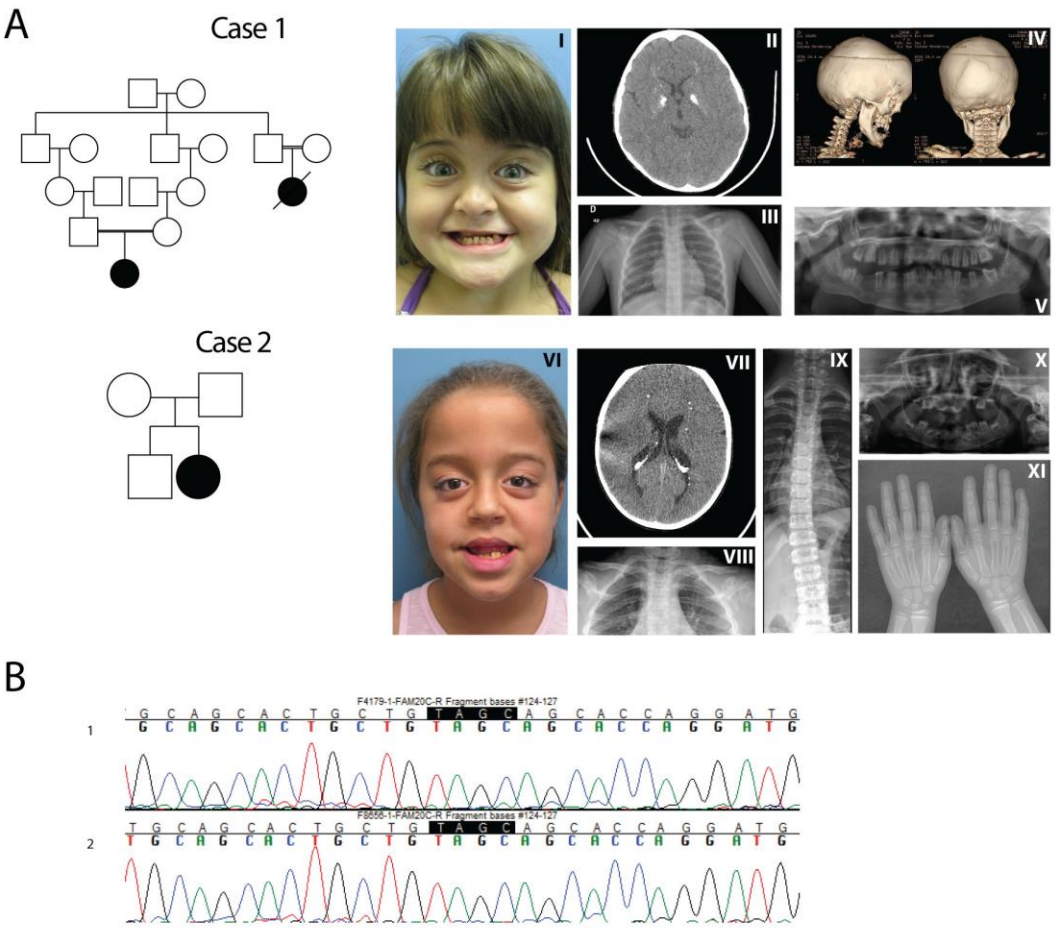

Figure 1: A) Pedigrees, facial defects(I and VI), CT scans(II, IV and VII), radiographs (III, VIII, IX and XI) and orthopantomogram (V and X) highlighting the clinical features of patients 1 and 2. Patient 1 exhibits premature sagittal closure, and hand, , thorax and spine X-rays showing ivory epiphyses in the hands, short clavicles and scoliosis in patient 2. Orthopantomogram: patient 1 (8yo): enlarged pulp chambers, enamel hypoplasia and vertical maxillary deficiency; patient 2 (6 yo): Early loss of deciduous teeth and vertical maxillary deficiency) c.1487C>T; p.P496L mutation detected by sanger sequencing in both patients (reverse strand sequence shown here).

Variants in FAM20C: review of the literature

Diagnosis of craniosynostosis can only be done by radiography or preferably by tomography. Only 25 out of the 38 cases so far reported in the literature meet this diagnosis criteria, however head shape, an indirect consequence of premature suture closure, is described in all but 6 of the published cases. Therefore, we divided our analysis into direct evidence of craniosynostosis (with documented radiography or tomography analysis) and indirect evidence (with only head shape description).

For this analysis, only cases with a full clinical description were included and 3 of the 38 previously reported were excluded due to lack of published clinical data. As summarized in Table

I, among the thirty-five reviewed cases, four had direct evidence of craniosynostosis. Nineteen cases were severely affected and were aborted or died within the first year of life, while the remaining eighteen cases were alive at the time of the reports. In twenty-five cases the suture closure status was described, of which four (15%) stated that at least one suture was prematurely closed. In two of the craniosynostosis cases reported the sagittal suture was closed, one reported coronal suture closure and one was unspecified. Of the four reported cases with craniosynostosis, two were lethal.

When considering both direct and indirect evidence of craniosynostosis, out of the eleven cases, five had evidence of sagittal suture closure, five reported evidence of coronal suture closure and one was unspecified. Of the eleven reported cases with suspected craniosynostosis, five were lethal, and four had coronal suture closure (one was unspecified). To verify the possibility of lethality and suture closure being related, we compared the frequency of cases that were lethal with CS (5), lethal without CS (12), not lethal with CS (6) and not lethal without CS (7), expecting that if there is no correlation of both manifestations in Raine syndrome patients, all groups should occur in equal proportion. Cases without the suture status description were not considered. The distribution of lethality and craniosynostosis was similarly distributed among the groups (P=0.45).

There are currently 18 different genomic variants associated with Raine syndrome in 24 individuals: 16 single nucleotide variants, of which 10 are reported in homozygosity and 6 were found in compound heterozygotes, one chromosome abnormality defined by a pseudodicentric chromosome 7, and one homozygous deletion of 7p22.3.

All mutations described so far are located within the CCD, the only domain in FAM20, and most of them in the kinase activity site of the protein (Figure 2)(TAGLIABRACCI et al., 2012). Four of the mutations are localized in the metal binding sites predicted by sequence similarity, two of them lethal. No mutations were found in the Signaling Peptide.

Of 11 cases with direct or indirect evidence of craniosynostosis, 8 had mutations identified, corresponding to 6 different single nucleotide variations and one chromosomal aberration. When considering patients with direct evidence of craniosynostosis only two mutations were found, p.P496L and 45, XY psudic (7;7) (p22;p22).

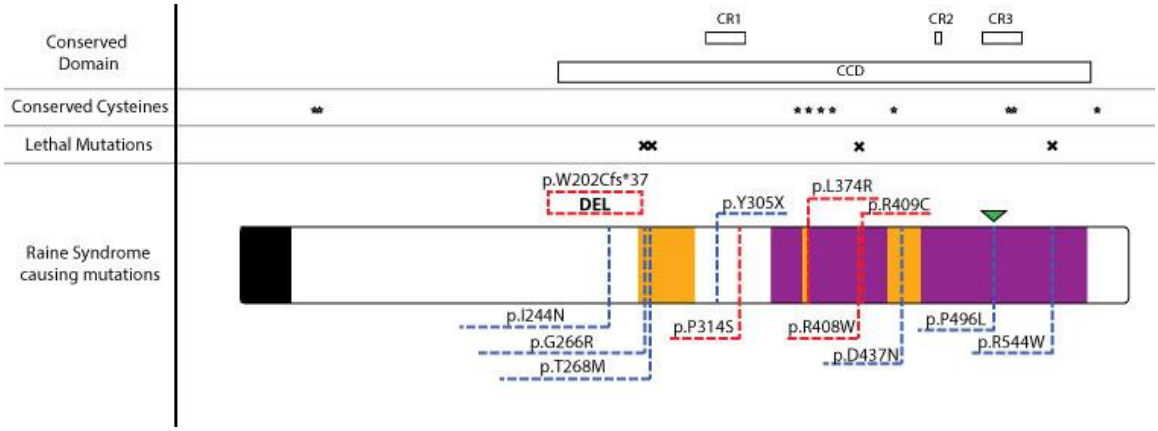

Figure 2: FAM20C protein with functional and conserved domains (Modified from Nalbant et al 2005) and distribution of the pathogenic variants so far associated with Raine syndrome. Dark yellow indicates the putative metal binding sites, purple indicates the kinase domain, black indicates the signaling peptide dashed lines indicate known single nucleotide mutations (blue: cases with evidence for craniosynostosis (direct or indirect); red: all cases with no evidence for craniosynostosis); Del indicates the frameshift deletion identified in case 1 from Acevedo et al, 2015, crosses indicate lethal mutations, stars indicate conserved cysteines. The green arrow indicates the p.P496L mutation described in this clinical report. Chromosomal aberrations involving the whole gene were not represented in this figure. CCD indicates the common conserved domain, CR1, CR2 and CR3 indicate the 3 conserved regions described by Nalbant et al, 2005.

Discussion

In this paper we present two unrelated cases of Raine syndrome harboring the p.P496L mutation. Both patients had similar non-lethal phenotypes, characterized by facial dysmoprhisms, enamel defects and intracranial calcifications. In addition, one of the patients also presented sagittal suture premature closure. The mutation p.P496L has been previously described in two siblings from a consanguineous marriage, who also have sagittal craniosynostosis and a similar non-lethal phenotype, thus suggesting that this mutation may be associated with a complete penetrance for the non-lethal phenotype(ACEVEDO; POULTER, 2015) and it is also commonly associated with sagittal synostosis. The novel cases reported here make p.P496L the mutation with the greater number of unrelated individuals so far reported. Interestingly, all cases are of Brazilian origin, thus possibly representing a founder effect of this variant. Indeed both families described in this paper were originally from the Ceará state, a northeast state with high inbreeding rates (BRITO et al., 2012).

One of the recurring features of Raine syndrome is craniosynostosis, present in approximately 16% of the cases (table I). The incidence of craniosynostosis in Raine syndrome (RS) has not been thoroughly studied yet and it is unknown if there is correlation between genotype and

penetrance of this phenotype. Several authors have described lethal RS cases with direct and indirect evidence of craniosynostosis(KINGSTON; FREEMAN; HALL, 1991; KOCHAR; CHOUDHARY; GADODIA, 2010; SIMPSON et al., 2007b), conversely 10 other cases of non-lethal RS with evidence of craniosynostosis have been published to date (table I). We did not find any evidence of correlation between lethality and therefore, the severity of the phenotype does not seem enough to explain the presence of craniosynostosis in the syndrome.

Pathogenic mutations in FAM20C are known to alter mineralization metabolism(KINOSHITA et al., 2014).FAM20C is part of the FAM family of secreted protein kinases, comprised of three members with high homology(ISHIKAWA et al., 2012). The FAM genes, contain only two domains, a signaling peptide responsible for the export of the protein to the extracellular matrix (ECM), and the CCD domain responsible for the ion binding and kinase activity. The CCD domain has 3 highly conserved regions named CR1-3 and 10 serines that are conserved in all isoforms in most species. It has been shown that Raine syndrome mutations, both missense and frameshift, decrease the kinase activity as well as the secretion of FAM20C[10].The impact of the p.P469L mutation in protein function is unknown, yet the localization within the kinase domain suggests that it impacts the ion binding or the phosphorylation capacity of the protein(Figure 2).

FAM20C phosphorylates proteins with the S-x-E motifs, including the SIBLING family of proteins, like OPN, DMP1 and DPP(TAGLIABRACCI et al., 2012). Osteopontin (OPN) has 7 phosphorylation residues, of which 6 are serines[11]. OPN phosphorylation is necessary for its function in bone remodeling[12]. OPN can both inhibit and promote tissue mineralization depending on its phosphorylation level, while dephosphorylated OPN has no effect on tissue mineralization, phosphorylated OPN inhibits mineralization(GERICKE et al., 2005). DMP1 and DPP phosphorylation is also necessary to bone remodeling, leading to the formation of highly organized mineralized collagen fibrils, similar to mineralized fibrils in bone and dentin(DESHPANDE; FANG; ZHANG, 2011). The sutural complex ECM structural elements are mainly COLI and COLIII(CARINCI et al., 2005), OPN is expressed in the adjacent bone, but not in the fibrous tissue of the suture. Therefore, due to FAM20C role in phosphorylation of SIBLING proteins, it must be a key protein in regulating the sutural complex mineralization.

One possible explanation to the incomplete penetrance of craniosynostosis in Raine syndrome is that different mutations in *FAM20C* might have variable impacts in protein function, leading to different phenotypes. If this hypothesis is true one would expect that the same mutation would cause the same phenotype. Indeed, the non-lethal phenotypes in RS with p.P496L variants were very similar. Further, seven mutations have been identified in more than one case, and, with the

exception of one case harboring p.P496L, all have so far been consistent about suture closure. It is thus possible that the presence of CS in Raine syndrome may be related to specific mutations, even though we cannot discard that that other loci or environmental factors might also influence the presence of CS.

Complete deletion or truncating the protein is not enough to cause craniosynostosis (cases 2 and 16, table 1). MA Simpson, 2007 described a lethal form caused by a pseudodicentric chromosome 7, resulting in the deletion of the 7p telomeric region that had evidence of premature closure of cranial sutures, however, as this chromosomal aberration involves FAM20C and 4 other loci, FLJ45445, which has an unclassified transcription discrepancy; LOC730345, LOC730346, and LOC651986, loci identified by *in silico* automated analysis and without any known function. We cannot rule out the possibility that the deletion of these loci are responsible for the craniosynostosis Pathogenic missense mutations in FAM20C seem to severely reduces the kinase activity of FAM20C (ISHIKAWA et al., 2012). In a compound heterozygote patient for missense variants in *FAM20C*, it was observed that while one of the mutations (p.I241N) resulted in undetectable levels of OPN phosphorylation, the other mutation (p.G261R) resulted in a tenfold reduction of kinase activity. All other 5 missense mutations analyzed had no detectable levels of kinase activity, also they were found in patients without confirmed craniosynostosis. Considering that complete deletion of *FAM20C* does not result in CS and that the compound heterozygous missense mutations analyzed preserved part of the kinase activity of FAM20C, it is possible that missense mutations that confer a less drastic reduction in FAM20C kinase activity are more likely to result in craniosynostosis.

In summary, we have found that there is no correlation between presence of cranioynostosis and lethality and the low penetrance for craniosynostosis in Raine syndrome may be related to the type and localization of the missense variant in *FAM20C*. Description of a larger number of cases combined with functional analysis of the variants will be important to validate this hypothesis.

Table I: Review of the literature of all cases of Raine syndrome regarding genomic variants, lethality, suture closure and number of cases

	Variant	Lethal < 1 year	craniosynostosis	Evidence for craniosynostosis	number of cases	Reference
Missense and Loss of Function						
	c.731 T>A (p.I244N) c.796 G>A (p.G266R)	no	scaphocephaly	skull morphology	1	(SIMPSON et al., 2009)
	c.784 + 5 g > c ; p.W202Cfs*37	no	no	CT scan	3	(ACEVEDO; POULTER, 2015)
	c.803 C > T, p.T268M	no	dolicocephaly	skull morphology	2	(RAFAELSEN; RÆDER; FAGERHEIM, 2013)
	c.914+5G>C / c.1404-1G>A	yes	no	NA	1	(SIMPSON et al., 2007a)
	c.940C>T p.P314S	no	no	X-ray	3	(KOOB et al., 2011)
	c.1093G>A p.G365R	yes	NA	NA	1	(SIMPSON et al., 2007a)
	c.1094G>A p.G365Q /c.1322-2A>G	yes	NA	NA	1	(SIMPSON et al., 2007a)
	c.1121T>G p.L374R	yes	no	X-Ray	3	(HÜLSKAMP; WIECZOREK; RIEDER, 2003)
	c.1222C > T, R408W	no	no	CT scan and X-ray	1	(TAKEYARI et al., 2014)
	c.1225C>T:p.R409C	yes	no	CT scan and X-ray	1	(SEIDAHMED et al., 2015)
	c.1309 G>A p.D437N	no	brachycephaly	skull morphology	1	(SIMPSON et al., 2009)
	c.1487C > T; p.P496L	no	sagittal	CT scan	2	(ACEVEDO; POULTER, 2015)
	c.1603C>T p.R544W	yes	no	CT scan and X-ray	1	(KOCHAR; CHOUDHARY; GADODIA, 2010)
	c.1603C>T p.R544W	yes	ridged coronal	X-Ray	1	(KINGSTON; FREEMAN; HALL, 1991)
Chromosomal rearrangements						
	45, XY psudic (7;7) (p22;p22)	yes	yes	X-Ray	1	(SIMPSON et al., 2007a)
	del 7p22.3	yes	no	CT scan and X-ray	1	(ABABNEH; ALSWAID; YOUSSEF,

						2013)
No Mutation Described						
	not described	yes	no	X-Ray	1	(MANE; COATES; MCDONALD, 1996)
	not described	no	not described	NA	1	(GÜNEŞ; KURTOĞLU; ÇETIN, 2005)
	not described	yes	not described	NA	1	(GREENBERG et al., 1991)
	not described	yes	not described	NA	1	(REJJAL, 1998)
	not described	yes	no	Autopsy	3	(RICKERT et al., 2002)
	not described	yes	ridged coronal	X-Ray	1	(RAINE et al., 1989)
	not described	no	no	X-Ray	1	(ACOSTA; PERES; CHIMELLI, 2000)
	not described	yes	not described	NA	1	(MICHAEL; NELSON; ORTMEIER, 2011)
	not described	yes	coronal	Autopsy	1	(CHITAYAT et al., 2007)
	not described	yes	ridged coronal	skull morphology	1	(SIMPSON et al., 2007a)
	not described	no	not described	NA	1	(VISHWANATH; SRINIVASA, 2014)
	not described	yes	no	X-Ray	1	(KAN; KOZLOWSKI, 1992a)

II. Exome sequencing of atypical cases of syndromic craniosynostosis.

Atique, R; Yamamoto, G; Rocha, K; Ezquina, S; Aguena, M; Tavares, VL; Brito, LA; Bertola, D; Passos-Bueno, MR

Abstract

Craniosynostosis are a heterogeneous group of diseases characterized by early closure of cranial sutures. So far, 57 genes have been associated with craniosynostosis, however they only explain approximately 23% of all cases. Many of the cases without a molecular diagnosis are small pedigrees or simplex cases which difficult the identification of the mutations responsible for the malformations. In this work we use whole exome sequencing to identify the mutations in four familial and three simplex cases. We were unable to identify the mutations responsible for the cases presented here, however we delineated several mutations in genes associated with pathways involved in suture development and patency maintenance. This work helps with the identification of new mutations in craniosynostosis with several candidate mutations that are strong candidate for further studies.

Resumo

As craniossinostoses são doenças heterogêneas caracterizadas pelo fechamento precoce das suturas cranianas. Até o momento 57 genes foram associados às craniossinostoses, nas mutações nesses genes só explicam cerca de 23% de todos os casos. Muitos dos casos sem um diagnóstico molecular definido são famílias pequenas ou casos únicos, o que dificulta a identificação das mutações responsáveis pelas malformações. Nesse trabalho nós usamos o sequenciamento do exoma complete para identificar as mutações responsáveis em quatro casos familiais e 3 casos únicos. Mutações únicas não foram identificadas, no entanto várias mutações candidatas em vias associadas ao desenvolvimento das suturas foram identificadas. Nosso trabalho ajuda no delineamento de novas mutações associadas às craniossinostoses ao propor novos genes candidatos à estudos mais aprofundados.

Introduction

Craniosynostosis are a heterogeneous group of craniofacial malformations characterized by early closure of the cranial sutures. It affects 1 in every 2000-3000 live births (COHEN JR.; MACLEAN, 2000). Craniosynostosis can be divided in two clinical groups: isolated (non-syndromic), or associated with other defects, such as limb and other craniofacial malformations, commonly referred as syndromic forms(KIMONIS et al., 2007).

Mutations in 57 genes have been shown to be involved with the biology of primary craniosynostosis, including *FGFR1*, *FGFR2* and *FGFR3* (Apert, Crouzon, Pfeiffer, Muenke and Baller-Gerold syndromes), *TWIST1* (Saethre-Chotzen syndrome), *ERF*, *TCF12*, *IL11RA*, *TGFBR1*, among others(TWIGG; WILKIE, 2015a). A plethora of molecular pathways have been linked to CS, as expected by the genetic heterogeneity so far reported, including but not limited to, SHH, WNT, NOTCH/EPH, RAS/MAPK, and STAT3(TWIGG; WILKIE, 2015a). These genes participate in different steps of bone formation such as embryological patterning of skeletal structures, osteogenic differentiation, cell proliferation, and bone resorption. Disturbances in this pathway are believed to alter the fine equilibrium of bone growth and suture patency present in the suture tissue, leading to premature suture closure. Of all syndromes with mapped genes, thirty seven are of autosomal dominant inheritance (of which seventeen are loss of function, and sixteen are confirmed as gain of function mutations), eighteen are autosomal recessive, one is x-linked dominant, and one is x-linked recessive(HEUZÉ et al., 2014b). Even though several genes have been related to craniosynostosis, 76% (HEUZÉ et al., 2014b; WILKIE et al., 2010)of all cases still lack a definitive molecular diagnosis. New techniques such as next generation sequencing have permitted the investigation of rare alleles in previously not described loci. This strategy has already proved effective in identifying new loci associated with craniosynostosis (SHARMA et al., 2013; TWIGG et al., 2013). The identification of new loci and new pathogenic variants associated with craniosynostosis could lead to a more thorough understanding of the molecular pathways and cellular processes involved in the pathophysiology of the disease as well as lead to better diagnostic tools, genetic counseling, and, possibly, new treatments. However, the lack of familial cases and the high genetic heterogeneity is, currently, a challenge. It has also been shown that the probability of recurrent closure of the sutures after surgery correlates with the genetic defect. In this work we aim to identify new causative mutations in rare cases of atypical craniosynostosis using whole exome sequencing.

Materials and Methods

DNA Preparation

DNA was purified from peripheral blood (according to standard protocols) or saliva (collected with Oragene® saliva collection kits OG-500 and OG-575; DNA GenotekInc, Ottawa, Canada), following manufacturer's instructions.

Library Construction and Exome Sequencing

Library preparation and exome capture were performed with Illumina'sTruSeq Sample Prep and Exome Enrichment Kits, for individuals from families CR45, CR157, and F1903. Nextera Rapid Capture Exome was used for individuals from family CR293. Library quantification was performed with KAPA Library Quantification kit (KAPA Biosystems), through real-time quantitative PCR. Paired-end sequencing was performed on a HiScanSQ (Illumina) for families CR45, CR157, and F1903, and on a HiSeq 2500 (Illumina) for family CR293.

Exome Data Processing

Sequences were aligned to the hg19 reference genome with Burrows-Wheller Aligner (BWA; http://bio-bwa.sourceforge.net). Genome indexing, realignment of reads and duplicate removal were performed with Picard (http://broadinstitute.github.io/picard/). Variants were then called using Genome Analysis Toolkit package (GATK; https://www.broadinstitute.org/gatk/), and subsequently annotated with ANNOVAR (http://www.openbioinformatics.org/annovar/).

Variant Selection

The variants were filtered by first excluding the variants that were incompatible with the mendelian model proposed for each family. Additionally, variants were further filtered to exclude the heterozygous variants with less than 3 reads presenting the mutated allele to exclude false positive variants present.

Afterwards the remaining variants were selected according to read quality, including variants with a quality score of over 30. Hypervariable genes were also excluded from analysis. Finally, the variants were filtered by population frequency (MAF <0,01) and by the mutation effect in the final transcript, including only variants that were nonsynonymous or loss of function (frameshift

insertions, frameshift deletions and stopgains). The remaining refined list was then submitted to a series of prioritization strategies. The selection was based on both the results from the VarElect tool as well as from the literature description of each gene. Genes that were expressed in the affect tissues in mouse embryo were defined according to the MGI database (http://www.informatics.jax.org/expression.shtml). Other bioinformatics tools were used to assess conservation and predictions of protein damage (SIFT (http://sift.jcvi.org), Polyphen-2 (http://genetics.bwh.harvard.edu/pph2/), Mutation Taster and PhastCons (http://www.mutationtaster.org). PubMed, OMIM and GeneCards databases were also examined. Collectively, these analyses provided the basis for a list of the best candidate variants.

We also considered the pLI (probability of LoF intolerance) index. It is calculated according to Lek et al(LEK et al., 2016)) and indicates how tolerant a gene is to LoF mutations. A pLI of 1 indicate total intolerance to LoF and 0 total tolerance.

Aditionally, variants found in simplex cases were subdivided in three categories, de novo variants with equal allelic balance; i.e. variants in which the mutant and wild alleles are present in approximately equal proportion in number of reads (40-60%) by NGS, variants with low allelic balance; i.e. variants in which the proportion of mutant alleles are present in lower (10-40%) proportion in comparison with the wild allele, and rare homozygous/hemizygous variants.

Sanger Sequencing

Variants classified as best candidates were visually inspected using Integrative Genomics Viewer (IGV) software (Broad Institute of MIT and Harvard). Sanger sequencing was used for variant validation and, whenever appropriate, for mutation screening in additional relatives. PCR primers were designed with Primer Designing Tool web interface (NCBI). The primers used were:

Gene	Forward	Reverse
DOCK6	TTAGGGACACACCCGTAAAC	TCTCTCCGTGTAGAACTCCT
COL5A3	GGTCTACACTGATCACCCAC	TCTCCTAGAGCCTTAGGGTG
FGFRL1	CAAAGATGGCGGACAAGG	GTAGTTGACGCTCAGGCT
GJB2	CTCCTAGTGGCCATGCAC	CAATGCGTTAAACTGGCTTT
WNT2B	GGAGCTATGCTGAGACCGGG	TCACCAGTCGTGTAAGACGC
RND2	TCCCTTGACCAGGATCTGTA	GATGAGAGCTTCACTCGCTA

SNW1	CTTAAGCCTGCTTGTGTTTGA	ATTTGTCAGCTGCTCGAACT
DDX23	CCCTGTTTACCACAGGATCG	AACAAAGCCCCAAGATAGCC

PCR products were sequenced with ABI 3730 DNA Analyzer (Applied Biosystems), and sequences were visualized using Sequencher® 5.2 analysis software (Gene Codes).

Results

The cohort here studied was composed of four (CR45, CR157, F1903, F8552) familial cases with more than one proband per family sequenced and by three sporadic cases (CR293, F8463 and f9320). All families were of Brazilian descent. The clinical phenotypes, as briefly described below, were atypical and no obvious syndromes were identified. Nevertheless, all probands were submitted to target sequencing of the 20 genes most commonly associated with craniosynostosis (*ALPL, ALX4, CHST3, EFNB1, ERF, FGFR1, FGFR2, FGFR3, GLI3, IL11RA, JAG1, POR, RAB23, RECQL4, RUNX2, TCF12, TGFBR1, TGFBR2, TWIST1, ZIC1*)(HEUZÉ et al., 2014b). No pathogenic mutations were detected.

Due to the negative results in genes linked to known craniosynostostic syndromes, 11 subjects from the four familial cases and 4 probands from the families with simplex cases were submitted to whole exome sequencing. The sequencing resulted in an average of 179390.8 variants per individual (Table I). The genes were than filtered according to the methodology described above and the resulting candidate variants were validated by sanger sequencing.

Allelic balance as a variant filter

Due to the great number of variants found by whole exome sequencing we tested whether the allelic balance (AB) could be a useful tool in restricting the number of variants in whole exome sequencing analysis. We gathered data from multiple variants previously tested by other members of our group, analyzing a total of 60 variants found by whole exome sequencing which were also validated by Sanger sequencing to test whether allelic balance could be a predictor of false positives, an inherent flaw of NGS.

Of the 60 variants validated (fig. 1), 53 (88,3%) were also validated by sanger sequencing, which means they are true variants. 38 of the validated variants are within the interval we previously defined as equal allelic balance (0.41-0.6), while 15 have lesser or higher allelic balances. With the exception of one variant, variants found by NGS but not validated by Sanger sequencing, i.e. false positives, were all outside of the equal allelic balance interval. Four of the false positive variants were in the 0.21-0.4 interval, while two were in the 0.91-1 interval.

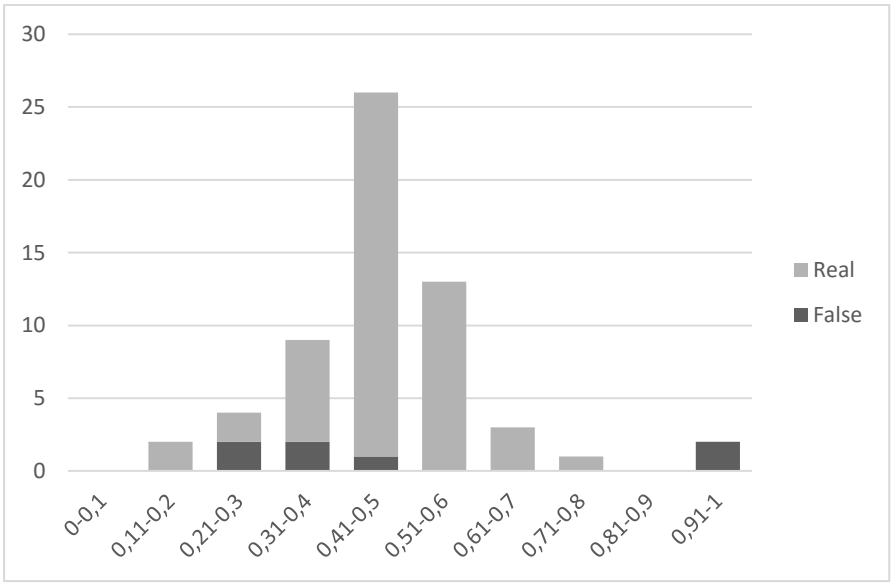

Figure 1: Number of real and false positive variants by allelic balance found in 60 variants from multiple sequences by validating variants found in whole exome sequencing using sanger sequencing. Variants that were detected by both techniques were labeled "Real" and variants with conflicting results are labeled "False".

We next analyzed some of the variants found in the cohort studied in this paper (table I): *DOCK6* (AB=0.48), *COL5A3* (0.49), *FGFRL1* (0.41/0.45/0.33), *GJB2* (0.66), *SMARCA1* (0.21), *WNT2B* (0.48/0.6), *RND2* (0.43/0.56), *SNW1* (0.19/0.35) and *DDX23* (0.46). The variant found in *SMARCA1* and *FGFRL1* were false positives while the variants found in *DOCK6, COL5A3, GJB2, WNT2B, RND2, SNW1* and *DDX23* were validated. The false positives identified had AB of 0.41/0.45/0.33 (*FGFRL1*, for each proband) and 0.21 (*SMARCA1*), which is unexpected, given that the variant found in *FGFRL1* was shared between three probands and had allelic balance of nearly 0.4 for each one.

Table I: Variants revalidated by Sanger sequencing in the atypical craniosinostosys cohort.

Family	Gene	Variant	Type	Qual	Coverage	Allelic Balance	Status
CR45	COL5A3	NM_015719:exon58:c.C4157T:p.P1386L	nonsynonymous SNV	1624	73/30/32	0.49/0.63/0.53	Real
	DOCK6	NM_020812:exon42:c.C5324A:p.S1775X	stopgain	1621	56/39/41	0.48/0.46/0.43	Real
CR157	FGFRL1	NM_021923:exon2:c.A167C:p.D56A	nonsynonymous SNV	175	49/44/39	0.41/0.45/0.33	False
F1903	GJB2	NM_004004:exon2:c.G402T:p.W134C	nonsynonymous SNV	667	6	0.66	Real*
F8463	SMARCA1	NM_001282874:exon11:c.C1471A:p.L491M	nonsynonymous SNV	37	23	0.21	False
F8552 and F8566	WNT2B	NM_024494:exon1:c.T143A:p.L48Q	nonsynonymous SNV	1637	115/45	0.48/0.6	Real
	RND2	NM_005440:exon3:c.C236A:p.S79Y	nonsynonymous SNV	949	74/30	0.43/0.56	Real
	SNW1	NM_012245:exon4:c.G370C:p.V124L	nonsynonymous SNV	406	51/31	0.19/0.35	Real
F9320	DDX23	NM_004818:exon12:c.G1441A:p.A481T	nonsynonymous SNV	165	24	0.46	Real

Qual: GATK base quality, **Allelic balance** is defined as the number of reads of the mutated allele divded by total coverage for the nucleotide.

*The variant was validated but the genotype called was incorrect.

Clinical synopsis of familial cases

CR45 family is non-consanguineous. The family consists of an affected father, a non-affected mother and two affected children. Two of the affected individuals (CR45-1 and CR45-2) presented craniosynostosis of the coronal while the third one (CR45-4) presented sagittal suture closure. All affected probands had congenital or very early in life cataracts, blue sclera, deformities of the hand and feet including metatarsus adductus, severe hypoplasia of first metatarsals and of the distal phalanges, and finger-like halluces (Figure 1 A). The phenotype segregation in the family was suggestive of autosomal dominant inheritance. The family was initially described in(PASSOS-BUENO et al., 1997) . All three probands from family CR45 were sequenced. After the removal of common, low quality and variants that were not inherited by both children, there were 27 (Table SI) variants left, 20 missenses and 7 LoF. The best variants

were then selected according to the function of the mutated genes, as described in the methodology section. The best candidate variants selected were c.C4157T:p.P1386L in *COL5A3* and c.C5324A:p.S1775X in *DOCK6*.

CR157 family consists of an affected father and two affected daughters from different unaffected non-consanguineous mothers. The affected propositus presented craniosynostosis of the coronal, sagittal and metopic sutures, trigonocephalic skull, hipoplastic supraorbital crest, shallow eye orbits, and palpebral ptosis (Figure 1B). The phenotype segregation in the family was suggestive of autosomal dominant inheritance. The probands from family CR157 were sequenced, resulting in 26 variants after filtering, 25 missenses and 1 LoF. The best variants were than selected according to the function of the mutated genes, as described in the methodology section. The best candidate variant selected was c.G1520A:p.R507Q in *TGFBR3.*

F8552 and F8566: Dizygotic twin brothers, unrelated and healthy parents. Born of C-section at 36 weeks, both were hospitalized for 18 days due to feeding difficulties. F8552 presented sagittal craniosynostosis, brachycephalic fistula, phimosis and hydroceles. F8566 presented closure of the sagittal and coronal sutures, brachycephalic fistula, branchial fistula, phimosis and hydroceles. Both brothers were sequenced and rare shared variants were selected. The patients presented 32 rare shared variants, 29 with equal allelic balance and 3 with low allelic balance. The index also presented 1 rare hemizygous variant in *RAB40AL*. According to gene function analysis and the clinical manifestations, the most likely variant to be causing the phenotype are p.S79Y in *RND2* and p.L48Q in *WNT2B* (tables SI and SII). We also sequenced the variants found in F8552-1 and F8566-1 in their parents (F8566-2 and F8566-3) to see whether the variants were de novo or inherited. We found that the variants in *WNT2B, RND2* and *SNW1* were inherited.

F1903 is a non-consanguineous family of four consisting of unaffected mother and father and affected monozygotic twin sisters. Both sisters presented premature metopic suture closure diagnosed at birth, sudden severe alopecia at age 2, dystrophic nails, and psoriasis (Figure 1C). We have hypothesized that the phenotype could represent a *de novo* change representing and autosomal dominant condition or alternatively, an autosomal recessive condition. The parents and one proband (F1903-2) were sequenced. The variants that were *de novo* (autosomal dominant) and bi-allelic (autosomal recessive) were considered in this family, resulting in 16 and 4 final variants, respectively (Table I). The best variants were then selected according to the function of the mutated genes, as described in the methodology section and resulted in 20

variants. The resulting analysis elected one homozygous variant in *GJB2* (c.G402T:p.W134C)

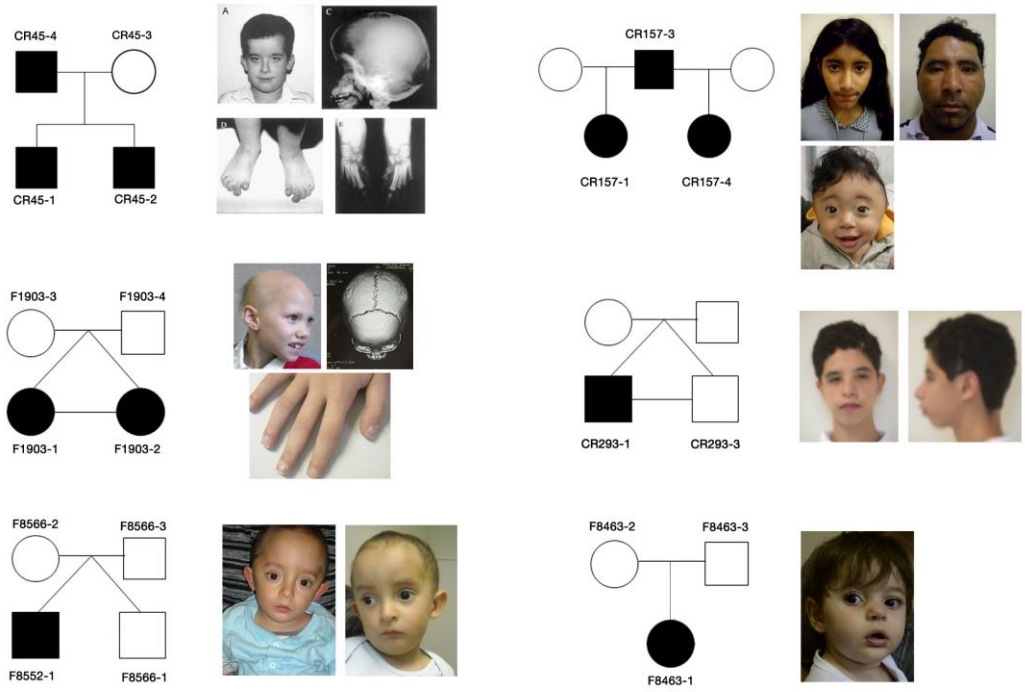

Figure 1: Pedigrees and physical characteristics of CR45 , F1903 , CR157 , CR293 , F8552-1, F8566 and F8463.

Table I: Number of variants per individual after variant selection steps. Raw: total number of variants; Mendelian: variants were filtered according to the inheritance hypothesis for each family; LOWQUAL: variants with a quality score under 30 were excluded; MAF<0,01: Variants that had a frequency higher than 0,01 in 1000 genomes consortium, NHLBI Exome Sequencing Project, ExaC consortium and in a local database of 600 healthy individuals were excluded; Nonsynonimous/LOF/InDel: only variants that resulted in an amino acid exchange, premature stop codons or frameshift insertions and deletions were considered

	Raw	Mendelian	Lowqual	MAF<0.01	Nonsynonimous/ LOF/InDel
CR45	201104	27406	24386	1873	27
CR157	228895	36890	33875	3317	26
F1903					
AD	110991	62378	56685	1395	16
AR	110991	47928	45249	1556	4
CR293	244973	18685	14849	3409	7
F8463	193595	9036	7444	910	9
F8552	175421	107307	100646	1898	33
F9320	146265	5724	4672	707	6

Table II: Main candidate variants selected.

Family	Gene	Position (hg19)	Variant	Type	Qual	*In silico predictions** SIFT / Polyphen-2 HD; HV / Mutation Taster / ExAC	Frequency ExAC / 1kGP / ESP6500 / CEGH60+	Coverage	Allelic Balance
CR45	*COL5A3*	Chr19:10079400	NM_015719:exon58:c.C4157T:p.P1386L	nonsynonymous SNV	1624	T/D/D/D/0	0,008/0/0/0	73/30/32	0.49/0.63/0.53
	DOCK6	Chr19:11313297	NM_020812:exon42:c.C5324A:p.S1775X	stopgain	1621	T/NA/NA/A/0	0,008/0/0/0	56/39/41	0.48/0.46/0.43
CR157	*TGFBR3*	Chr1:92184912	NM_021923:exon2:c.A167C:p.D56A	nonsynonymous SNV	1411	T/B/B/N/0.01	0/0/0/0	46/42/33	0.41/0.4/0.33
CR293	*EGR1*	Chr5:137803186	NM_001964:exon2:c.T1048C:p.S350P	nonsynonymous SNV	186	D/D/D/D/0,67	0/0/0,0004/0	52/51/103	0.5
F1903	*GJB2*	20763319	NM_004004:exon2:c.G402T:p.W134C	nonsynonymous SNV	667	D/D/D/D/0	0/0/0/0,0008	6	0.66
F8552 and F8566	*WNT2B*	Chr1:113052027	NM_024494:exon1:c.T143A:p.L48Q	nonsynonymous SNV	1637	T/D/P/D/0.29	0/0/0/0	115/45	0.48/0.6
	RND2	Chr17:41179245	NM_005440:exon3:c.C236A:p.S79Y	nonsynonymous SNV	949	D/D/D/D/0	0/0/0/0	74/30	0.43/0.56
	SNW1	Chr14:78205365	NM_012245:exon4:c.G370C:p.V124L	nonsynonymous SNV	406	T/B/B/D/D/1	0/0/0/0	51/31	0.19/0.35
F9320	*DDX23*	Chr12:49228222	NM_004818:exon12:c.G1441A:p.A481T	nonsynonymous SNV	165	D/D/D/D/1	0/0/0/0	24	0.46

Qual: GATK base quality (minimum threshold fixed as 30); **HD:** Polyphen-2 HumDiv; **HV:** Polyphen-2 HumVar; **1kGP:** 1000 Genomes Project; **ExAC:** Exome Aggregation Consortium; **ESP6500**: Exome Sequencing Project database; **CEGH60+**: in-house database (Centro de Estudos do Genoma Humano e Células-Tronco); **na:** not available. **D:** damaging; **P:** possibly damaging; **B:** Benign; **T:** tolerated. Allelic balance is defined as the number of reads of the mutated allele divided by total coverage for the nucleotide
.

Clinical synopsis of simplex cases

F8463-1: A 4 years old girl, daughter to healthy unrelated parents. The craniosynostosis was first noted at 3 months old and confirmed at 5 months. The patient presented closure of the right coronal suture. No other defects were reported. All three family members were sequenced and *de novo* mutations were selected. The index presented 9 de novo mutations, all with low allelic balance. The index presented no rare homozygous variants.

F9320: A 18 years old woman daughter to healthy, unrelated parents. No previous family history of congenital malformations was reported. The affected proband presented craniosynostosis of the sagittal and coronal sutures, ventricular dilation, short stature, macrocephaly, facial asymmetry, shallow eye orbits and ocular proptosis, pectus excavatum, hand digits presented camptodactyly. All three family members were sequenced and de novo mutations were selected. The index patient presented 5 *de novo* rare mutations, 2 with an equal allelic balance and 3 with a low allelic balance. The index also presented 1 rare homozygous variant. According to gene function analysis and the clinical manifestations, the best candidate variant is p.A481T in *DDX23*.

CR293 family consists of a pair of monozygotic twins (CR293-1 and CR293-3). CR293-1 exhibits coronal suture craniosynostosis, palpebral ptosis, cardiopathy, and partial syndactilly (Figure 1D). In contrast, CR293-3, his twin brother, is not affected. Due to the discordant phenotype of the twins, we sequenced both brothers and selected the mutations present in the affected propositus, but not in the unaffected brother reasoning that a de novo pathogenic mutation has arisen in CR293-1. The best variants were than selected according to the function of the mutated genes, as described in the methodology section. This analysis resulted in 7 variants, all missense. The best candidate variant found was c.T1048C:p.S350P in *EGR1*, as we assumed that the craniosynostosis has arisen as a de novo mutation.

Discussion

In this work we have sequenced the whole exome of fifteen patients with atypical syndromic craniosynostosis in whom no obvious exposure of teratogenic environmental factors during pregnancy were identified. With the exception of F1903, all families had probands with early closure of the coronal suture. Sagittal craniosynostosis was observed in CR45, CR157, F8552-1, F8566 and F9320 affected probands, and metopic closure was observed in F1903 and CR293 affected probands. Interestingly heterogeneity of suture fusion was observed in familial cases. Coronal and multisuture craniosynostosis have been considered an indicative of genetic causes underlying the disease (WILKIE et al., 2010). F1903 only had metopic suture closure, however, the homogenous syndromic phenotype presented by both monozygotic twins favors a genetic cause.

The analysis revealed several possible mutations that could explain the phenotype of each case. Syndromic craniosynostosis are genetic heterogeneous malformations, therefore we do not expect the mutations found in the affected individuals studied here to be part of a common pathway, but rather part of different processes involved in suture closure. As reviewed by Twigg et al, 2015(TWIGG; WILKIE, 2015a), the main processes involved in suture closure are stem cell specification and migration, lineage commitment, boundary formation, osteogenic differentiation, bone homeostasis, and neural crest specification, migration and maturation. Also, due to the different embryological origins of the cranial sutures, different molecular pathways controlling specific biological functions are more recurrently associated with CS of each suture. The pathways with predominately coronal suture involvement are WNT, NOTCH/EPH and RAS/MAPK (TWIGG; WILKIE, 2015a). During craniofacial development these pathways control biological functions, mainly stem cell lineage commitment, boundary formation and integrity, and the balance between osteogenic differentiation and proliferation.

The observed proportion of de novo mutations observed here are higher than observed in the literature when we did not take into account allelic balance. Kong et al., 2012 found that from 78 parent offspring trios only 73 de novo mutations were observed, or, a proportion of 0,93 de novo variant per individual. However, they only considered true heterozygotes (here called equal allelic balance mutations) in their analysis, if the same methodology is applied to our data F8463 and F1903 exhibits no equal allelic balance mutations and F9320 exhibits 2 (the other cases can't be compared due to absence of data from both parents). Our data supports the

strategy proposed by Kong et al, 2012, that only variants with allelic balance between 0,4 and 0,6 should be considered true in large scale experiments. However, this strategy underestimates the total number of de novo variants, as we have seen, 15 of the 53 (28%) real variants had allelic balances outside the 0,4-0,6 range. Allelic balance alone is not enough to disregard any variant, as we were able to find mutations with allelic balance as low as 0.16. However, efforts to validate NGS findings would be better spent on variants with allelic balance outside the 0.4-0.6 interval. We, therefore, only validated candidate variants outside the equal allelic balance range.

From the variants detected in the CR45 family the strongest candidates were variants in the *COL5A3* and *DOCK6* genes (Table II). *COL5A3* transcribes the alpha-3 chain of collagen V. Collagen V is a heterotrimer made of alpha-1 (*COL5A1*), alpha-2 (*COL5A3*), and alpha-3 chains (IMAMURA; SCOTT; GREENSPAN, 2000). Mutation in *COL5A1* and *COL5A2* cause Ethler-Danlos syndrome(DE PAEPE; MALFAIT, 2012), a connective tissue defect that causes, among other things, blue sclera. *COL5A3* mutations do not cause any known genetic conditions, and are marked in ExaC with a pLI index of 0, which means that stop gain and essential splice site mutations in this gene are seem more frequently than expected in controls. Therefore, due to the frequency of mutations in controls and the absence of hand and feet phenotypes in malformations with mutation in collagen genes, *COL5A3* is an improbable candidate gene for the syndrome. The p.P1386L variant in COL5A3 was also observed in one control, according to ExAC, however the sequencing was low quality and they do not confirm the variant call.

DOCK6 encodes a member of the dedicator of cytokinesis (DOCK) family of atypical guanine nucleotide exchange factors. Guanine nucleotide exchange factors interact with small GTPases and are components of intracellular signaling networks. *DOCK6* is essential to actin cytoskeletal reorganization by activating the Rho GTPases Cdc42 and Rac1(CÔTÉ; VUORI, 2002). Homozygous mutations in this gene are associated with Adams-Oliver syndrome 2. Adams-Oliver syndrome 2 is an autosomal recessive congenital anomaly with variable involvement of the brain, eyes, and cardiovascular systems(SHAHEEN et al., 2011). Cataracts and finger shortening have been described in the syndrome. However, as it is both a heterozygous mutation and it is not predicted to have a major impact on the protein, it is unlikely that the p.S1775X mutation in *DOCK6* causes the syndrome.

The analysis of the CR157 family's exome sequencing revealed variants in 26 possible candidate genes, of which 2 stand out as more functionally relevant: missense variants in *TGFBR3* and *FGFRL1* (Tables I and II). *FGFRL1* was detected as a false positive and therefore discarded.

TGFBR3 encodes the transforming growth factor (TGF)-beta type III receptor. The encoded receptor is a membrane proteoglycan that often functions as a co-receptor with other TGF-beta receptor superfamily members(MORÉN; ICHIJO; MIYAZONO, 1992). Other TGF-beta receptors are involved in syndromic craniosynostosis like Loeys-Dietz Syndrome types 1 and 2, caused by mutations in *TGFBR1* and *TGBR2*, respectively(AKUTSU et al., 2007). However, the phenotype of Loeys-Dietz syndrome involves arterial tortuosity, aneurisms, cleft palate and bifid uvula, which are all absent in the clinical phenotype of the family. Also, the *in silico* prediction of damage to protein function suggests that the mutation is benign. Mutations in the neighboring nucleotides and amino acids are rare, according to ExAC.

The affected propositi in the F1903 pedigree are homozygotic twins, and therefore only one of the sisters was sequenced (F1903-2). The parents were unaffected and there were no other affected family members, thus the phenotype was analyzed as either AD, in which the mutation is considered to be *de novo*, or AR.

The AR analysis revealed 4 candidate variants (Table SIV). Mutations in *GJB2* are associated with 7 phenotypes, all of which show varying degrees of skin dysplasia, including alopecia, nail dystrophy, and neurosensorial deafness, the latter not present in our patients(CHAN; CHANG, 2014). The p.W134C variant is predicted to be highly damaging to the resulting protein by removing an alpha-coil from the second transmembrane domain. The mutation was initially found to be homozygous, however sanger sequencing demonstrated that it is in heterozygosity and that it was inherited from the mother.

The mother is also unaffected, which can be explained by two hypotheses: the phenotype is not completely penetrant or another hit is necessary to cause the phenotype. The second hit would probably be on another protein that constitutes gap junctions. Mutations in both *GJB6* and *GJB2* have been related to Clouston syndrome(LIU et al., 2015; MARKOVA et al., 2016), a genetic disease characterized by partial to complete alopecia, nail dystrophy and palmoplantar hyperkeratosis. Clouston syndrome cases with mutations in GJB2 are rare, in one report the affected individual was a double heterozygote for mutations in GJB6 and GJB2, and in other two report a heterozygous mutation in GJB2 was present, but both patients had hearing-loss, also all patients had hipotrichosis, including complete loss of the eyebrows and eye lashes, and nail dystrophy, similarly to F1903-1 and F1903-2. Three variants in GJB6 were found in F1903 (data not shown) but were too common to explain the phenotype (MAF 0.23-0.35).

The CR293 family presented one proband with craniosynostosis with a monozygotic unaffected twin brother. Of the 7 variants found, none have a strong functional relationship with suture

development and patency. The only gene indirectly related to craniosynostosis was *EGR1*, which is expressed in pharyngeal endoderm during craniofacial development when submitted to FGF signaling(LARBUISSON et al., 2013). In ExAC it is documented that there is one synonymous mutation in the same amino acid as the p.S350P mutation in EGR1; there is also a frameshift deletion encompassing Serine 350 with a frequency of 0.0006193 in the control population, rendering it unlikely to cause a severe, easily noticeable phenotype; however the p.S350P mutation could lead to a gain of function, thus having a different effect than de deletion found in controls.

No mutations within the selection criteria were detected in F8463(Table SII). Due to the single sided nature of the craniosynostosis it is possible the phenotype of this index affected patient is due to somatic genetic mosaicism, which would not be easily detected in DNA from blood samples. Mosaicism is increasingly being detected by NGS sequencing (GAJECKA, 2016; HAGUE et al., 2016; QIN et al., 2016; TANIGUCHI-IKEDA et al., 2016), however, the effective detection of mosaicism requires a mean coverage of 800 reads per base pair, well beyond the coverage used in this study, thus we would not expect to identify these mutations in our data. Alternatively, we cannot discard the possibility that the mutation could be in non-coding regions of the genome.

F8552 and F8566 are dizygotic twins, thus mutations in homozygosis are more likely to be causative of their syndrome. Whole exome analysis only revealed one rare mutation in homozygosis in *RAB40AL* (Table SIV), however LoF mutations in this gene have been linked to X-linked mental retardation(SAITO-OHARA et al., 2002), a severe form of cognitive impairment not observed in our patients. Therefore, mutations in *RAB40AL* are unlikely to be causative of the phenotype. Heterozygous mutations in RND2 and WNT2B (Table II) were also found in both brothers, RND2 is part of the RAS/MAPK pathway(LARTEY et al., 2006), closely linked to several forms of syndromic CS, WNT2B is part of the WNT pathway, integral to osteogenic differentiation(DAY et al., 2005; LING; NURCOMBE; COOL, 2009).

Finally, F9320 exhibited a variant in DDX23 (Table II), a DEAD box protein that participates in the spliceossome formation (MÖHLMANN et al., 2014). Even though DDX23 is not directly related to CS, it has been shown that its orthologue in C. elegans is required for cell differentiation of most tissues (KONISHI; UODOME; SUGIMOTO, 2008). It is possible that DDX23 could be involved in the balance between cell proliferation and differentiation in the suture complex, that when disturbed can lead to premature suture closure

Notch signaling is a major pathway in bone biology, participating in the patterning, growth and homeostasis of skeletal tissue. NOTCH are transmembrane receptors that, when activated translocate into the nucleus to act as an expression regulator. It regulates WNT and BMP pathways and is downstream of the TWIST pathway, all related to CS in humans(HORI et al., 2013). Notch signaling works mainly in two ways: by acting in cell differentiation and in patterning, organizing different cell types in a field, and by instructing the formation of a third cell type in the border between two cell types, as seem in the coronal suture. Mice harboring a conditional knockout of JAGGED1 in the coronal suture, a ligand of NOTCH, exhibit closure of the coronal suture and, as well as in defects in the osteogenic/non-osteogenic boundary (YEN; TING; MAXSON, 2010). Also, mutations in NOTCH2 and JAGGED1 cause Alagille syndrome, which presents craniosynostosis (ODA et al., 1997).

WNT2B encodes a ligand of the WNT pathway, which is regulated by NOTCH signaling(ZAMUROVIC et al., 2004). *SNW1* is involved in NOTCH1-mediated transcriptional activation and is also believed to interact with SKI, a TGF-B repressor in which mutations cause Shprintzen-Goldberg syndrome(WU et al., 2011). Finally, DDX23 has a less strong connection to NOTCH signaling, interacting with SNW1 during spliceosomal formation (KONCZ et al., 2012). Interestingly, F8552-1 and F8566-1 have two different variants in the NOTCH signaling pathway, WNT2B and SNW1. Even though both mutations were inherited, the lack of phenotype of the parents could be due to each parent only being heterozygote to one of the mutations, while the indexes were double heterozygotes.

The small size of the pedigrees as well as the rarity and heterogeneity of syndromic craniosynostosis represented the main limiting factors of our study. Somatic mosaicism might be another confounding factor. It is well known the power of the analysis of large families, but this is very uncommon among patients with syndromic forms of craniosynostosis. From the 6 strategies previously suggested in the literature (GILISSEN et al., 2012) we were able to use the *de novo*, candidate gene, and linkage based strategies. It should also be noted that variants outside of the exome coverage would not be detected by our methods. Several recent studies have successfully identified new loci and variants associated with craniosynostosis (CARMIGNAC et al., 2012; RAUCH et al., 2015; SHARMA et al., 2013; THAM et al., 2015). Their experimental design differed from ours due to the number of affected individuals studied: Tham et al studied 6 individuals from 5 families. Rauch et al studied two unrelated individuals, Sharma et al studied 347 samples from unrelated cases, Carmignac studied 4 families, including one family with a 4 generation pedigree. The studied of unrelated affected individuals seems to be a major factor in determining the variants associated with rare phenotypes. The study of rare syndromes in small

pedigrees is a challenge even after the advent of NGS, and the results presented here will only be further refined by sequencing similar cases or by other investigative approaches, such as *in vivo* and *in vitro* studies. Expanding our knowledge of suture biology is essential to better diagnose and propose novel treatments to rare syndromic craniosynostosis.

Supplementary Tables

Table SI: Variants detected by whole exome sequencing in each family after the filtering steps described in the methodology section.

CR45

Gene	Mutation Type	Mutation
ENSA	nonsynonymous SNV	NM_207045:exon1:c.T26A:p.V9E
FMN2	nonsynonymous SNV	NM_020066:exon5:c.C2855G:p.A952G
FANCD2	frameshift deletion	NM_001018115:exon15:c.1278_1278del:p.L426fs
XYLB	nonsynonymous SNV	NM_005108:exon7:c.T536C:p.I179T
DCP1A	frameshift deletion	NM_001290207:exon6:c.963delT:p.S321fs
KIAA2018	frameshift deletion	NM_001009899:exon7:c.3047delA:p.N1016fs
CP	nonsynonymous SNV	CP:NM_000096:exon1:c.C146T:p.T49M
MRPL47	nonsynonymous SNV	NM_177988:exon3:c.T14C:p.L5P
PROM1	nonsynonymous SNV	NM_001145849:exon1:c.G3A:p.M1I
LIAS	nonsynonymous SNV	NM_001278590:exon4:c.G376A:p.A126T
NFKBIE	nonsynonymous SNV	NM_004556:exon1:c.G17C:p.S6T
LRRC1	nonsynonymous SNV	NM_018214:exon11:c.C1045T:p.R349W
DFNA5	nonsynonymous SNV	NM_001127453:exon3:c.G241A:p.E81K
HOXA2	nonsynonymous SNV	NM_006735:exon2:c.C785T:p.P262L
HIBADH	nonsynonymous SNV	NM_152740:exon7:c.C767A:p.T256N
BAZ1B	nonsynonymous SNV	NM_032408:exon7:c.A1955G:p.N652S
PRRC2B	nonsynonymous SNV	NM_013318:exon26:c.C5897T:p.S1966F
ATP8A2	frameshift insertion	NM_016529:exon22:c.1869_1870insTT:p.G623fs

HERC1	nonsynonymous SNV	NM_003922:exon67:c.G12574A:p.A4192T
CLEC18C	nonsynonymous SNV	NM_173619:exon1:c.G70A:p.A24T
BZRAP1	frameshift insertion	NM_024418:exon21:c.4067_4068insCA:p.P1356fs
ARL16	nonsynonymous SNV	NM_001040025:exon1:c.G132T:p.Q44H
NPC1	nonsynonymous SNV	NM_000271:exon17:c.A2603T:p.D868V
COL5A3	nonsynonymous SNV	NM_015719:exon58:c.C4157T:p.P1386L
DOCK6	stopgain	NM_020812:exon42:c.C5324A:p.S1775X
ZNF527	frameshift insertion	NM_032453:exon5:c.901_902insTGTG:p.P301fs
RDH13	nonsynonymous SNV	NM_001145971:exon3:c.C280T:p.R94W

CR157

Gene	**Mutaion Type**	**Mutation**
LOC391003,PRAMEF22	nonsynonymous SNV	NM_001099850:exon2:c.G845A:p.G282D
C1orf177	frameshift deletion	NM_001110533:exon9:c.1101delG:p.K367fs
TGFBR3	nonsynonymous SNV	NM_001195683:exon10:c.G1520A:p.R507Q
VCAM1	nonsynonymous SNV	NM_080682:exon5:c.T956C:p.M319T
FGFRL1	nonsynonymous SNV	NM_021923:exon2:c.A167C:p.D56A
KIAA1211	nonsynonymous SNV	NM_020722:exon8:c.C2048G:p.P683R
CDH18	nonsynonymous SNV	NM_001167667:exon6:c.C725T:p.A242V
CCNI2	nonsynonymous SNV	NM_001039780:exon1:c.C307T:p.P103S
ASCC3	nonsynonymous SNV	NM_006828:exon40:c.G6263C:p.R2088T
KCNH2	nonsynonymous SNV	NM_000238:exon5:c.G917A:p.G306E
SPATA31C2	nonsynonymous SNV	NM_001166137:exon4:c.C3346A:p.Q1116K
HOXC4	nonsynonymous SNV	NM_153633:exon1:c.C128T:p.S43L
GIT2	nonsynonymous SNV	NM_001135213:exon6:c.A494G:p.E165G
CNTNAP4	nonsynonymous SNV	NM_138994:exon12:c.C1697G:p.S566C
SCARF1	nonsynonymous SNV	NM_003693:exon11:c.C2302T:p.P768S

SPAG9	nonsynonymous SNV	NM_001251971:exon3:c.C394T:p.P132S

F1903

Autossmal Dominant

Gene	Mutation Type	Mutation
PDE4D	nonsynonymous SNV	NM_006203:exon1:c.C7T:p.H3Y
ITGB8	nonsynonymous SNV	NM_002214:exon3:c.G256T:p.V86F
TUBB8	nonsynonymous SNV	NM_177987:exon2:c.T151C:p.Y51H
SEMA4G	nonsynonymous SNV	NM_001203244:exon10:c.C1310A:p.T437K
VAX1	nonsynonymous SNV	NM_001112704:exon1:c.A12T:p.K4N
CDK2AP2	nonsynonymous SNV	NM_001271849:exon2:c.A8G:p.Y3C
PRKRIR	nonsynonymous SNV	NM_004705:exon3:c.C242T:p.A81V
PRKRIR	nonsynonymous SNV	NM_004705:exon3:c.G233A:p.R78Q
GXYLT1	nonsynonymous SNV	NM_001099650:exon4:c.A677G:p.N226S
TVP23B	nonsynonymous SNV	NM_016078:exon7:c.C594A:p.N198K
ZNF519	stopgain	NM_145287:exon3:c.C1009T:p.Q337X
PQLC1	nonsynonymous SNV	NM_001146345:exon5:c.C722A:p.A241E
PTPRS	nonsynonymous SNV	NM_130854:exon11:c.G1919T:p.G640V
SSBP4	nonsynonymous SNV	NM_001009998:exon7:c.G493A:p.A165T
TUBGCP6	nonsynonymous SNV	NM_020461:exon4:c.C1168T:p.P390S
KDM6A	nonsynonymous SNV	NM_001291418:exon22:c.T3220C:p.C1074R

Autossomal Recessive

Gene	**Mutation Type**	**Mutation**
ZDHHC13	nonsynonymous SNV	NM_001001483:exon14:c.G1089T:p.L363F
GJB2	nonsynonymous SNV	NM_004004:exon2:c.G402T:p.W134C
GOLGA6L4	nonsynonymous SNV	NM_001267536:exon6:c.G696T:p.Q232H
GP6	frameshift insertion	NM_001083899:exon8:c.1666dupA:p.T556fs

CR293

Gene	Mutation Type	Mutation
NBPF10	nonsynonymous SNV	NM_001039703:exon56:c.A7124G:p.H2375R
EGR1	nonsynonymous SNV	NM_001964:exon2:c.T1048C:p.S350P
ANKRD30B	nonsynonymous SNV	NM_001145029:exon24:c.A2206G:p.T736A
MBD3L5	nonsynonymous SNV	NM_001136507:exon2:c.G370A:p.G124S
ANKLE1	nonsynonymous SNV	NM_001278444:exon8:c.G1925T:p.C642F
EIF6	nonsynonymous SNV	NM_181466:exon2:c.A143G:p.E48G
MN1	nonsynonymous SNV	NM_002430:exon1:c.G1174C:p.G392R

Table SII: Rare variants with equal allelic balance present in simpex cases

Family	Gene	Position (hg19)	Variant	Type	Qual	*In silicopredictions* SIFT / Polyphen-2 HD; HV / MutationTaster	Frequency ExAC / 1kGP / ESP6500 / CEGH60+
F8463							
	NA	NA	NA	NA	NA	NA	NA
F8552 and F8566							
	GPR157	chr1:9164639	NM_024980:c.A847T:p.T283S	nonsynonymous SNV	1042	T/D/D/D	0/0/0/0
	EXOSC10	chr1:11139866	NM_001001998:c.A1651T:p.I551F	nonsynonymous SNV	641	D/D/D/D	0/0/0/0
	WNT2B	chr1:113052027	NM_024494:c.T143A:p.L48Q	nonsynonymous SNV	1637	T/D/P/D	0/0/0/0
	POLR3GL	chr1:145457977	NM_032305:c.C283G:p.Q95E	nonsynonymous SNV	1658	T/B/B/D	0/0/0/0
	LAD1	chr1:201356001	NM_005558:c.488delG:p.G163fs	frameshiftdeletion	1630	NA/NA/NA/NA	0/0/0/0
	MKRN2	chr3:12623410	NM_001271707:c.G943A:p.E315K	nonsynonymous SNV	788	T/D/P/D	0/0/0/0
	CYP8B1	chr3:42916129	NM_004391:c.C1180G:p.P394A	nonsynonymous SNV	1076	D/D/D/D	0/0/0/0
	FBXW12	chr3:48436108	NM_001159927:c.A1169T:p.Y390F	nonsynonymous SNV	1294	D/D/P/N	0/0/0/0
	CRYBG3	chr3:97596474	NM_153605:c.G6436A:p.A2146T	nonsynonymous SNV	2858	T/B/B/N	0/0/0/0
	PABPC4L	chr4:135121727	NM_001114734:c.G622A:p.A208T	nonsynonymous SNV	680	NA/NA/NA/NA	0/0/0/0
	GGCT	chr7:30544279	NM_001199815:c.G47C:p.S16T	nonsynonymous SNV	1102	T/B/B/N	0/0/0/0

	YKT6	chr7:44246083	NM_006555:c.A287G:p.K96R	nonsynonymous SNV	1277	T/P/P/D	0/0/0/0
	KANK1	chr9:712884	NM_153186:c.G1644T:p.Q548H	nonsynonymous SNV	1441	T/P/B/D	0/0/0/0
	TRIM14	chr9:100850083	NM_014788:c.C998G:p.A333G	nonsynonymous SNV	150	T/P/P/N	0/0/0/0
	SLC34A3	chr9:140128639	NM_001177316:c.T1004A:p.L335H	nonsynonymous SNV	2108	D/D/D/D	0/0/0/0
	FRMD4A	chr10:13698791	NM_018027:c.A2798G:p.Q933R	nonsynonymous SNV	1973	D/B/B/D	0/0/0/0
	TRPC6	chr11:101324404	NM_004621:c.A2621G:p.K874R	nonsynonymous SNV	1353	T/P/B/D	0/0/0/0
	FAM186A	chr12:50749761	NM_001145475:c.A854G:p.Q285R	nonsynonymous SNV	1047	T/B/B/N	0/0/0/0
	SLC39A9	chr14:69919985	NM_001252150:c.C431A:p.S144Y	nonsynonymous SNV	321	T/D/P/D	0/0/0/0
	TMEM121	chr14:105995556	NM_025268:c.G385T:p.V129L	nonsynonymous SNV	430	D/D/D/D	0/0/0/0
	SLC9A3R2	chr16:2086816	NM_001252073:c.G349T:p.V117L	nonsynonymous SNV	2897	T/D/D/D	0/0/0/0
	PKD1	chr16:2142055	NM_000296:c.C11401A:p.L3801M	nonsynonymous SNV	909	T/D/D/N	0/0/0/0
	PKD1	chr16:2168136	NM_000296:c.C857G:p.S286C	nonsynonymous SNV	1864	T/D/P/D	0/0/0/0
	N4BP1	chr16:48595503	NM_153029:c.G1051A:p.V351I	nonsynonymous SNV	1637	D/B/B/D	0/0/0/0
	RND2	chr17:41179245	NM_005440:c.C236A:p.S79Y	nonsynonymous SNV	949	D/D/D/D	0/0/0/0
	ACTG1	chr17:79478321	NM_001199954:c.C695T:p.S232F	nonsynonymous SNV	423	D/P/P/D	0/0/0/0
	FN3K	chr17:80706786	NM_022158:c.C524G:p.A175G	nonsynonymous SNV	1776	NA/P/B/D	0/0/0/0
	TFF2	chr21:43770029	NM_005423:c.A190C:p.T64P	nonsynonymous SNV	1489	NA/B/B/N	0/0/0/0
	YDJC	chr22:21984285	NM_001017964:c.C19A:p.R7S	nonsynonymous SNV	1219	D/P/P/N	0/0/0/0
F9320							
	TAS2R19	chr12:11175041	NM_176888:c.G130A:p.A44T:	nonsynonymous SNV	65	D/P/P/N	0/0/0/0
	DDX23	chr12:49228222	NM_004818:c.G1441A:p.A481T:	nonsynonymous SNV	165	D/D/D/D	0/0/0/0

Table SIII: Rare variants with low allelic balance present in the indexes patients

Family	Gene	Position (hg19)	Variant	Type	Qual	*In silicopredictions* SIFT / Polyphen-2 HD; HV / MutationTaster	Frequency ExAC / 1kGP / ESP6500 / CEGH60+
F8463							
	SLMAP	chr3:57743457	NM_007159:c.C79A:p.P27T	nonsynonymous SNV	36	T/D/P/D/D	0/0/0/0
	CADPS	chr3:62459879	NM_183393:c.C3209A:p.T1070K	nonsynonymous SNV	42	T/B/B/D/D	0/0/0/0
	ZAR1	chr4:48493132	NM_175619:c.G824T:p.R275L	nonsynonymous SNV	31	T/P/B/NA/N	0/0/0/0

	ATP6V0E1	chr5:172410936	NM_003945:c.C73A:p.P25T	nonsynonymous SNV	48	D/D/D/D/D	0/0/0/0
	NACA	chr12:57113654	NM_001113203:c.A1660G:p.K554E	nonsynonymous SNV	34	D/B/B/NA/N	0/0/0/0
	RPL19	chr17:37358635	NM_000981:c.178_179del:p.R60fs	Frameshift deletion	767	NA/NA/NA/NA/NA	0/0/0/0
	TBCD	chr17:80878454	NM_005993:c.G2061T:p.L687F	nonsynonymous SNV	41	NA/D/D/N/D	0/0/0/0
	KCNK15	chr20:43379328	NM_022358:c.C842A:p.A281D	nonsynonymous SNV	34	T/B/B/N/N	0/0/0/0
	SMARCA1	chrX:128631855	NM_001282874:c.C1471A:p.L491M	nonsynonymous SNV	37	D/D/D/U/D	0/0/0/0
F8552 and F8566							
	OTOP1	chr4:4228377	NM_177998:c.C215T:p.A72V	nonsynonymous SNV	363	T/P/B/N/D	0/0/0/0
	SNW1	chr14:78205365	NM_012245:c.G370C:p.V124L	nonsynonymous SNV	406	T/B/B/D/D	0/0/0/0
	CATSPERD	chr19:5739390	NM_152784:c.513_514insTA:p.T171fs	Frameshift insertion	778	NA/NA/NA/NA/NA	0/0/0/0
F9320							
	ZNF860	chr3:32031995	NM_001137674:c.T1424C:p.I475T	nonsynonymous SNV	31	NA/P/D/NA/N	0/0/0/0
	VAX1	chr10:118897556	NM_001112704:c.A12T:p.K4N	nonsynonymous SNV	64	D/D/P/N/N	0/0/0/0
	ZNF681	chr19:23927110	NM_138286:c.C1242A:p.S414R	nonsynonymous SNV	41	T/B/B/NA/N	0/0/0/0

Table SIV: Rare homozygous and hemizygous variants

Family	**Gene**	**Position (hg19)**	**Variant**	**Type**	**Qual**	***In silico predictions*** **SIFT / Polyphen-2 HD; HV / Mutation Taster**	**Frequency** **ExAC / 1kGP / ESP6500 / CEGH60+**
F8368	MAGEB1	chrX:30269602	NM_177404:c.C992T:p.T331I	nonsynonymous SNV	2145	T/B/B/NA/N	0/0/0/0
F8463	NA	NA	NA	NA	NA	NA	NA
F8552 and F8566	RAB40AL	chrX:102192733	NM_001031834:c.A487T:p.I163F	nonsynonymous SNV	1220	D/D/P/U/D	0/0/0/0
F9320	KIR3DL3	chr19:55239223	NM_153443:c.G502A:p.V168I	nonsynonymous SNV	6638	T/B/B/N	0/0/0/0

III. Cell type-dependent non-specific FGF signaling in Apert Syndrome

Yeh, E *; Atique, R*; Fanganiello, RD; Yumi, D; Ishiy, FAA; Passos Bueno, MR.

Abstract

Apert Syndrome (AS) is one of the most severe forms of craniosynostosis. It is caused by gain-of-function mutations in the receptor FGFR2, which leads to ligand-receptor promiscuity. Here, we aimed to better understand the behavior of MSCs and of fibroblastoid cells, cellular populations that are part of the suture complex, when stimulated with different FGFs. We also aimed to verify whether FGFR2 specificity loss due to AS syndrome mutations would change their signaling behavior. We tested this hypothesis through cell proliferation and differentiation assays as well as through gene expression profiling. We found that FGF19 and FGF10 increase proliferation of fibroblastoid cells harboring the FGFR2 p.S252W mutation, but not of mutant mesenchymal stem cells (MSCs). FGF19 and FGF10 were associated with different expression profiles in p.S252W cells. Further, in accordance to our gene expression microarray data, FGF19 decreases bone differentiation rate of mutant fibroblastoid cells and increases bone differentiation rate of MSCs. This effect in osteogenesis seems to be mediated by BMP signaling. The present data indicate that non-natural FGFR2 ligands, such as FGF10 and FGF19, are important factors in the pathophysiology of AS. Further research is needed to determine the role of modulation of MSC proliferation or use of FGF19 or anti-BMP2 as inhibitors of osteogenesis in AS subjects' cells, and if these findings can be used in the clinical management of AS.

Resumo

A síndrome de Apert é uma das formas mais severas de craniossinostose. Ela é causada por mutações do tipo ganho de função no receptor FGFR2, o que leva à uma perda de especificidade entre o receptor e seus ligantes. Nesse trabalho nosso objetivo foi melhor compreender o comportamento de células tronco mesenquimais (MSCs) e células fibroblastóides, populações celulares que compõe o complexo sutural, quando estimuladas com diferentes FGFs. Nós também buscamos identificar se a perda de especificidade de FGFR2 devido à mutação causadora da S. de Apert alterariam seus comportamentos e sinalização. Nós testamos essa hipótese através de ensaios de proliferação e diferenciação celular além da identificação do perfil transicional dessas células. Nós descobrimos que FGF19 e FGF10 aumentam a taxa de proliferação de células fibroblastóides com a mutação p.S252W em FGFR2, mas não causam o mesmo efeito em MSCs mutantes. Tratamento com FGF10 e FGF19 resultaram em perfis de expressão gênica distintos em células mutantes. Além disso, de acordo com os dados de expressão gênica, FGF19 foi capaz de diminuir a taxa de diferenciação osteogênica em fibroblastóides mutantes mas aumenta a taxa de diferenciação osteogênica em MSCs. Esse efeito na osteogênese é mediado por sinalização por BMP. Os dados aqui apresentados indicam que ligantes não naturais de FGFR2 como FGF19 e FGF10 têm um papel importante na patofisiologia da S. de Apert. Estudos mais aprofundados são necessários para determinar o papel da modulação da proliferação de MSCs e se o uso de FGF19 e anticorpos anti-BMP2 seriam de serventia clínica no tratamento da S. de Apert.

Introduction

Through binding to Fibroblast Growth Factor Receptors (FGFRs), Fibroblast Growth Factors (FGFs) regulate several fundamental cellular processes, including proliferation, differentiation, regulation of cell cycle, metabolism and survival (BEENKEN; MOHAMMADI, 2009; LEMMON; SCHLESSINGER, 2010). FGFRs are highly conserved tyrosine kinase transmembrane receptors, present from cnidarian to chordates (REBSCHER et al., 2009). A hallmark of FGFRs is the alternative transcription into different isoforms, altering the extracellular Ig-like loops, responsible for ligand binding specificity. There are 4 genes that transcribe 7 different isoforms of FGFRs in humans, and each binds to a subset of the 22 known FGFs, i.e. FGFR2b binds specifically to FGFs 1, 3, 7, 10 and 22, and FGFR2c binds to FGFs 1, 2, 4, 6, 9, 17 and 18.(ORNITZ et al., 1996; XU; LIU; ORNITZ, 2000)

To initiate the FGF-FGFR signaling cascade, a FGF must bind to a FGFR, which dimerizes and undergoes transactivation through tyrosine autophosphorylation. The main downstream signaling pathways activated by FGF-FGFR binding are RAS/MAPK, PI3K and PLC pathways(TURNER; GROSE, 2010) .Since FGF-FGFR signaling has a ubiquitous role in development and in maintenance of homeostasis, germline gain-of-function mutations affecting this circuitry have disruptive consequences in several organs. Impairment or abnormalities in FGF-FGFR signaling has been linked to several diseases, including cancer, rickets, cleft lip and palate, skeletal dysplasias, and craniosynostosis(HUNTER et al., 2007; ITOH; ORNITZ, 2011). Apert Syndrome is one of the most severe forms of syndromic craniosynostosis(COHEN, 2002) and is characterized by premature closure of the coronal sutures, agenesis of the metopic and sagittal sutures, severe syndactyly of hands and feet and joint malformations (COHEN, 1995). Craniofacial surgery is required to release increased intracranial pressure as well as to normalize skull appearance. Nonetheless, re-synostosis is a frequent hurdle after surgical intervention in Apert patients.

Among the best characterized *FGFR2* recurrent mutations leading to Apert Syndrome (AS) are p.S252W (contributing to approximately 75% of the cases) and p.P253R (accounting for almost 25% of the cases). Both p.S252W and p.P253R mutations are located in the extracellular portion of FGFR2 and cause loss of ligand binding specificity of the mesenchymal expressed isoform (FGFR2c) and of the epithelial expressed isoform (FGFR2b), leading to promiscuous receptors

that can be activated by any of the FGF molecules, as demonstrated by plasmon resonance experiments (GREEN; WALSH; DOHERTY, 1996; IBRAHIMI et al., 2004; WILKIE et al., 2002). Crystal structure analysis of the interaction between FGFs and FGFR2 with p.S252W or p.P253R mutations has shown that FGFs with a hydrophobic amino acid at the residue corresponding to phe21 in FGF2 have increased affinity for p.S252W FGFR2 (IBRAHIMI et al., 2001). Therefore, as a consequence of p.S252W and p.P253R mutations, aberrant signaling caused by promiscuous FGF-FGFR2 bindings is proposed as the molecular cause of Apert Syndrome(PARK; BELLUS; JABS, 1995; SLANEY et al., 1996).

We have previously established that the p.S252W FGFR2 germline gain-of-function mutation is associated with a specific gene expression signature, comprised of transcripts not only associated with the overstimulation of the FGFR2 canonical downstream pathway, but also of transcripts that contribute to novel pathological signaling (FANGANIELLO et al., 2007). Moreover, we showed that this mutation has a more drastic effect in periosteal fibroblastoid cells than in mesenchymal stem cells (MSCs) and that this cell-type specific effect may contribute to the pathophysiology of AS (YEH et al., 2011), during both embryogenesis and childhood development. Even though different ligands can bind to FGFR2 and are considered to activate the same downstream networks, each ligand can produce a specific cellular behavior and, although receptor promiscuity is well established as the molecular cause of AS(BRIGHTMAN; FELL, 2000), the functional effects of the binding of different FGFs that do not naturally bind to FGFR2 in the cellular phenotype of AS is currently unknown. This knowledge is essential to better understand the pathophysiology of Apert syndrome as well as to tackle the problem of resynostosis in AS following surgical intervention with a pharmacological strategy(WALL et al., 1994).

Here, we hypothesized that stimulation by different FGFs leads to distinct cellular behaviors in periosteum-derived fibroblastoid cells and in MSCs from AS subjects harboring the p.S252W mutation in FGFR2. We aimed to investigate changes dependent on the cellular context at the molecular and at the cellular levels elicited by activation of p.S252W FGFR2 by different ligands.

Methodology

Subjects

Coronal suture periosteal tissue from four unrelated AS subjects (p.S252W mutation in FGFR2) and from three age- and sex-matched control subjects (WT) were obtained as previously described(FANGANIELLO et al., 2007; YEH et al., 2011, 2013). The presence of the p.S252W FGFR2 mutation was confirmed by direct DNA sequencing and expression of the mesenchyme-specific isoform of FGFR2 in the primary fibroblastoid cells was examined by Western Blot and RT-PCR. Only the expression of the FGFR2c isoform in control and AS periosteal cells, with no apparent difference between these two, was observed(FANGANIELLO et al., 2007; YEH et al., 2011, 2013).

The project was approved by the Research Ethics Committee - Human subjects (Comitê de Ética em Pesquisa – Seres Humanos) at the Institute of Biosciences/University of Sao Paulo (protocol # 024 / 2004) and was performed according to the amended Declaration of Helsinki. All patients and controls were already enrolled for treatment and surgery at the Department of Plastic Surgery, School of Medicine, University of Sao Paulo, when we contacted them. Thus, those who declined to participate or otherwise did not participate were not disadvantaged in any other way by not participating in the study. Appropriate informed consent was obtained for the donation of the periosteum, a tissue that is usually discarded during surgical treatment, so that this procedure would represent no harm for any of the subjects. Because all the participants were under the age of 18, legal guardians gave written consent on behalf of them.

Cell Culture

Periosteal overlying the coronal suture harvested from AS patients or control individuals were used for both fibroblast and MSC extraction, as previously described(FANGANIELLO et al., 2007; YEH et al., 2011, 2013) Primary fibroblastoid cells (WT: n=3; p.S252W FGFR2: n=3) were grown in fibroblast growth medium (DMEM High-Glucose, 20% fetal bovine serum [FBS; GIBCO] and 100 U/mL penicillin and 100 µg/mL streptomycin [1% Penicillin Streptomycin; GIBCO]). MSCs (WT: n=3; p.S252W FGFR2: n=3) were grown in MSC growth medium (DMEM/F12, 10 %FBS,1% Nonessential aminoacids, 1% penicillin/Streptomycin). Cells were passaged at near confluency with trypsin-EDTA. All cells were cultured in a humidified incubator at 37°C and 5% CO_2. All tests were performed between the third and the fifth subcultures. To further attest that both the surgical isolation of periosteum and the cell culture expansion procedure were leading to a

homogeneous cell sample, we compared gene expression of MSC-specific and Fibroblast-specific markers(HALFON et al., 2011) in our cultures. Regardless of the presence of the FGFR2 gene mutations, fibroblastoid cell lines showed 1.48-fold higher expression of *MMP1* and 1.74-higher expression of *MMP3* compared to MSCs, while MSC lines had 1.77-fold increased expression of *VCAM1* and 1.15-fold increased expression of *ITGA11* compared to fibroblastoid lines.

We performed experiments in technical triplicates in each of the 12 cell lines. For all the experiments, we used all twelve cell lines for each condition, the exceptions are indicated by an "n" value. Thus we tried to ensure that the results we obtained were representative of the biological variance seen in human patients.

Exogenous FGF treatment

Periosteal fibroblastoid cells were grown until they reached 80% of confluency. Cells were washed with 1x PBS and then were serum starved for 24h in DMEM High-Glucose not supplemented with FBS. After this period, control condition cultures were grown in DMEM High-Glucose, 0.5% FBS while experimental condition cultures, in DMEM High-Glucose , 0.5% FBS [GIBCO] supplemented with recombinant human FGF2, FGF10 or FGF19 (PeproTech, Rocky Hill, NJ, USA – diluted in 1x PBS –Phosphate Buffered Saline- to a final concentration of 2000 pM). Similar phosphorylation level of both WT and p.S252W FGFR2c was observed when treated with 2000 pM of FGF (YU et al., 2000).

Cell proliferation analysis

A density of 10,000 cells/cm^2 was plated to each well of a 12-well flat bottom plate in fibroblast growth medium. After 24h, when total cell adhesion was verified, the fibroblastoid cells were serum-starved for 24h and MSCs for 48h. At the initial time point (0h), we changed the starvation medium (fibroblast growth medium or MSC growth medium without FBS) for the respective cell growth medium or starvation medium supplemented with FGFs. At the indicated time points, the cells were trypsinized and counted using Guava EasyCyte Flow Cytometer (Guava Technologies).

RNA extraction

Cells at a confluency of 80% in 25 cm^2 cell culture flasks were used for FGFs 10, and 19 treatment followed by microarray and qRT-PCR assays. Following 24h of exogenous FGF treatment, total RNA was isolated using Nucleospin RNA kit (Macherey-Nagel, Düren, Germany).

Microarray Assays

For each RNA sample, cDNA was generated with the Affymetrix GeneChip WT cDNA Synthesis and Amplification Kit (Affymetrix, Santa Clara, California) following the manufacturer's instructions. cDNA was fragmented and end labeled with the Affymetrix GeneChip WT Terminal Labeling Kit (Affymetrix, Santa Clara, California). Approximately 5.5 µg of labeled DNA target was hybridized to the Affymetrix GeneChip Human Gene 1.0 ST array (Affymetrix, Santa Clara, California)(which interrogates 28869 well-annotated genes) at 45°C for 16h per manufacturer's recommendation. Hybridized arrays were washed and stained on an Affymetrix GeneChip Fluidics Station 450 (Affymetrix, Santa Clara, California) and scanned on an Affymetrix GCS 3000 (Affymetrix, Santa Clara, California).

Intensity data were subjected to Robust Multichip Average (RMA) and afterwards, to identify differentially expressed genes (DEGs), we used the Limma (WETTENHALL; SMYTH, 2004) and Rank -Prod (HONG et al., 2006) methods, available in the R/Bioconductor package, both with p-value ≤ 0.05 adjusted by False Discovery Rate (FDR) correction factor. In order to minimize biological variations and focus on the effect of the ligand, we compared the expression data of all three treated fibroblast populations, whether harboring the p.S252W mutation in FGFR2 or WT, with the corresponding expression data of the same three untreated fibroblast populations. We extracted the genes that were commonly selected by the two different methods (RankProd and Limma) as significantly differentially expressed (DEGS) in order to minimize false positive occurrence. The Limma method performs statistical analysis based on a moderate t-statistics to test the average difference in log expression levels between the treated and the control groups for each gene (TUSHER; TIBSHIRANI; CHU, 2001). The RankProd is a rank-based non-parametric method that uses geometric mean rank for each gene and its distribution is estimated by randomly permuting the observed ranks. The permutation principle partly alleviates the small sample sizes issue, enhancing the robustness against outliers (SAEYS; INZA; LARRAÑAGA, 2007). To analyze the result, we used QIAGEN's Ingenuity Pathway Analysis (IPA® , QIAGEN Redwood City, www.qiagen.com/ingenuity) software for generating gene interaction networks and functional classification of DEGS, the gene interaction network were generated by using the core analysis default settings, considering only direct relationships indicated by the curated databases available from the software publisher; DAVID was used for the enrichment of gene ontology and GT (GeneTrail) for analysis of over-or under representation of biological categories and pathways.

Hierarchical clustering was performed by average linkage of genes and arrays utilizing GEne Cluster 3.0 and visualized with Treeview. (DE HOON et al., 2004)

Reverse Transcription Reactions and Quantitative Real Time PCR

Complementary DNA (cDNA) was produced from 1 μg of total RNA using Superscript II reverse transcription kit (Invitrogen, Carlsbad, CA, USA). qRT-PCR, assay was performed using approximately 20 ng of cDNA and SYBR Green PCR master mix in an ABI Prism 7500 system (Applied Biosystems, California, USA). Primers were designed with Primer Express software V.2.0 (Applied Biosystems, California, USA) and the amplification efficiency (E) of each primer was calculated according to the equation: E=10(-1/slope). The expression data of the studied transcripts was determined by relative quantification in comparison to endogenous controls (*GAPDH*, *HMBS*, *HPRT1* and *SDHA*). Primers' amplification efficiencies (E) were determined by serial cDNA dilutions expressed in $\log_{10}$ in which $E = 10^{-1/slope}$. Expression of target genes was assessed relative to a calibrator cDNA pool (ΔCt). We verified the gene expression stability of endogenous controls through geNorm VBA applet designed for Microsoft Excel (VANDESOMPELE et al., 2002). Samples from all cells analyzed previously in Microarray assay were run in technical triplicates, and the threshold suggested by the instrument software was used to calculate Ct. Primers used in this study are summarized in Supplementary Table 1. To assess the statistical significance of the correlation between microarray assay data and the qRT-PCR results we used the nonparametric two-tailed Spearman correlation test, with p-values of less than 0.05 considered to be statistically significant.

In vitro osteogenic differentiation

To induce osteogenic differentiation, periosteal fibroblastoid cells and MSCs from three AS patients and from three controls were plated in 24-well plates (5×10^3 cells/cm^2) and cultured for three weeks in osteogenic medium (DMEM Low-Glucose, 0.5% FBS [GIBCO], 0.1 mM dexamethasone (Sigma-Aldrich Corp., St. Louis, MO), 50 mM ascorbate-2-phosphate (Sigma-Aldrich), 10 mM β-glycerophosphate (Sigma-Aldrich), and 1% Penicillin Streptomycin [GIBCO]). For the co-culture assay, the cells were plated at the same concentration onto 12-mm transwell inserts of 12-well plates, 0.4 μm pore size (Corning Costar). Media changes occurred every three to four days.

Alkaline phosphatase activity was assessed on the 9th day of differentiation through a biochemical assay. The cells were provided with phosphatase substrate (Sigma-Aldrich) and the

resulting p-nitrophenol was measured colorimetrically by the use of a Multiskan EX ELISA plate reader (Thermo Scientific) at 405 nm.

After 14 and 21 days, calcified matrix production was analyzed by alizarin red staining and quantification was done as previously described(GREGORY et al., 2004).

In vivo osteogenic differentiation

A 4.5 mm in diameter ceramic scaffold (60% hydroxyapatite and 40% of β-tricalcium phosphate; CellceramScaffdex^{TM}) was moistened with osteogenic medium and mixed with 10^6 human fibroblastoid cells or MSCs. The cells attached to the scaffold were pre-differentiated in osteogenic medium and incubated at 37^{o}C in 5% CO2 for five days.

For the *in vivo* differentiation we used 8 non-immunosuppressed (NIS) Wistar rats (all males, aged 2 months, weighing a maximum of 200 g as previously described by our group and approved by the ethical committee of our Institute (DE MENDONÇA COSTA et al., 2008; YEH et al., 2011). We used a trephine bur of 4.5 mm diameter to obtain two cranial critical defects which were made in the parietal region, lateral to the sagittal suture, where two scaffolds were implanted per animal, one side being filled by biomaterial alone (left defect) and the other by the biomaterial associated with cells (right defect). The animals were kept in ventilated racks with standard conditions of temperature and lighting (22^{o}C, 12 h light cycling per day) with free access to food and water. Four weeks after surgery, the rats were sacrificed in a CO^2 chamber, as previously described by our group and approved by the ethical committee of our Institute(DE MENDONÇA COSTA et al., 2008; YEH et al., 2011). The calvaria was removed and fixed in 10% formalin for 24h and then decalcified in 5% formic acid for 48h and embedded in paraffin. Slices of 5 µm were obtained and stained with hematoxylin and eosin.

We analyzed three transversal 4 µm slices of the calvaria with 10 µm of distance of each animal. Ossification area of each defect was calculated through Axio Vision Carl Zeiss based on 10x amplified images obtained from Axio Observer.A1 Carl Zeiss microscope. The percentage of the defect area that ossified at the right side was normalized by the percentage of the defect area that ossified at the left side, so that for each animal we obtained 3 ratio values.

Statistical analysis

Continuous variables were expressed by mean and standard deviation, and the groups were compared by Student's t-test. A p value < 0.05 was considered statistically significant. The tests were performed using the GraphPadInStat software (GraphPad).

Results

Exogenous FGF10 and FGF19 increases proliferation in fibroblastoid cells harboring p.S252W FGFR2 mutation

In order to verify if different FGFs lead to similar functional changes in p.S252W FGFR2 cells (BEENKEN; MOHAMMADI, 2009), we selected FGFs that comprehensively represent all the 6 FGF subfamilies known, and based on the knowledge that FGFs overall have increased affinity for p.S252W FGFR2(IBRAHIMI et al., 2004). We first screened the effect of 7 FGFs (FGF2, FGF7, FGF8, FGF9, FGF10, FGF18 and FGF19) in the proliferation of p.S252W FGFR2 fibroblastoid cells (n=1) compared with WT fibroblastoid cells (n=1), in technical triplicates. As expected, only FGF2-treated control fibroblastoid cells showed a significant increase in proliferation (25%, $p<0.05$) compared with untreated WT cells. Conversely, the proliferation of p.S252W FGFR2 fibroblastoid cells was significantly increased when treated with FGF2 (100%, $p<0.05$), FGF10 (75%, $p<0.05$), or FGF19 (125%, $p<0.01$) (Figure 1A and 1B). Noteworthy, both FGF10 and FGF19 are not natural ligands of the wild-type mesenchymal isoform of FGFR2, expressed in fibroblastoid cells (IBRAHIMI et al., 2004). Moreover, different than most FGFs, which works in a paracrine fashion, FGF19 is one of the 3 FGFs (*i.e.* FGF19, FGF21, and FGF23) that have a systemic effect.

We further confirmed this result in an additional set of p.S252W FGFR2 fibroblastoid cells (n=2) and WT fibroblastoid cells (n=2), all in technical triplicates and in passages 4 to 5 (Figure 1C and 1D). All mutant cells showed a significant increase in proliferation in the presence of FGF2, FGF10 or FGF19 (Figure 1D) while, confirming our previous results, the only significant increase observed in WT fibroblastoid cells was in the presence of FGF2 (Figure 1C).

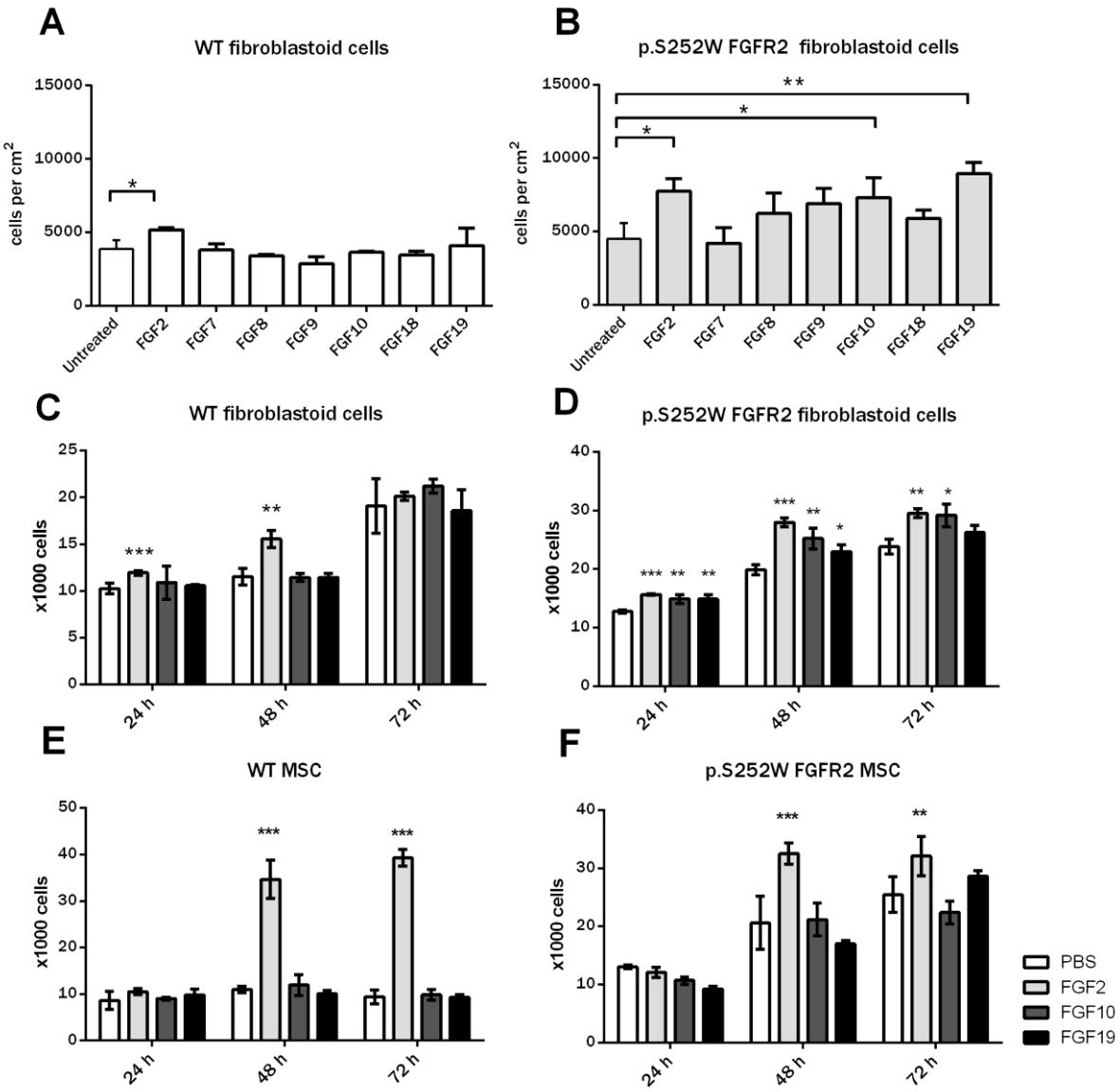

Figure 1: Cell proliferation rate of **A-** wild-Type fibroblastoid cells and **B-** p.S252W fibroblastoid cells (after initial time point 0h, we changed the starvation medium for the respective cell growth medium or starvation medium supplemented with FGFs). Cell proliferation rate after different treatments with PBS (control), FGF2, 10 and 19 in **C-** wild-Type fibroblastoid cells, **D-** p.S252W fibroblastoid cells, **E-** wild-Type mesenchymal stem cells and **F-** p.S252W mesenchymal stem cells. At the indicated time points, the cells were trypsinized and counted using Guava EasyCyte Flow Cytometer (Guava Technologies). Values represent means +/- SD, $p<0.05$ (*), $p<0.01$ (**), $p<0.001$ (***).

FGF10 and FGF19 have distinct effects on gene expression profile of p.S252W FGFR2 fibroblastoid cells

We have previously shown that activation of p.S252W FGFR2 by FGF2 not only exacerbates FGFR2 the canonical downstream signaling pathway but also induces abnormal novel molecular pathways (YEH et al., 2011). Based on these previous observations and the more significant effects of FGF10 and FGF19 in the proliferation rate of p.S252W FGFR2 cells, two questions arise: 1) what are the downstream signaling circuitries activated by non-natural ligands binding to p.S252W FGFR2; and 2) whether this molecular signature is similar for FGF19 and FGF10. To address these questions, we performed whole transcriptome analysis in FGF10 and FGF19 treated p.S252W FGFR2 and WT fibroblastoid cells.

As expected, no significant functional enrichment of differentially expressed genes (DEGs) was observed in WT fibroblastoid cells when cells were treated with FGF10, since FGF10 does not bind to any of the FGFRs expressed in tissues of mesenchymal origin (IBRAHIMI et al., 2004; ZHANG et al., 2006). Contrariwise, treatment with FGF10 resulted in 59 DEGs in p.S252W FGFR2 fibroblastoid cells (Supplementary Table 2), of which, 10 are genes associated with inflammatory diseases (*HLA-DMA*, *OR12D3*, *MOG*, *RING1*, *TCF19, C6ORF15*, *CLIC2*, *LY6G5C*, *POP* e *XCL1*), and immune response was the most enriched biological process (IPA: $p<0.001$; GT: $p<0.001$). The most enriched gene interaction network, containing 8 out of the 59 genes, is associated with cellular development and cell cycle (Figure 2A), and central nodes of this network are transcription regulators EZH2, E2F1 and TP53(Figure 2B), which are all key players in cell growth and development (GARKAVTSEV et al., 2001; TIFFEN et al., 2015; WU et al., 2001). Between the DEGs in WT cells treated with FGF10 and p. S252W cells treated with FGF10, there were 5 transcripts in common (Figure 2D), four of which had opposite pattern of regulation: IGHV3-11-001 (Immunoglobulin Heavy Variable 3-11; Fold-change in WT: -4.15, FC in p.S252W: 3.17), LOC100132785 (gene of unknown function; FC in WT: -1.45, FC in p.S252W: 3.01), GOLGA6L1 (Golgin A6 family-like 1; FC in WT: 3.85, FC in p.S252W: -2.33), noncoding RNA: Mitochondrial tRNA pseudogene (FC in WT: 0.997, FC in p.S252W: -1.56). A non-coding RNA: small nucleolar RNA pseudogene transcript was the only one downregulated with FGF10 treatment in both wild type and p.S252W fibroblastoid cells.

Treatment of wild-type fibroblastoid cells with FGF19 is associated with the differential expression of 45 genes (Supplementary Table 3) and the most enriched biological function among these DEGs was also immune response (IPA: $p<0.001$; GT: $p<0.05$). Accordingly, 6 DEGs formed an interaction network enriched for antigen presentation and immune response (Figure

2B). SMARCA4 and STAT3 are the two central nodes of this network (Figure 2B). One of the signaling pathways associated with FGFR activation is the JAK-STAT pathway(RAWLINGS; ROSLER; HARRISON, 2004), which leads to nuclear translocation of STAT transcription factors, including STAT3. Likewise, SMARCA4 is a transcriptional activator. Both proteins are essential from early development and knockout of either gene is embryonically lethal (BULTMAN et al., 2000; TAKEDA et al., 1997). Addition of FGF19 to p.S252W FGFR2 fibroblastoid cell culture led to differential expression of 46 genes (Supplementary Table 4). The most enriched cellular functions were immune response (IPA: $p<0.05$; GT: $p<0.05$), cell proliferation (IPA: $p<0.05$; GT<0.05) and ossification (IPA: $p<0.005$; GT<0.01) (Figure 2C). Central nodes of this network are STAT genes (STAT1 and STAT3), likely activated by the same mechanism as in WT cells treated with FGF19, and IRF genes (IRF3, IRF5 and IRF8)(Figure 2C). IRF genes encode interferon regulatory factors, transcription factors used in the JAK-STAT signaling pathway(DARNELL; KERR; STARK, 1994). There were two transcripts in common listed in WT cells treated with FGF19 and p. S252W cells treated with FGF19: non-coding RNA (ENST00000364918; FC in WT: -0.96, FC in p.S252W: 0.64) and non-coding RNA Mitochondrial tRNA pseudogene (ENST00000386778; FC in WT: 6.3, FC in p.S252W: 0.65). We selected 12 of the differentially expressed genes identified in the microarray experiments and performed qRT-PCR in order to corroborate the statistical analysis done in the microarray dataset. We selected genes based on two different criteria: 1) genes that were found differentially expressed in more than one microarray comparison; 2) Genes with the highest fold-change within each comparison. The genes chosen by criteria 1 were: *ARL17*, *BAT3*, *FAM60A*, *TCF19* and *HLA-DMA*. The genes chosen by criteria 2 were: *CFHR1*, *CLIC2, MGP, CKS2, DDX58, OAS3,* and *SAMHD1*. The ΔΔCt from qRT-PCR and fold-change from the microarray experiment showed significant correlation (Supplementary Figure 1), thus validating the microarray gene expression analysis.

To further address the question of whether non-natural FGF ligands lead to different downstream effects of mutant FGFR activation, we compared the results of p.S252W fibroblastoid cells treated with FGF10 and FGF19 and compared to the FGF2 activated cells (previously published in (YEH et al., 2013)). Comparison of gene regulation between canonical (FGF2 treated) and non-canonical (FGF10 treated or FGF19 treated) FGFR2 activation showed that each FGF led to distinct DEG: only one transcript was found in common between the three conditions, RNA5SP502 (RNA, 5S ribosomal pseudogene 502) (Figure 2D). Hierarchical clustering of the DEGs of each of the 3 conditions further attests that the molecular signature for FGF10 and FGF19 are different from the canonical FGFR2c activation gene expression profile, but they are distinct of each other (Figure 2E).

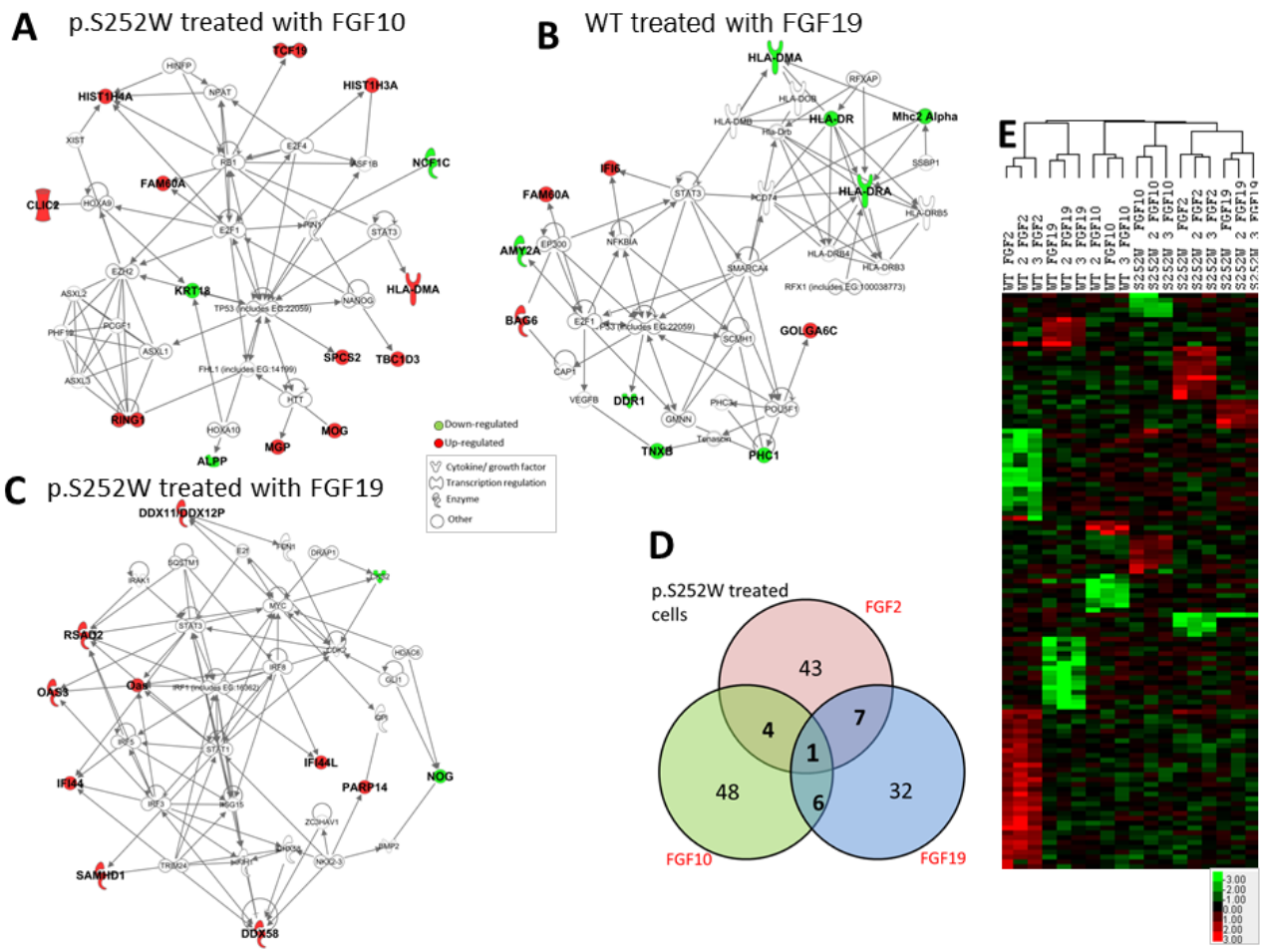

Figure 2: Most relevant Gene interaction networks based on DEGs after treatment of Fibroblastoid cells with exogenous FGFs. A: p.S252W treated with FGF10; B: WT cells treated with FGF19; C: p.S252W cells treated with FGF19. Genes shown in bold lettering are differentially expressed genes, genes colored in red are overexpressed in the experiment and genes colored in green are underexpressed. The symbols are representative of the molecule class that the protein encoded by each gene belongs. The lines represent the interaction between molecules, straight lines represent binding, lines ending in arrowheads represent activation. D- Venn diagram showing the number of common DEGs between cells harboring the mutant FGFR2 receptor in response to FGF2 (from previously published data, Yeh et al., 2013), to FGF10 and to FGF19. E- Hierarchical clustering of the microarray data of all lines treated with FGF2 (from previously published Yeh et al., 2013), FGF10 and FGF19.

FGF19 has opposite effects in the osteogenesis of p.S252W FGFR2 MSCs and fibroblastoid cells

Work by our group and others have previously shown that p.S252W and p.P253R mutations in FGFR2 respond differently to environmental factors depending on their cellular context, both *in vitro* and *in vivo*. Thus, we also analyzed cellular phenotypes in MSCs harboring the p.S252W in FGFR2, in response to FGFs10 and 19 and compared these results with those observed in fibroblastoid cells.

First, we verified if treatment with FGFs 2, 10 and 19 had different effects in p.S252W FGFR2 MSCs when compared with wild-type MSCs. Proliferation of both p.S252W MSCs and wild-type MSCs was only significantly increased when adding FGF2 to the medium, but not when adding FGF10 or FGF19 (Figure 1E and 1F).

Our microarray gene expression analysis has shown that FGF19, but not FGF10, alters the transcription of genes associated with ossification, one of the main physiological functions altered in Apert Syndrome. Moreover, a direct connection between FGF19 and Apert syndrome has not yet been suggested. Therefore, we next aimed to dissect the impact of FGF 19 in *in vitro* osteogenesis using different cellular context and in *in vivo* bone formation; FGF10 has been considered as additional control of the experiments. WT and p.S252W FGFR2 periosteal fibroblastoid cells and MSCs were treated with osteogenic induction medium supplemented with FGFs 10 or 19. As anticipated by the microarray results, no significant difference in osteogenic differentiation induced by FGF10 was observed in neither cell types (data not shown). In osteogenic medium supplemented with FGF19, no difference was observed at early and late time points of osteogenesis in both cell types, as attested by analysis of alkaline phosphatase enzyme activity at day 9 and alizarin red-S staining at day 21 of *in vitro* osteogenesis (Figure 3). However, by mid-osteogenesis (day 14), FGF19 significantly inhibited ossification in p.S252W FGFR2 fibroblastoid cells ($p<0.001$, Figure 3B), while in p.S252W FGF2 MSCs, FGF19 did not interfere in the osteogenic effect (Figure 3E), as shown by alizarin red-S staining.

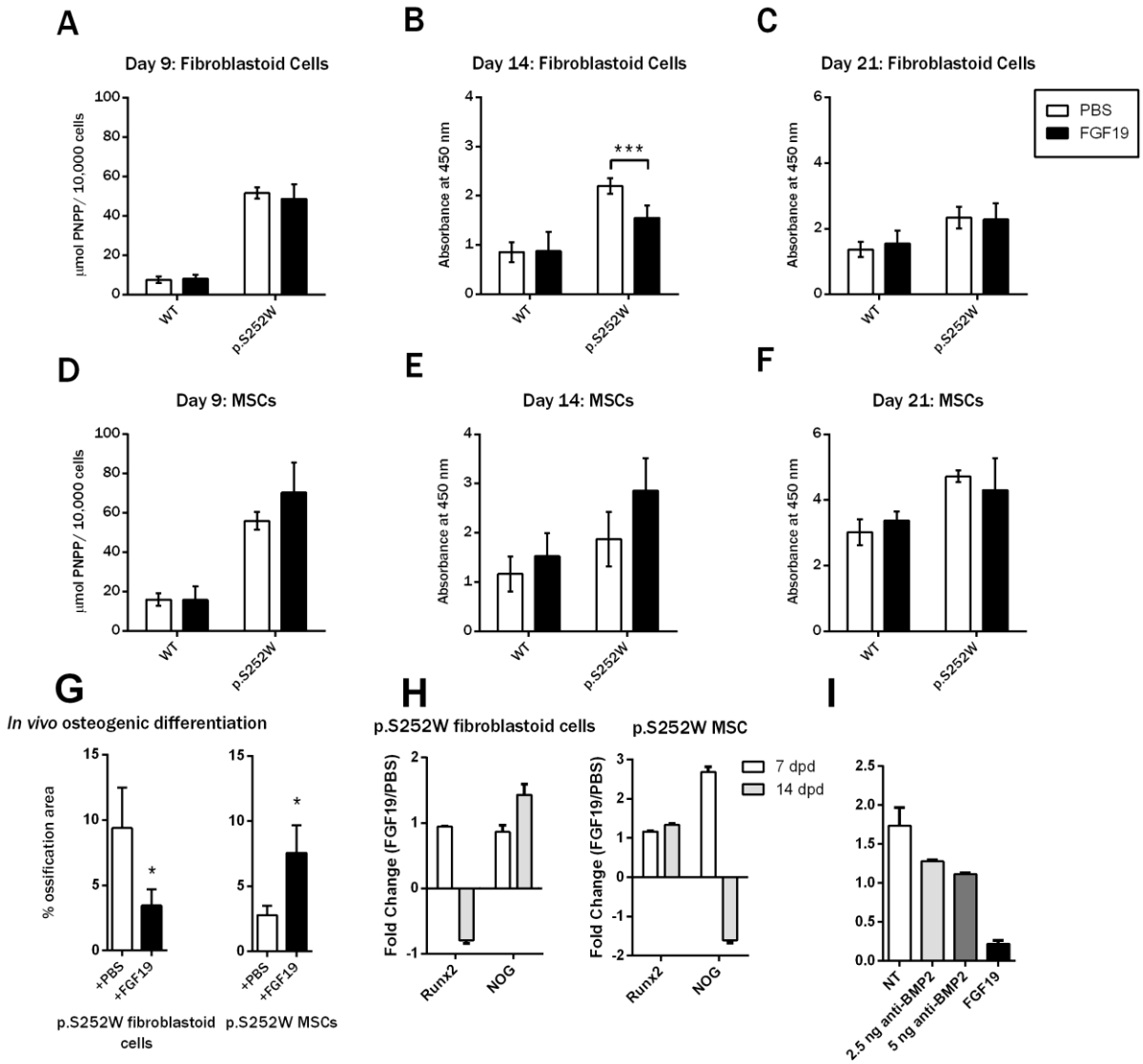

Figure 3: Comparison of in vitro osteogenic differentiation of fibroblastoid cells **A** (Alkaline Phosphatase activity quantification at 9 days) **B** and **C** (Alizarin Red S staining at 14 and 21 days); Comparison of in vitro osteogenic differentiation of mesenchymal stem cells **D** (Alkaline Phosphatase activity quantification at 9 days) **E** and **F** (Alizarin Red S staining at 14 and 21 days); Quantification of in vivo ossification using **G-**p.S252W fibroblastoid cells and **H-**p.S252W mesenchymal stem cells (Ossification area of each defect was calculated through Axio Vision Carl Zeiss based on 10x amplified images obtained from Axio Observer). **I-** Effects of anti-BMP2 antibody compared to FGF19 shown by Alizarin red staining quantification in co-cultures of periosteal p. S252W FGFR2 fibroblastoid and MSCs. Values represent means +/- SD, $p<0.05$ (*), $p<0.01$ (**), $p<0.001$ (***).

We next aimed to validate the differential effect of FGF19 in the osteogenic potential of p.S252W FGFR2 MSCs and fibroblastoid cells in an *in vivo* model. We adopted a bilateral cranial critical-size defect model using Wistar non-immunosuppressed rats as previously described by our group (DE MENDONÇA COSTA et al., 2008; YEH et al., 2011). Fibroblastoid cells harboring the p.S252W FGFR2 were pre-differentiated for 5 days with osteogenic medium. Defects where we introduced biomaterial associated with p.S252W FGFR2 fibroblastoid cells with FGF19-containing heparin beads displayed less ossification when compared with defects where we inserted the biomaterial associated with p.S252W FGFR2 fibroblastoid cells and without FGF19 (saline vs. +FGF19: $p<0.05$; figure 3G). On the other hand, in defects where we introduced the biomaterial associated with p.S252W FGFR2 pre-differentiated MSCs and FGF19-containing heparin beads, the bone neo-formation was increased compared with the defects where we inserted the biomaterial associated with p.S252W FGFR2 MSCs without FGF19 (saline vs. +FGF19: $p<0.05$; Figure 3H). In all groups, abundant loose connective tissue was observed filling the scaffolds' pores in a heterogeneous distribution, showing the adhesion and cellular maintenance ability of this biomaterial. Bone tissue was distributed radially in the pores of all groups but a consistent and broad distribution of bony islands, including in the central areas of the implants, was observed when p.S252W FGFR2 MSCs were associated with FGF19 or when p.S252W FGFR2 fibroblastoid cells were transplanted free of recombinant FGF19.

FGF19 affects osteogenesis of p.S252W FGFR2 fibroblastoid cells through BMP signaling

One of the differentially expressed genes with the highest fold-change (FC=-2.4) induced by the presence of FGF19 in p.S252W FGFR2 fibroblastoid cells was *NOG*, which encodes the BMP signaling inhibitor NOGGIN. NOGGIN is well established in the literature as a suppressor of bone formation *in vitro* and *in vivo* (WAN et al., 2007; WARREN et al., 2003; WU et al., 2003). The transcription factor *RUNX2* is a master regulator of osteoblast differentiation (KRONENBERG, 2003; KRONENBERG et al., 2004; SCHROEDER; JENSEN; WESTENDORF, 2005) and *BMP* signaling is required for RUNX2-dependent osteogenesis (LEE et al., 2003). Hence, in order to better determine the molecular mechanism underlying the differential effect of FGF19 in p.S252W FGFR2 fibroblastoid cells compared with p.S252W MSCs, we analyzed gene expression of these two pivotal osteogenesis markers, NOG and RUNX2, up to mid-osteodifferentiation (Figure 4).

Analysis of NOG and RUNX2 expression in WT MSCs throughout osteodifferentiation shows that expression of both genes is highly correlated (Figure 4A, $R2=0.78$; $p<0.0001$).

At 14 days of *in vitro* osteodifferentiation, *RUNX2* gene expression was downregulated by FGF19 (Figure 4C), while *NOG* was upregulated by FGF19 (Figure 4B) in p.S252W FGFR2 fibroblast. This is in agreement with the decrease in osteogenesis induced by FGF19 in p.S252W FGFR2 fibroblastoid cells cell cultures (Figure 3B). Moreover, only in the presence of FGF19 the expression levels of RUNX2 and NOG are significantly associated (Spearman correlation: R^2=8571, p-value=0.01, Figure 4E), suggesting NOG and RUNX2 expression are independent in p.S252W FGFR2 fibroblastoid cells undergoing osteodifferentiation, but are both influenced by FGF19.

Meanwhile, in p.S252W FGFR2 MSCs, *RUNX2* gene expression is slightly upregulated by FGF19 (Figure 4G), while *NOG* is downregulated by FGF19 (Figure 4F). Expression levels of these two genes are not correlated in p.S252W MSC cells even when treated with FGF19 (Figure 4G and 4I). These data suggest that decreased osteogenesis induced by FGF19 activation of the mutant FGFR2 is likely associated with inhibition of BMP signaling by NOGGIN. They also suggest that NOGGIN and BMP signaling are potentially key regulators of p.S252W FGFR2 fibroblastoid cells` osteogenesis

Previously, we have shown that the premature suture fusion and resynostosis in AS subjects are likely the result of perturbations in FGF-FGFR2 signaling and in interactions between fibroblasts and MSCs at the cranial suture complex (FANGANIELLO et al., 2007; YEH et al., 2011). To test if the effect of BMP2 inhibition or addition of FGF19 affects the interaction between the two cell population with the p.S252W mutation, we used a co-culture system to simulate the *in vivo* anatomic niche between the fibroblastoid cells and MSCs in the periosteum, allowing the paracrine signaling without physical cell interaction.. As expected, we observed decreased formation of mineralized nodules as we increased the concentration of BMP2 antibody (Figure 3I). Similarly, FGF19 decreased osteogenesis in the co-cultures when compared with inhibition of BMP2 (Figure 3I).

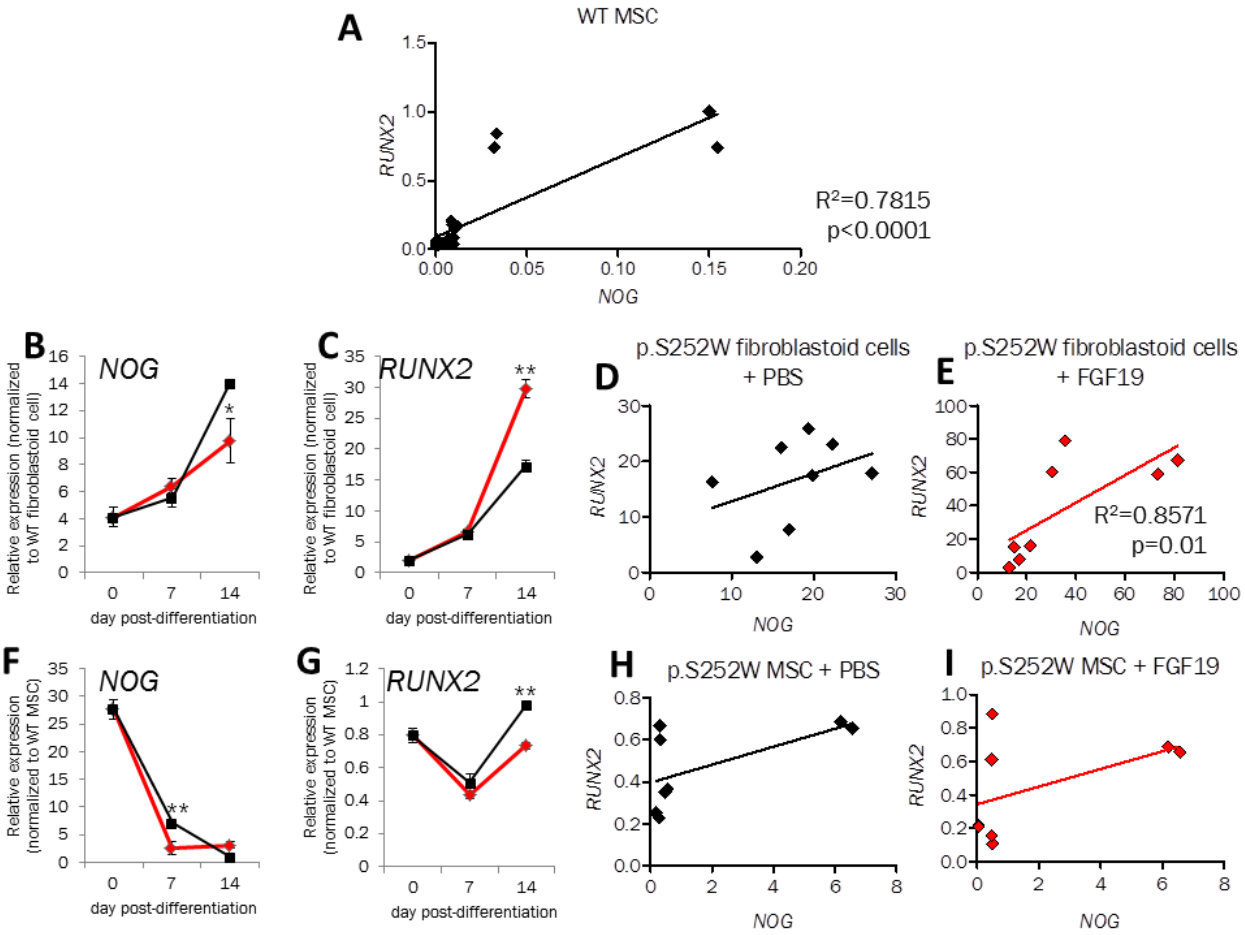

Figure 4. A- Correlation between the gene expression of *RUNX2* and *NOG* in WT MSCs in control osteoblastic differentiation conditions. Expression levels of *NOG* **(B)** and *RUNX2* **(C)** during early and mid-differentiation in p.S252W fibroblastoid cells, and correlation between these gene expression in p.S252W fibroblastoid cells without **(D)** and with FGF19 **(E)** during osteodifferentiation. Expression levels of *NOG* **(F)** and *RUNX2* **(G)** during early and mid-differentiation in p.S252W fibroblastoid cells, and correlation between these gene expression in p.S252W fibroblastoid cells without **(H)** and with FGF19 **(I)** during osteodifferentiation. p<0.05 (*), p<0.01 (**), p<0.001 (***).

Discussion

The current model for cranial suture closure in AS is that imbalance of osteogenic proliferation/differentiation causes deregulation of cell cycle at the suture site and that osteogenic differentiation mediated by FGFR2 signaling leads to premature suture closure (MORRISS-KAY; WILKIE, 2005; TWIGG; WILKIE, 2015b). It is well established that FGFR2 gain-of-function mutations disturb ligand-receptor specificity and ligand-receptor binding stoichiometry,

but their effects on cellular behavior in response to different FGFs are poorly defined. Here, we aimed to characterize these effects in AS subjects` cells harboring the p.S252W mutation in FGFR2.

First, we used cell proliferation assays as a screening method to select which FGFs affects p.S252W FGFR2 mutant cell proliferation most significantly. As expected, proliferation of wild-type fibroblastoid cells increased when exposed to FGF2, a natural ligand of FGFR2c, the receptor isoform expressed in mesenchymal tissues. Even though FGFs 7 and 18 are also natural ligands of FGFR2c, they did not alter cell proliferation in wild-type fibroblastoid cells. Conversely, p.S252W FGFR2 fibroblastoid cells proliferated more when exposed to FGF2, FGF10 and FGF19. Since increased cell proliferation has been reported in cells harboring the p.S252W FGFR2 mutation (FANGANIELLO et al., 2007; HOLMES et al., 2009; MIRAOUI et al., 2009; WANG et al., 2002; YANG et al., 2008b), we suggest that signaling by FGF10 and FGF19 is also an important factor leading to the altered proliferation seen in p.S252W FGFR2 fibroblastoid cells. While there is no previous information about the functional effect of FGF19 in p.S252W cells, there are several evidences reported in the literature that corroborate that illegitimate binding of FGFR2 to FGF10 is strongly implicated in the coronal suture pathology in Apert syndrome: interaction of FGF10 with FGFR2 harboring the p.S252W has been shown by different approaches in both human and murine cells (WILKIE et al., 2002; YU et al., 2000) further, the high local concentrations of FGF10, which is expressed in tissues of mesenchymal origin, allows an abnormal autocrine signaling loop through the pathological activation of mutant p.S252W FGFR2 (TWIGG; WILKIE, 2015b).

Through transcriptome analysis in p.S252W FGFR2 fibroblastoid cells, we show that the most relevant signaling pathways induced by FGF10 and FGF19 do not coincide with those regulated by FGF2 (YEH et al., 2013). In addition, our microarray analysis suggests that FGF10 led to an increase in the signaling pathways involved in immune response. Even though this correlation is still poorly explored in the literature, this finding goes along with the emerging evidence of a link between craniosynostosis and immunity, as suggested by the role of IL11RA-STAT3 pathway in craniosynostosis (NIEMINEN et al., 2011; TWIGG; WILKIE, 2015b).

FGF19 is an atypical FGF that acts as a hormone, and is found in the bloodstream and the receptor with the highest affinity for the endocrine FGF19 is FGFR4, which is also expressed in these cells (data not shown). It was validated in different cell lines (Hela, HEK293 and DU145) that stimulation of FGFR4 by FGF19 leads to inhibition of the NFKβ, a factor involved in inflammatory response(DRAFAHL et al., 2010). Interestingly, through microarray analysis in

fibroblastoid cells, we found that FGF19 also leads to an enrichment of genes associated with inflammatory/immune response in both WT and p.S252W FGFR2 fibroblastoid cells. Even though these data need to be further validated, we speculate that this could be due to the activation of FGFR4 by FGF19. We also observed enrichment in transcripts associated with osteogenesis in p.S252W FGFR2 fibroblastoid cells, which in turn, might be triggered by the non-natural FGF19-p.S252W FGFR2 binding.

Literature concerning p.S252W and p.P253R mutations in FGFR2 have yielded different and even contradictory results regarding their effects in cellular phenotypes (HEUZÉ et al., 2014a; MORITA et al., 2014; SUZUKI et al., 2012; WANG et al., 2002; YANG et al., 2008b; YOKOTA et al., 2014). We have previously shown that p.S252W mutation in FGFR2 confers a less drastic abnormal cell phenotype in MSCs when compared with fibroblastoid cells (YEH et al., 2011), suggesting that in order to understand the pathophysiology of FGFR2 mutations we need to take the cellular context into consideration. Therefore, we assayed proliferation and osteodifferentiation in cell types found in the coronal suture periosteal tissue (MSCs and fibroblastoid cells). Differently from what we observed in the screening for FGF-mediated alterations in cell proliferation in p.S252W FGFR2 fibroblastoid cells, only FGF2 increased proliferation in both WT and p.S252W FGFR2 MSCs. No effect was observed associated with FGF10 or FGF19 treatment.

The microarray finding that FGF19 caused differential expression of osteogenesis-related genes in p.S252W FGFR2 fibroblastoid cells prompted us to investigate the effects of FGF19 treatment during osteodifferentiation in both fibroblastoid cells and MSCs. In the mutant fibroblastoid cells, FGF19 decreased bone formation both *in vitro* and *in vivo*, corroborating the gene expression findings. In p.S252W MSCs, FGF19 did not affect osteogenic differentiation *in vitro*, while it increased differentiation in our *in vivo* model. This result is not actually discordant if taken into account that *in vitro* osteogenic differentiation lasts 21 days, while in the *in vivo* experiment the cells are pre-differentiated for 5 days before transplanted to the critical defect in the rat and the animal is sacrificed 4 weeks later: the *in vivo* model rather shows the long-term effect of FGF19 in p.S252W MSCs osteodifferentiation. Nevertheless, these results highlight the opposing phenotypic effect of FGF19 in AS-derived cells with the same mutation.

The analysis of the expression profile of *NOG* and *RUNX2* during *in vitro* osteogenesis showed that both genes correlate only in the p.S252W fibroblastoid cells when treated with FGF19, but not without FGF19 stimulation. This was not observed in p.S252W MSCs. FGF and BMP signaling are known to crosstalk and interact during bone development (NAKAMURA et al.,

2005; ORNITZ; MARIE, 2015), but this is the first time an endocrine FGF has been shown to affect BMP signaling in p.S252W FGFR2 cells.

In summary, data presented in this manuscript suggest that FGF10 and FGF19 are important factors contributing to the pathophysiology of AS by overstimulating proliferation or osteogenesis depending on the cellular context. Based on these findings, the relative balance of MS and fibroblastoid cells should be a variable to be considered in the regulation of the rate of suture fusion in Apert patients. Future studies to investigate the inhibition of MSC proliferation or use of FGF19 or anti-BMP2 as inhibitors of osteogenesis in AS subjects' cells are important to shed light in the clinical management of AS.

DISCUSSÃO GERAL

O objetivo central dessa tese foi investigar novos mecanismos moleculares atuantes na patofisiologia das craniossinostoses. Essa investigação foi feita tanto sobre os aspectos genéticos quanto sobre os eventos moleculares e celulares resultantes das mutações que causam formas graves de craniossinostose sindrômica. Dessa maneira podemos subdividir esse trabalho em duas frentes: variantes associadas às craniossinostoses e, efeitos funcionais da mutação p.S252W em FGFR2.

Os trabalhos referentes às variantes associadas às craniossinostoses foram divididos de acordo com o histórico genético e clínico das famílias, no capítulo 1 analisamos o caso de uma paciente filha de um casamento consanguíneo com síndrome de Raine, cuja identificação também nos permitiu identificar a mutação responsável em outra paciente com uma forma clinicamente semelhante. No capítulo 2 foram analisados casos atípicos familiais de craniossinostose sem mutações em genes previamente relacionados às craniossinostoses. O que permitiu a busca por mutações em todos os casos foi a disponibilidade de técnicas de sequenciamento em larga escala, a qual utilizamos para o sequenciamento de todas as regiões codificadoras do genoma, regiões na qual se encontram a maior parte das mutações causadoras de doenças genéticas em humanos.

As técnicas de sequenciamento em larga escala foram revolucionárias no estudo da genética humana, no entanto uma série de desafios novos foram abertos após sua implementação, em especial a necessidade da criação e refinamento de técnicas de análise de dados devido ao grande volume de dados gerados. Nesse sentido nossos dados contribuíram para o aperfeiçoamento das metodologias de análise ao nos permitiram concluir que em casos de doenças autossômicas dominantes sem loci previamente relacionado o sequenciamento de duas gerações é insuficiente, orientação importante ao iniciar a investigação de doenças raras. Também deve-se incluir o balanço alélico como fonte potencial de informações para a filtragem de dados de sequenciamento. No caso de variantes missense e indels em heterozigose, balanços alélicos abaixo de 0,4 devem ser validados por meio de outras técnicas antes de serem considerados para a análise, também se faz desnecessário a princípio a validação de variantes com balanço alélico entre 0,4 e 0,6, pois, como visto no capítulo 2, apenas 1 variante com balanço alélico entre 0,4 e 0,6 foi um achado falso positivo.

Além das respostas aos desafios técnicos apresentados os dados dos capítulos referentes a investigação de novos loci associados às craniossinostoses também expandem nosso conhecimento em relação à biologia das suturas cranianas. No capítulo 1 vimos que mutações específicas em FAM20C têm efeitos distintos sobre as suturas, podendo causar desde craniossinostose até agenesia de suturas, efeitos usualmente negligenciados em outros trabalhos que estudaram a síndrome de Raine. Interessantemente, pacientes com perda parcial da função da proteína FAM20C apresentam o fechamento da sutura, no entanto só há um único trabalho que estuda o impacto das mutações sobre a ação cinase da proteína e, portanto, para termos uma conclusão mais firme, mais estudos funcionais seriam necessários. O capítulo 2 propõe uma série de novos loci, desde genes associados à outras formas de doenças genéticas como GJB2 até genes muito pouco estudados como DDX23, expandindo ainda mais a já vasta heterogeneidade genética das craniossinostoses. Também foram encontradas mutações potencialmente patogênicas em genes da via NOTCH, como WNT2B, SNW1 e mesmo DDX23. Devido à grande variedade de loci envolvidos no processo de formação e de manutenção das suturas é esperado que mutações em diversos genes possam abalar o fino equilíbrio necessário para a manutenção da abertura da mesma.

Por fim o estudo funcional de células de periósteo proveniente de pacientes com síndrome de Apert mostrou um resultado surpreendente, FGF19, uma molécula sem ação na forma selvagem de FGFR2, causa efeitos distintos em tipos celulares diferentes quando portando a mutação p.S252W em FGFR2. Como revisto na introdução geral, o fino balanço entre proliferação e diferenciação das células tronco no complexo sutural é responsável pelo crescimento dos ossos cranianos ao mesmo tempo em que mantém um estoque de células indiferenciadas e uma matriz não ossificada para manter a sutura aberta (TWIGG; WILKIE, 2015a). A resposta ao FGF19 na síndrome de Apert pode afetar esse balanço ao promover a diferenciação das células tronco mesenquimais em osteoblastos, depletando o estoque de células indiferenciadas e levando à ossificação prematura da sutura coronal. FGF19, por ser um FGF de ação endócrina pode estar presente durante o desenvolvimento da sutura e promover a ossificação prematura da sutura em células portadoras da mutação p.S252W, sem, no entanto, ter ação sobre células selvagens.

Em conclusão o presente estudo permitiu o melhor delineamento das craniossinostoses, tanto ao eleger loci candidatos a serem causais de formas atípicas de craniossinostose quanto ao aprofundar o conhecimento em relação da patofisiologia das síndromes de Raine e Apert.

RESUMO

As craniossinostoses são malformações craniofaciais caracterizadas pelo fechamento precoce de uma ou mais suturas cranianas. Elas são doenças congênitas e são causadas por mutações em diversos genes devido ao grande número de vias envolvidas na formação e manutenção das suturas cranianas. Embora mutações em 53 genes já tenham sido descritas o conhecimento da genética e da patofisiologia das craniossinostoses ainda é incompleto. Nesse trabalho tivemos como objetivo a identificação de novas mutações associadas às craniossinostoses bem como o aprofundamento do conhecimento sobre a atuação dessas mutações em células humanas por meio de estudos funcionais. Para identificarmos novas mutações utilizamos metodologias de sequenciamento em larga escala conhecidas como sequenciamento de noiva geração (NGS). Identificamos a mutação causal em uma paciente proveniente de um casamento consanguíneo portadora da síndrome de Raine (p.P496L em *FAM20C*). Também delimitamos à poucas mutações candidatas outros onze casos atípicos de craniossinostose

Por fim estudamos os efeitos de diferentes FGFs sobre o comportamento de células com a mutação mais comum causadora da S. de Apert, p.S252W em *FGFR2*. Descobrimos que os FGFs10 e 19 têm ações distintas sobre o perfil transcricional e sobre a taxa de proliferação de células mutantes. Também descobrimos que as células tronco mesenquimais e as células fibroblastóides têm comportamentos distintos ao serem tratadas com FGF19.

Os resultados aqui apresentados serão de grande serventia para o melhor delineamento da biologia das suturas cranianas e da patofisiologia das craniossinostoses.

Abstract

Craniosynostosis are craniofacial malformations defined by early closure of the cranial sutures. They are congenital diseases caused by mutations in several genes due to the diversity of pathways involved in the development and maintenance of the cranial sutures. Even though 53 genes have already been linked to various forms of craniosynostosis, the knowledge about the genetics and pathophysiology is incomplete. In this work we aimed to identify new mutations associated with craniosynostosis as well as to further the knowledge of how those mutations act in human cells. To identify new variants associated with craniosynostosis we used large scale sequencing techniques known as next generation sequencing (NGS). We were able to identify the causal mutation in one patient from a consanguineous marriage with Raine syndrome (p.P496L in *FAM20C*). We also were able to elect candidate mutations in other eleven cases of atypical craniosynostosis.

Lastly, we studied the effects of different FGFs over the behavior of human cells harboring the most common Apert syndrome mutation, p.S252W in FGFR2. We discovered that FGFs 10 and 19 have different effects over the transcriptional profile and proliferation rate of mutant cells. We also found that FGF19 have opposite effects in mesenchymal stem cells and fibroblastoid cells osteogenic differentiation.

The results shown here will be of great service to better understand the biology of cranial suture and the pathophysiology of craniosynostosis.

BIBLIOGRAFIA

ABABNEH, F.; ALSWAID, A.; YOUSSEF, T. Hereditary deletion of the entire FAM20C gene in a patient with Raine syndrome. **American Journal of**, 2013.

ACEVEDO, A.; POULTER, J. Variability of systemic and oro-dental phenotype in two families with non-lethal Raine syndrome with FAM20C mutations. **BMC medical**, 2015.

ACOSTA, A.; PERES, L.; CHIMELLI, L. Raine dysplasia: a Brazilian case with a mild radiological involvement. **Clinical**, 2000.

AKUTSU, K. et al. Phenotypic Heterogeneity of Marfan-Like Connective Tissue Disorders Associated With Mutations in the Transforming Growth Factor-β Receptor Genes. **Circulation Journal**, v. 71, n. 8, p. 1305–1309, 1 ago. 2007.

BEENKEN, A.; MOHAMMADI, M. The FGF family: biology, pathophysiology and therapy. **Nature reviews. Drug discovery**, v. 8, n. 3, p. 235–53, mar. 2009.

BRIGHTMAN, F. A.; FELL, D. A. Differential feedback regulation of the MAPK cascade underlies the quantitative differences in EGF and NGF signalling in PC12 cells. **FEBS Letters**, v. 482, n. 3, p. 169–174, out. 2000.

BRITO, L. A. et al. IRF6 is a risk factor for nonsyndromic cleft lip in the Brazilian population. **American journal of medical genetics. Part A**, v. 158A, n. 9, p. 2170–5, set. 2012.

BULTMAN, S. et al. A Brg1 Null Mutation in the Mouse Reveals Functional Differences among Mammalian SWI/SNF Complexes. **Molecular Cell**, v. 6, n. 6, p. 1287–1295, dez. 2000.

CARINCI, F. et al. Apert and Crouzon Syndromes: Clinical Findings, Genes and Extracellular Matrix. **Journal of Craniofacial Surgery**, v. 16, n. 3, p. 361–368, maio 2005.

CARMIGNAC, V. et al. In-frame mutations in exon 1 of SKI cause dominant Shprintzen-Goldberg syndrome. **American journal of human genetics**, v. 91, n. 5, p. 950–7, 2 nov. 2012.

CHAN, D. K.; CHANG, K. W. GJB2-associated hearing loss: Systematic review of worldwide prevalence, genotype, and auditory phenotype. **The Laryngoscope**, v. 124, n. 2, p. E34–E53, fev. 2014.

CHITAYAT, D. et al. Raine syndrome: A rare lethal osteosclerotic bone dysplasia. Prenatal diagnosis, autopsy, and neuropathological findings. **American Journal of**, 2007.

COHEN JR., M. M.; MACLEAN, R. E. **Craniosynostosis. Diagnosis, Evaluation and Management**. Second ed. New York: Oxford University Press, 2000.

COHEN, M. M. Craniosynostoses: phenotypic/molecular correlations. **American journal of medical genetics**, v. 56, n. 3, p. 334–9, 10 abr. 1995.

COHEN, M. M. Malformations of the craniofacial region: evolutionary, embryonic, genetic, and clinical perspectives. **American journal of medical genetics**, v. 115, n. 4, p. 245–68, 30 dez. 2002.

CÔTÉ, J.-F.; VUORI, K. Identification of an evolutionarily conserved superfamily of DOCK180-related proteins with guanine nucleotide exchange activity. **Journal of cell science**, v. 115, n. Pt 24, p. 4901–13, 15 dez. 2002.

DARNELL, J. E.; KERR, I. M.; STARK, G. R. Jak-STAT pathways and transcriptional activation in response to IFNs and other extracellular signaling proteins. **Science (New York, N.Y.)**, v. 264, n. 5164, p. 1415–21, 3 jun. 1994.

DAY, T. F. et al. Wnt/beta-catenin signaling in mesenchymal progenitors controls osteoblast and chondrocyte differentiation during vertebrate skeletogenesis. **Developmental cell**, v. 8, n. 5, p. 739–50, maio 2005.

DE HOON, M. J. L. et al. Open source clustering software. **Bioinformatics (Oxford, England)**, v. 20, n. 9, p. 1453–4, 12 jun. 2004.

DE MENDONÇA COSTA, A. et al. Reconstruction of large cranial defects in nonimmunosuppressed experimental design with human dental pulp stem cells. **The Journal of craniofacial surgery**, v. 19, n. 1, p. 204–210, 2008.

DE PAEPE, A.; MALFAIT, F. The Ehlers-Danlos syndrome, a disorder with many faces. **Clinical Genetics**, v. 82, n. 1, p. 1–11, jul. 2012.

DECKELBAUM, R. A. et al. Regulation of cranial morphogenesis and cell fate at the neural crest-mesoderm boundary by engrailed 1. **Development (Cambridge, England)**, v. 139, n. 7, p. 1346–58, abr. 2012.

DESHPANDE, A.; FANG, P.; ZHANG, X. Primary structure and phosphorylation of dentin matrix protein 1 (DMP1) and dentin phosphophoryn (DPP) uniquely determine their role in biomineralization. 2011.

DRAFAHL, K. A. et al. The receptor tyrosine kinase FGFR4 negatively regulates NF-kappaB signaling. **PloS one**, v. 5, n. 12, p. e14412, 2010.

FANGANIELLO, R. D. et al. Apert p. Ser252Trp mutation in FGFR2 alters osteogenic potential and gene expression of cranial periosteal cells. **Molecular Medicine**, v. 13, n. 7-8, p. 422, 2007.

FAUNDES, V.; CASTILLO-TAUCHER, S. Raine syndrome: An overview. **European journal of**, 2014.

FLÜCK, C. E. et al. Mutant P450 oxidoreductase causes disordered steroidogenesis with and without Antley-Bixler syndrome. **Nature genetics**, v. 36, n. 3, p. 228–30, mar. 2004.

FRIESEL, R. E. Constitutive Activation of Fibroblast Growth Factor Receptor-2 by a Point Mutation Associated with Crouzon Syndrome. **Journal of Biological Chemistry**, v. 270, n. 44, p. 26037–26040, 3 nov. 1995.

GAJECKA, M. Unrevealed mosaicism in the next-generation sequencing era. **Molecular genetics and genomics : MGG**, v. 291, n. 2, p. 513–30, abr. 2016.

GALVIN, B. D. et al. Constitutive receptor activation by Crouzon syndrome mutations in

fibroblast growth factor receptor (FGFR)2 and FGFR2/Neu chimeras. **Proceedings of the National Academy of Sciences**, v. 93, n. 15, p. 7894–7899, 23 jul. 1996.

GARKAVTSEV, I. V et al. The Bloom syndrome protein interacts and cooperates with p53 in regulation of transcription and cell growth control. **Oncogene**, v. 20, n. 57, p. 8276–80, 13 dez. 2001.

GERICKE, A. et al. Importance of phosphorylation for osteopontin regulation of biomineralization. **Calcified tissue international**, v. 77, n. 1, p. 45–54, jul. 2005.

GILISSEN, C. et al. Disease gene identification strategies for exome sequencing. **European journal of human genetics : EJHG**, v. 20, n. 5, p. 490–7, maio 2012.

GREEN, P. J.; WALSH, F. S.; DOHERTY, P. Promiscuity of fibroblast growth factor receptors. **BioEssays : news and reviews in molecular, cellular and developmental biology**, v. 18, n. 8, p. 639–46, ago. 1996.

GREENBERG, F. et al. Molecular analysis of the Smith-Magenis syndrome: a possible contiguous-gene syndrome associated with del(17)(p11.2). **American journal of human genetics**, v. 49, n. 6, p. 1207–18, dez. 1991.

GREGORY, C. A. et al. An Alizarin red-based assay of mineralization by adherent cells in culture: comparison with cetylpyridinium chloride extraction. **Analytical biochemistry**, v. 329, n. 1, p. 77–84, 2004.

GÜNEŞ, T.; KURTOĞLU, S.; ÇETIN, N. Raine syndrome associated with cytomegalovirus infection. **Turkish journal of …**, 2005.

HAGUE, J. et al. Molecularly proven mosaicism in phenotypically normal parent of a girl with Freeman-Sheldon Syndrome caused by a pathogenic MYH3 mutation. **American journal of medical genetics. Part A**, v. 170, n. 6, p. 1608–12, jun. 2016.

HALFON, S. et al. Markers distinguishing mesenchymal stem cells from fibroblasts are downregulated with passaging. **Stem cells and development**, v. 20, n. 1, p. 53–66, jan. 2011.

HARADA, M. et al. FGF9 monomer-dimer equilibrium regulates extracellular matrix affinity and tissue diffusion. **Nature genetics**, v. 41, n. 3, p. 289–98, mar. 2009.

HEUZÉ, Y. et al. Quantification of facial skeletal shape variation in fibroblast growth factor receptor-related craniosynostosis syndromes. **Birth defects research. Part A, Clinical and molecular teratology**, v. 100, n. 4, p. 250–9, abr. 2014a.

HEUZÉ, Y. et al. Closing the Gap: Genetic and Genomic Continuum from Syndromic to Nonsyndromic Craniosynostoses. **Current genetic medicine reports**, v. 2, n. 3, p. 135–145, 1 set. 2014b.

HOLMES, G. et al. Early onset of craniosynostosis in an Apert mouse model reveals critical features of this pathology. **Developmental biology**, v. 328, n. 2, p. 273–84, abr. 2009.

HONG, F. et al. RankProd: a bioconductor package for detecting differentially expressed genes in meta-analysis. **Bioinformatics (Oxford, England)**, v. 22, n. 22, p. 2825–7, 15 nov. 2006.

HORI, K. et al. Notch signaling at a glance. **Journal of Cell Science**, v. 126, n. 10, p. 2135–2140, 15 maio 2013.

HÜLSKAMP, G.; WIECZOREK, D.; RIEDER, H. Raine syndrome: report of a family with three affected sibs and further delineation of the syndrome. **Clinical**, 2003.

HUNTER, D. J. et al. A genome-wide association study identifies alleles in FGFR2 associated with risk of sporadic postmenopausal breast cancer. **Nature genetics**, v. 39, n. 7, p. 870–4, jul. 2007.

IBRAHIMI, O. A. et al. Structural basis for fibroblast growth factor receptor 2 activation in Apert syndrome. **Proceedings of the National Academy of Sciences of the United States of America**, v. 98, n. 13, p. 7182–7, 19 jun. 2001.

IBRAHIMI, O. A. et al. Biochemical analysis of pathogenic ligand-dependent FGFR2 mutations suggests distinct pathophysiological mechanisms for craniofacial and limb abnormalities. **Hum Mol Genet**, v. 13, p. 2313–2324, 2004.

IMAMURA, Y.; SCOTT, I. C.; GREENSPAN, D. S. The pro-alpha3(V) collagen chain. Complete primary structure, expression domains in adult and developing tissues, and comparison to the structures and expression domains of the other types V and XI procollagen chains. **The Journal of biological chemistry**, v. 275, n. 12, p. 8749–59, 24 mar. 2000.

ISHIKAWA, H. et al. The Raine syndrome protein FAM20C is a Golgi kinase that phosphorylates bio-mineralization proteins. **PLoS One**, 2012.

ITOH, N.; ORNITZ, D. M. Fibroblast growth factors: from molecular evolution to roles in development, metabolism and disease. **Journal of biochemistry**, v. 149, n. 2, p. 121–30, 1 fev. 2011.

JIANG, X. et al. Tissue Origins and Interactions in the Mammalian Skull Vault. **Developmental Biology**, v. 241, n. 1, p. 106–116, 2002.

JOHNSON, D. et al. **Expression patterns of Twist and Fgfr1, -2 and -3 in the developing mouse coronal suture suggest a key role for Twist in suture initiation and biogenesisMechanisms of Development**. [s.l: s.n.].

JOHNSON, D. et al. A novel mutation, Ala315Ser, in FGFR2: a gene-environment interaction leading to craniosynostosis? **European journal of human genetics : EJHG**, v. 8, n. 8, p. 571–7, ago. 2000b.

JOHNSON, D.; WILKIE, A. O. M. Craniosynostosis. **European journal of human genetics : EJHG**, v. 19, n. 4, p. 369–76, abr. 2011.

JUSTICE, C. M. et al. A genome-wide association study identifies susceptibility loci for nonsyndromic sagittal craniosynostosis near BMP2 and within BBS9. **Nature genetics**, v. 44, n. 12, p. 1360–4, dez. 2012.

KAN, A. E.; KOZLOWSKI, K. New distinct lethal osteosclerotic bone dysplasia (Raine syndrome). **American Journal of Medical Genetics**, v. 43, n. 5, p. 860–864, jul. 1992a.

KAN, A. E.; KOZLOWSKI, K. New distinct lethal osteosclerotic bone dysplasia (Raine syndrome). **American Journal of Medical Genetics**, v. 43, n. 5, p. 860–864, 15 jul. 1992b.

KATAYAMA, Y.; HOUSE, C.; UDAGAWA, N. Casein kinase 2 phosphorylation of recombinant rat osteopontin enhances adhesion of osteoclasts but not osteoblasts. **Journal of cellular**, 1998.

KIMONIS, V. et al. Genetics of craniosynostosis. **Seminars in pediatric neurology**, v. 14, n. 3, p. 150–61, set. 2007.

KINGSTON, H. M.; FREEMAN, J. S.; HALL, C. M. A new lethal sclerosing bone dysplasia. **Skeletal Radiology**, v. 20, n. 2, p. 117–119, fev. 1991.

KINOSHITA, Y. et al. Functional analysis of mutant FAM20C in Raine syndrome with FGF23-related hypophosphatemia. **Bone**, 2014.

KLEIN, R. et al. Eph/ephrin signalling during development. **Development (Cambridge, England)**, v. 139, n. 22, p. 4105–9, nov. 2012.

KOCHAR, G.; CHOUDHARY, A.; GADODIA, A. Raine syndrome: a clinical, radiographic and genetic investigation of a case from the Indian subcontinent. **Clinical**, 2010.

KONCZ, C. et al. The Spliceosome-Activating Complex: Molecular Mechanisms Underlying the Function of a Pleiotropic Regulator. **Frontiers in Plant Science**, v. 3, p. 9, 2012.

KONG, A. et al. Rate of de novo mutations and the importance of father's age to disease risk. **Nature**, v. 488, n. 7412, p. 471–5, 23 ago. 2012.

KONISHI, T.; UODOME, N.; SUGIMOTO, A. The Caenorhabditis elegans DDX-23, a homolog of yeast splicing factor PRP28, is required for the sperm-oocyte switch and differentiation of various cell types. **Developmental dynamics : an official publication of the American Association of Anatomists**, v. 237, n. 9, p. 2367–77, set. 2008.

KOOB, M. et al. Raine syndrome: expanding the radiological spectrum. **Pediatric radiology**, 2011.

KRONENBERG, H. M. Developmental regulation of the growth plate. **Nature**, v. 423, n. 6937, p. 332–6, 15 maio 2003.

KRONENBERG, H. M. et al. Twist Genes Regulate Runx2 and Bone Formation. **Developmental Cell**, v. 6, n. 3, p. 317–318, mar. 2004.

KURATANI, S.; MATSUO, I.; AIZAWA, S. **Developmental patterning and evolution of the mammalian viscerocranium: Genetic insights into comparative morphologyDevelopmental Dynamics**, 1997.

LAJEUNIE, E. et al. Clinical variability in patients with Apert's syndrome. **Journal Of Neurosurgery**, v. 90, n. 3, p. 443–447, 1999.

LAJEUNIE, E. et al. Mutation screening in patients with syndromic craniosynostoses indicates that a limited number of recurrent FGFR2 mutations accounts for severe forms of Pfeiffer syndrome. **European journal of human genetics : EJHG**, v. 14, n. 3, p. 289–98, mar. 2006.

LARBUISSON, A. et al. Fgf receptors Fgfr1a and Fgfr2 control the function of pharyngeal endoderm in late cranial cartilage development. **Differentiation; research in biological diversity**, v. 86, n. 4-5, p. 192–206, jan. 2013.

LARTEY, J. et al. Expression of RND proteins in human myometrium. **Biology of reproduction**, v.

75, n. 3, p. 452–61, set. 2006.

LAZARUS, J. E. et al. Fibroblast growth factor expression in the postnatal growth plate. **Bone**, v. 40, n. 3, p. 577–86, mar. 2007.

LEE, M.-H. et al. BMP-2-induced Runx2 expression is mediated by Dlx5, and TGF-beta 1 opposes the BMP-2-induced osteoblast differentiation by suppression of Dlx5 expression. **The Journal of biological chemistry**, v. 278, n. 36, p. 34387–94, 5 set. 2003.

LEK, M. et al. Analysis of protein-coding genetic variation in 60,706 humans. **bioRxiv**, p. 030338, 30 out. 2016.

LEMMON, M. A.; SCHLESSINGER, J. Cell signaling by receptor tyrosine kinases. **Cell**, v. 141, n. 7, p. 1117–34, 25 jun. 2010.

LEVI, B. et al. Cranial suture biology: from pathways to patient care. **The Journal of craniofacial surgery**, v. 23, n. 1, p. 13–9, jan. 2012.

LING, L.; NURCOMBE, V.; COOL, S. M. Wnt signaling controls the fate of mesenchymal stem cells. **Gene**, v. 433, n. 1-2, p. 1–7, 2009.

LIU, Y. T. et al. Novel mutations in GJB6 and GJB2 in Clouston syndrome. **Clinical and experimental dermatology**, v. 40, n. 7, p. 770–3, out. 2015.

MANE, K. AL; COATES, R.; MCDONALD, P. Intracranial calcification in Raine syndrome. **Pediatric radiology**, 1996.

MARKOVA, T. G. et al. Phenotype in a patient with p.D50N mutation in GJB2 gene resemble both KID and Clouston syndromes. **International journal of pediatric otorhinolaryngology**, v. 81, p. 10–4, 1 fev. 2016.

MEFFORD, H. C. et al. Copy number variation analysis in single-suture craniosynostosis: multiple rare variants including RUNX2 duplication in two cousins with metopic craniosynostosis. **American journal of medical genetics. Part A**, v. 152A, n. 9, p. 2203–10, set. 2010.

MERRILL, A. E. et al. Cell mixing at a neural crest-mesoderm boundary and deficient ephrin-Eph signaling in the pathogenesis of craniosynostosis. **Human molecular genetics**, v. 15, n. 8, p. 1319–28, 15 abr. 2006.

MICHAEL, K.; NELSON, D. M.; ORTMEIER, A. Raine Syndrome. **Journal of Diagnostic Medical Sonography**, v. 27, n. 4, p. 167–170, 1 jul. 2011.

MIRAOUI, H. et al. Fibroblast growth factor receptor 2 promotes osteogenic differentiation in mesenchymal cells via ERK1/2 and protein kinase C signaling. **The Journal of Biological Chemistry**, v. 284, n. 8, p. 4897–904, 2009.

MIURA, T. et al. Mechanism of skull suture maintenance and interdigitation. **Journal of anatomy**, v. 215, n. 6, p. 642–55, dez. 2009.

MOHAMMADI, M.; OLSEN, S. K.; IBRAHIMI, O. A. Structural basis for fibroblast growth factor receptor activation. **Cytokine & growth factor reviews**, v. 16, n. 2, p. 107–37, abr. 2005.

MÖHLMANN, S. et al. Structural and functional analysis of the human spliceosomal DEAD-box

helicase Prp28. **Acta crystallographica. Section D, Biological crystallography**, v. 70, n. Pt 6, p. 1622–30, jun. 2014.

MORÉN, A.; ICHIJO, H.; MIYAZONO, K. Molecular cloning and characterization of the human and porcine transforming growth factor-beta type III receptors. **Biochemical and biophysical research communications**, v. 189, n. 1, p. 356–62, 30 nov. 1992.

MORITA, J. et al. Soluble form of FGFR2 with S252W partially prevents craniosynostosis of the apert mouse model. **Developmental dynamics : an official publication of the American Association of Anatomists**, v. 243, n. 4, p. 560–7, abr. 2014.

MORRISS-KAY, G. M.; WILKIE, A. O. M. Growth of the normal skull vault and its alteration in craniosynostosis: insights from human genetics and experimental studies. **Journal of anatomy**, v. 207, n. 5, p. 637–53, nov. 2005.

NAKAMURA, Y. et al. Low dose fibroblast growth factor-2 (FGF-2) enhances bone morphogenetic protein-2 (BMP-2)-induced ectopic bone formation in mice. **Bone**, v. 36, n. 3, p. 399–407, mar. 2005.

NALBANT, D. et al. FAM20: an evolutionarily conserved family of secreted proteins expressed in hematopoietic cells. **BMC Genomics**, v. 6, n. 1, p. 11, 2005.

NAZZARO, A. et al. Prenatal ultrasound diagnosis of a case of Pfeiffer syndrome without cloverleaf skull and review of the literature. **Prenatal diagnosis**, v. 24, n. 11, p. 918–22, nov. 2004.

NIEMINEN, P. et al. Inactivation of IL11 signaling causes craniosynostosis, delayed tooth eruption, and supernumerary teeth. **American Journal of Human Genetics**, v. 89, n. 1, p. 67–81, 15 jul. 2011.

ODA, T. et al. Mutations in the human Jagged1 gene are responsible for Alagille syndrome. **Nature Genetics**, v. 16, n. 3, p. 235–242, jul. 1997.

OLDRIDGE, M. et al. De novo alu-element insertions in FGFR2 identify a distinct pathological basis for Apert syndrome. **The American Journal of Human Genetics**, v. 64, n. 2, p. 446–461, 1999.

OLIVEIRA, N. A J. et al. Further evidence of association between mutations in FGFR2 and syndromic craniosynostosis with sacrococcygeal eversion. **Birth defects research. Part A, Clinical and molecular teratology**, v. 76, n. 8, p. 629–33, ago. 2006.

ORNITZ, D. M. et al. Receptor specificity of the fibroblast growth factor family. **The Journal of biological chemistry**, v. 271, n. 25, p. 15292–7, 21 jun. 1996.

ORNITZ, D. M. FGFs, heparan sulfate and FGFRs: complex interactions essential for development. **BioEssays news and reviews in molecular cellular and developmental biology**, v. 22, n. 2, p. 108–112, 2000.

ORNITZ, D. M.; MARIE, P. J. Fibroblast growth factor signaling in skeletal development and disease. **Genes & development**, v. 29, n. 14, p. 1463–86, 15 jul. 2015.

PAN, D. et al. Twist-1 is a PPARdelta-inducible, negative-feedback regulator of PGC-1alpha in

brown fat metabolism. **Cell**, v. 137, n. 1, p. 73–86, 3 abr. 2009.

PARK, W. J.; BELLUS, G. A.; JABS, E. W. Mutations in fibroblast growth factor receptors: phenotypic consequences during eukaryotic development. **American journal of human genetics**, v. 57, n. 4, p. 748–54, out. 1995.

PASSOS-BUENO, M. et al. Genetics of craniosynostosis: genes, syndromes, mutations and genotype-phenotype correlations. **Craniofacial sutures: development, disease and treatment**, v. 12, p. 107–143, 2008.

PASSOS-BUENO, M. R. et al. **Pfeiffer mutation in an Apert patient: how wide is the spectrum of variability due to mutations in the FGFR2 gene?American Journal of Medical Genetics**Wiley Online Library, , 1997. Disponível em: <http://onlinelibrary.wiley.com/doi/10.1002/(SICI)1096-8628(19970808)71:2<243::AID-AJMG27>3.0.CO;2-D/abstract>

PRITCHARD, J. J.; SCOTT, J. H.; GIRGIS, F. G. The structure and development of cranial and facial sutures. **Journal of anatomy**, v. 90, n. 1, p. 73–86, jan. 1956.

QIN, L. et al. Detection and Quantification of Mosaic Mutations in Disease Genes by Next-Generation Sequencing. **The Journal of molecular diagnostics : JMD**, v. 18, n. 3, p. 446–53, maio 2016.

RAFAELSEN, S.; RÆDER, H.; FAGERHEIM, A. Exome sequencing reveals FAM20c mutations associated with fibroblast growth factor 23–related hypophosphatemia, dental anomalies, and ectopic. **Journal of Bone and**, 2013.

RAINE, J. et al. Unknown syndrome: microcephaly, hypoplastic nose, exophthalmos, gum hyperplasia, cleft palate, low set ears, and osteosclerosis. **Journal of medical genetics**, 1989.

RAUCH, F. et al. Cole-Carpenter syndrome is caused by a heterozygous missense mutation in P4HB. **American journal of human genetics**, v. 96, n. 3, p. 425–31, 5 mar. 2015.

RAWLINGS, J. S.; ROSLER, K. M.; HARRISON, D. A. The JAK/STAT signaling pathway. **Journal of cell science**, v. 117, n. Pt 8, p. 1281–3, 15 mar. 2004.

REBSCHER, N. et al. Conserved intron positions in FGFR genes reflect the modular structure of FGFR and reveal stepwise addition of domains to an already complex ancestral FGFR. **Development genes and evolution**, v. 219, n. 9-10, p. 455–68, out. 2009.

REJJAL, A. Raine syndrome. **American journal of medical genetics**, 1998.

RICKERT, C. et al. Neuropathology of Raine syndrome. **Acta**, 2002.

SAAD, F. A.; SALIH, E.; GLIMCHER, M. J. Identification of osteopontin phosphorylation sites involved in bone remodeling and inhibition of pathological calcification. **Journal of Cellular Biochemistry**, v. 103, n. 3, p. 852–856, 15 fev. 2008.

SAEYS, Y.; INZA, I.; LARRAÑAGA, P. A review of feature selection techniques in bioinformatics. **Bioinformatics (Oxford, England)**, v. 23, n. 19, p. 2507–17, 1 out. 2007.

SAITO-OHARA, F. et al. The Xq22 inversion breakpoint interrupted a novel Ras-like GTPase gene in a patient with Duchenne muscular dystrophy and profound mental retardation. **American**

journal of human genetics, v. 71, n. 3, p. 637–45, set. 2002.

SCHROEDER, T. M.; JENSEN, E. D.; WESTENDORF, J. J. Runx2: a master organizer of gene transcription in developing and maturing osteoblasts. **Birth defects research. Part C, Embryo today : reviews**, v. 75, n. 3, p. 213–25, set. 2005.

SEIDAHMED, M. Z. et al. Report of a case of Raine syndrome and literature review. **American Journal of Medical Genetics Part A**, v. 167, n. 10, p. 2394–2398, out. 2015.

SETO, M. L. et al. Isolated sagittal and coronal craniosynostosis associated with TWIST box mutations. **American journal of medical genetics. Part A**, v. 143, n. 7, p. 678–86, 1 abr. 2007.

SHAHEEN, R. et al. **Recessive Mutations in DOCK6, Encoding the Guanidine Nucleotide Exchange Factor DOCK6, Lead to Abnormal Actin Cytoskeleton Organization and Adams-Oliver SyndromeThe American Journal of Human Genetics**. [s.l: s.n.]. Disponível em: <http://www.sciencedirect.com/science/article/pii/S000292971100303X>. Acesso em: 16 dez. 2013.

SHARMA, V. P. et al. Mutations in TCF12, encoding a basic helix-loop-helix partner of TWIST1, are a frequent cause of coronal craniosynostosis. **Nature genetics**, v. 45, n. 3, p. 304–7, mar. 2013.

SIMPSON, M. et al. Mutations in FAM20C also identified in non-lethal osteosclerotic bone dysplasia. **Clinical**, 2009.

SIMPSON, M. A. et al. Mutations in FAM20C Are Associated with Lethal Osteosclerotic Bone Dysplasia (Raine Syndrome), Highlighting a Crucial Molecule in Bone Development. **The American Journal of Human Genetics**, v. 81, n. 5, p. 906–912, nov. 2007a.

SIMPSON, M. A. et al. Mutations in FAM20C Are Associated with Lethal Osteosclerotic Bone Dysplasia (Raine Syndrome), Highlighting a Crucial Molecule in Bone Development. **The American Journal of Human Genetics**, v. 81, n. 5, p. 906–912, nov. 2007b.

SLANEY, S. F. et al. Differential effects of FGFR2 mutations on syndactyly and cleft palate in Apert syndrome. **American journal of human genetics**, v. 58, n. 5, p. 923–32, maio 1996.

SUZUKI, H. et al. Apert syndrome mutant FGFR2 and its soluble form reciprocally alter osteogenesis of primary calvarial osteoblasts. **Journal of cellular physiology**, v. 227, n. 9, p. 3267–77, set. 2012.

TAGLIABRACCI, V. et al. Secreted kinase phosphorylates extracellular proteins that regulate biomineralization. 2012.

TAKEDA, K. et al. Targeted disruption of the mouse Stat3 gene leads to early embryonic lethality. **Proceedings of the National Academy of Sciences of the United States of America**, v. 94, n. 8, p. 3801–4, 15 abr. 1997.

TAKEYARI, S. et al. Hypophosphatemic osteomalacia and bone sclerosis caused by a novel homozygous mutation of the FAM20C gene in an elderly man with a mild variant of Raine. **Bone**, 2014.

TANIGUCHI-IKEDA, M. et al. Next-generation sequencing discloses a nonsense mutation in the

dystrophin gene from long preserved dried umbilical cord and low-level somatic mosaicism in the proband mother. **Journal of human genetics**, v. 61, n. 4, p. 351–5, abr. 2016.

TARTAGLIA, M. et al. Trp290Cys mutation in exon IIIa of the fibroblast growth factor receptor 2 (FGFR2) gene is associated with Pfeiffer syndrome. **Human genetics**, v. 99, n. 5, p. 602–6, maio 1997.

THAM, E. et al. Dominant mutations in KAT6A cause intellectual disability with recognizable syndromic features. **American journal of human genetics**, v. 96, n. 3, p. 507–13, 5 mar. 2015.

TIFFEN, J. C. et al. Targeting activating mutations of EZH2 leads to potent cell growth inhibition in human melanoma by derepression of tumor suppressor genes. **Oncotarget**, v. 6, n. 29, p. 27023–36, 29 set. 2015.

TURNER, N.; GROSE, R. Fibroblast growth factor signalling: from development to cancer. **Nature reviews. Cancer**, v. 10, n. 2, p. 116–29, fev. 2010.

TUSHER, V. G.; TIBSHIRANI, R.; CHU, G. Significance analysis of microarrays applied to the ionizing radiation response. **Proceedings of the National Academy of Sciences of the United States of America**, v. 98, n. 9, p. 5116–21, 24 abr. 2001.

TWIGG, S. R. F. et al. The origin of EFNB1 mutations in craniofrontonasal syndrome: frequent somatic mosaicism and explanation of the paucity of carrier males. **American journal of human genetics**, v. 78, n. 6, p. 999–1010, jun. 2006.

TWIGG, S. R. F. et al. Reduced dosage of ERF causes complex craniosynostosis in humans and mice and links ERK1/2 signaling to regulation of osteogenesis. **Nature genetics**, v. 45, n. 3, p. 308–13, mar. 2013.

TWIGG, S. R. F.; WILKIE, A. O. M. A Genetic-Pathophysiological Framework for Craniosynostosis. **The American Journal of Human Genetics**, v. 97, n. 3, p. 359–377, 2015a.

TWIGG, S. R. F.; WILKIE, A. O. M. New insights into craniofacial malformations. **Human molecular genetics**, v. 24, n. R1, p. R50–9, 15 out. 2015b.

VANDESOMPELE, J. et al. Accurate normalization of real-time quantitative RT-PCR data by geometric averaging of multiple internal control genes. **Genome biology**, v. 3, n. 7, p. RESEARCH0034, 18 jun. 2002.

VISHWANATH, B.; SRINIVASA, K. Raine syndrome. **Indian journal of human**, 2014.

VISSERS, L. E. L. M. et al. Heterozygous mutations of FREM1 are associated with an increased risk of isolated metopic craniosynostosis in humans and mice. **PLoS genetics**, v. 7, n. 9, p. e1002278, set. 2011.

WALL, S. A. et al. Fronto-orbital re-operation in craniosynostosis. **British Journal of Plastic Surgery**, v. 47, n. 3, p. 180–184, jan. 1994.

WAN, D. C. et al. Noggin suppression enhances in vitro osteogenesis and accelerates in vivo bone formation. **The Journal of biological chemistry**, v. 282, n. 36, p. 26450–9, 7 set. 2007.

WANG, X. et al. FAM20C plays an essential role in the formation of murine teeth. **Journal of**

Biological, 2012.

WANG, Y. et al. Abnormalities in cartilage and bone development in the Apert syndrome FGFR2 + / S252W mouse. **Development**, 2002.

WARREN, S. M. et al. The BMP antagonist noggin regulates cranial suture fusion. **Nature**, v. 422, n. 6932, p. 625–9, 10 abr. 2003.

WETTENHALL, J. M.; SMYTH, G. K. limmaGUI: a graphical user interface for linear modeling of microarray data. **Bioinformatics (Oxford, England)**, v. 20, n. 18, p. 3705–6, 12 dez. 2004.

WIELAND, I. et al. Mutations of the ephrin-B1 gene cause craniofrontonasal syndrome. **American journal of human genetics**, v. 74, n. 6, p. 1209–15, jun. 2004.

WILKIE, A. O. et al. Apert syndrome results from localized mutations of FGFR2 and is allelic with Crouzon syndrome. **Nature Genetics**, v. 9, n. 2, p. 165–172, 1995.

WILKIE, A. O. M. et al. FGFs, their receptors, and human limb malformations: clinical and molecular correlations. **American journal of medical genetics**, v. 112, n. 3, p. 266–78, 15 out. 2002.

WILKIE, A. O. M. et al. Clinical dividends from the molecular genetic diagnosis of craniosynostosis. **American journal of medical genetics. Part A**, v. 143A, n. 16, p. 1941–9, 15 ago. 2007.

WILKIE, A. O. M. et al. Prevalence and complications of single-gene and chromosomal disorders in craniosynostosis. **Pediatrics**, v. 126, n. 2, p. e391–400, ago. 2010.

WU, L. et al. The E2F1-3 transcription factors are essential for cellular proliferation. **Nature**, v. 414, n. 6862, p. 457–62, 22 nov. 2001.

WU, M. Y. et al. SNW1 Is a Critical Regulator of Spatial BMP Activity, Neural Plate Border Formation, and Neural Crest Specification in Vertebrate Embryos. **PLoS Biology**, v. 9, n. 2, p. e1000593, 15 fev. 2011.

WU, X.-B. et al. Impaired osteoblastic differentiation, reduced bone formation, and severe osteoporosis in noggin-overexpressing mice. **The Journal of clinical investigation**, v. 112, n. 6, p. 924–34, set. 2003.

XU, J.; LIU, Z.; ORNITZ, D. M. Temporal and spatial gradients of Fgf8 and Fgf17 regulate proliferation and differentiation of midline cerebellar structures. **Development (Cambridge, England)**, v. 127, n. 9, p. 1833–43, maio 2000.

YANG, F. et al. The study of abnormal bone development in the Apert syndrome Fgfr2+/S252W mouse using a 3D hydrogel culture model. **Bone**, v. 43, n. 1, p. 55–63, jul. 2008a.

YANG, F. et al. The study of abnormal bone development in the Apert syndrome Fgfr2+/S252W mouse using a 3D hydrogel culture model. **Bone**, v. 43, n. 1, p. 55–63, jul. 2008b.

YEH, E. et al. FGFR2 Mutation Confers a Less Drastic Gain of Function in Mesenchymal Stem Cells Than in Fibroblasts. **Stem Cell Reviews and Reports**, 2011.

YEH, E. et al. Novel molecular pathways elicited by mutant FGFR2 may account for brain

abnormalities in Apert syndrome. **PloS one**, v. 8, n. 4, p. e60439, 2013.

YEN, H.-Y.; TING, M.-C.; MAXSON, R. E. Jagged1 functions downstream of Twist1 in the specification of the coronal suture and the formation of a boundary between osteogenic and non-osteogenic cells. **Developmental Biology**, v. 347, n. 2, p. 258–270, 2010.

YOKOTA, M. et al. Therapeutic effect of nanogel-based delivery of soluble FGFR2 with S252W mutation on craniosynostosis. **PloS one**, v. 9, n. 7, p. e101693, 2014.

YU, K. et al. Loss of fibroblast growth factor receptor 2 ligand-binding specificity in Apert syndrome. **Proceedings of the National Academy of Sciences of the United States of America**, v. 97, n. 26, p. 14536–41, 19 dez. 2000.

ZAMUROVIC, N. et al. Coordinated Activation of Notch, Wnt, and Transforming Growth Factor- Signaling Pathways in Bone Morphogenic Protein 2-induced Osteogenesis: Notch TARGET GENE Hey1 INHIBITS MINERALIZATION AND Runx2 TRANSCRIPTIONAL ACTIVITY. **Journal of Biological Chemistry**, v. 279, n. 36, p. 37704–37715, 3 set. 2004.

ZHANG, X. et al. Receptor specificity of the fibroblast growth factor family. The complete mammalian FGF family. **The Journal of biological chemistry**, v. 281, n. 23, p. 15694–700, 9 jun. 2006.

ZHAO, H. et al. The suture provides a niche for mesenchymal stem cells of craniofacial bones. **Nature cell biology**, v. 17, n. 4, p. 386–96, abr. 2015.